CANADIAN THESES ON MICROFICHE

I.S.B.N.

THESES CANADIENNES SUR MICROFICHE

National Library of Canada
Collections Development Branch

Canadian Theses on
Microfiche Service

Ottawa, Canada
K1A 0N4

Bibliothèque nationale du Canada
Direction du développement des collections

Service des thèses canadiennes
sur microfiche

NOTICE

The quality of this microfiche is heavily dependent upon the quality of the original thesis submitted for microfilming. Every effort has been made to ensure the highest quality of reproduction possible.

If pages are missing, contact the university which granted the degree.

Some pages may have indistinct print especially if the original pages were typed with a poor typewriter ribbon or if the university sent us a poor photocopy.

Previously copyrighted materials (journal articles, published tests, etc.) are not filmed.

Reproduction in full or in part of this film is governed by the Canadian Copyright Act, R.S.C. 1970, c. C-30. Please read the authorization forms which accompany this thesis.

THIS DISSERTATION
HAS BEEN MICROFILMED
EXACTLY AS RECEIVED

AVIS

La qualité de cette microfiche dépend grandement de la qualité de la thèse soumise au microfilmage. Nous avons tout fait pour assurer une qualité supérieure de reproduction.

S'il manque des pages, veuillez communiquer avec l'université qui a conféré le grade.

La qualité d'impression de certaines pages peut laisser à désirer, surtout si les pages originales ont été dactylographiées à l'aide d'un ruban usé ou si l'université nous a fait parvenir une photocopie de mauvaise qualité.

Les documents qui font déjà l'objet d'un droit d'auteur (articles de revue, examens publiés, etc.) ne sont pas microfilmés.

La reproduction, même partielle, de ce microfilm est soumise à la Loi canadienne sur le droit d'auteur, SRC 1970, c. C-30. Veuillez prendre connaissance des formules d'autorisation qui accompagnent cette thèse.

LA THÈSE A ÉTÉ
MICROFILMÉE TELLE QUE
NOUS L'AVONS REÇUE

Canada

0-315-18034-X

15

National Library of Canada | Bibliothèque nationale du Canada

CANADIAN THESES ON MICROFICHE | *THÈSES CANADIENNES SUR MICROFICHE*

65943

NAME OF AUTHOR/*NOM DE L'AUTEUR* Yashpal I.R.K. Parmar

TITLE OF THESIS/*TITRE DE LA THÈSE* "NMR Studies of Human Plasma High Density Lipoproteins"

UNIVERSITY/*UNIVERSITÉ* Simon Fraser University

DEGREE FOR WHICH THESIS WAS PRESENTED/*GRADE POUR LEQUEL CETTE THÈSE FUT PRÉSENTÉE* Ph.D.

YEAR THIS DEGREE CONFERRED/*ANNÉE D'OBTENTION DE CE GRADE* 1985

NAME OF SUPERVISOR/*NOM DU DIRECTEUR DE THÈSE* R.J. Cushley, Professor

Permission is hereby granted to the NATIONAL LIBRARY OF CANADA to microfilm this thesis and to lend or sell copies of the film.

The author reserves other publication rights, and neither the thesis nor extensive extracts from it may be printed or otherwise reproduced without the author's written permission.

L'autorisation est, par la présente, accordée à la BIBLIOTHÈQUE NATIONALE DU CANADA de microfilmer cette thèse et de prêter ou de vendre des exemplaires du film.

L'auteur se réserve les autres droits de publication; ni la thèse ni de longs extraits de celle-ci ne doivent être imprimés ou autrement reproduits sans l'autorisation écrite de l'auteur.

DATED/*DATÉ* April 16, 85 SIGNED/*SIGNÉ*

PERMANENT ADDRESS/*RÉSIDENCE FIXÉ* [redacted]

NL-91 (3-74)

NMR STUDIES OF HUMAN PLASMA HIGH DENSITY LIPOPROTEINS

by

YASHPAL I. PARMAR

M.Sc., Department of Biological Sciences,

Brock University, St. Catharines (1979)

A THESIS SUBMITTED IN PARTIAL FULFILLMENT OF

THE REQUIREMENTS FOR THE DEGREE OF

DOCTOR OF PHILOSOPHY

in the Department

of

Chemistry

SIMON FRASER UNIVERSITY

April 1985

APPROVAL

Name: YASHPAL I. PARMAR

Degree: Doctor of Philosophy

Title of Thesis: NMR Studies of Human Plasma High Density Lipoproteins

Examining Committee: Chairman: Dr. F.W.B. Einstein

Dr. R.J. Cushley
Senior Supervisor

Dr. A.C. Oehlschlager

Dr. S. Aronoff

Dr. A.H. Burr
Department of Biological Sciences

Dr. I.C.P. Smith
External Examiner
Division of Biological Sciences
National Research Council
Ottawa

Date Approved: April 10, 1985

PARTIAL COPYRIGHT LICENSE

I hereby grant to Simon Fraser University the right to lend my thesis, project or extended essay (the title of which is shown below) to users of the Simon Fraser University Library, and to make partial or single copies only for such users or in response to a request from the library of any other university, or other educational institution, on its own behalf or for one of its users. I further agree that permission for multiple copying of this work for scholarly purposes may be granted by me or the Dean of Graduate Studies. It is understood that copying or publication of this work for financial gain shall not be allowed without my written permission.

Title of Thesis/Project/Extended Essay

"NMR Studies of Human Plasma High Density Lipoproteins"

Author:

(signature)

Yashpal I.R.K. Parmar

(name)

April 16, 85

(date)

ABSTRACT

Molecular motions and conformation(s) of lipids in human plasma high density lipoproteins, HDL_2 (density = 1.063-1.125 g/mL) and HDL_3 (density = 1.125-1.21 g/mL) have been studied by ^2H- and ^{31}P NMR. The acyl chain organization of lipids was quantified by the C-^2H bond order parameter, S_{CD}, which measures the time-averaged angular excursions of the C-^2H bond about the axis of motional averaging.

Selectively deuterated palmitic acids were incorporated (~5 mol %) into the surface monolayer of HDL_2 and HDL_3. At ~25°C the average order parameter, $\bar{S}_{CD}$, for the chain positions C_2 - C_6 = 0.32 and 0.38 for HDL_2 and HDL_3, respectively. For comparison, ~5 mol % selectively deuterated palmitic acid in sonicated unilamellar vesicles composed of phosphatidylcholine/sphingomyelin yielded $\bar{S}_{CD}$ = 0.09. This value is ~3-5 times lower than in HDL and ~2 times lower than phospholipid multilamellar liposomes. Possible reasons for the differences in the three systems are discussed.

Cholesteryl palmitate selectively deuterated along the acyl chain was incorporated into the core of reconstituted HDL. The ^2H NMR line widths (430-350 Hz) for the C_2 - C_6 deuterons are consistent with an average ester conformation wherein the ester acyl chain is extended. Using a radius, R = 4.0 nm, obtained from electron microscopy, a line width = 2350 Hz for a static all-trans C^2H_2 was calculated, indicating the presence of con-

siderable ester chain motions in the HDL core.

^2H longitudinal relaxation times T_1 (38.8 MHz; ~25°C) for deuterated palmitic acid in the monolayer of HDL_2 and HDL_3 and the core-located cholesteryl palmitate in reconstituted HDL were 15 ± 2 ms (C^2H_2) and 170 ±17 ms (C^2H_3). At 61.4 MHz and ~25°C T_1 = 23 ±2 ms for [5,5,6,6-$^2H_4$]- and 190 ±19 ms for [16,16,16-$^2H_3$] palmitic acid in HDL_3. The frequency dependence of T_1 suggests the presence of slow motions influencing T_1. Furthermore, HDL_3 tumbling (τ_t ~5 x 10^{-8} s) may also contribute to T_1.

The lateral diffusion coefficient of phospholipids in HDL_2 was (2±1) x 10^{-8} cm^2 s^{-1} at ~25°C. The ^{31}P residual chemical shift anisotropy (CSA), calculated from the field and viscosity dependence of ^{31}P NMR line width, was ~69 ppm and ~75 ppm, respectively. These values are larger than the CSA ~45 ppm in phospholipid bilayers, suggesting conformational and/or motional differences of the head group in the two systems.

DEDICATION

to my father (Kanwar Kashmira Singh)

ACKNOWLEDGEMENTS

I wish to express my sincere gratitude to my supervisor, Professor R. J. Cushley, for the invaluable advice and continuous support during the course of this study.

I am indebted to my committee members, Professors A. C. Oehlschlager and S. Aronoff for helpful comments. Further, I thank the past and present members of Dr. Cushley's group, in particular Ms. J. Thewalt, Drs. W. D. Treleaven, S. R. Wassall and H. Gorrissen for many informal discussions. The helpfulness of the Chemistry Department is also acknowledged.

TABLE OF CONTENTS

TABLE OF CONTENTS (Cont)

LIST OF TABLES

LIST OF FIGURES

INTRODUCTION

Plasma lipoproteins are lipid-protein complexes which act as vehicles for fat transport (1). Under fasting conditions these complexes can be classified into four types of lipoproteins on the basis of their size, hydrated density, chemical composition and electrophoretic mobility (Table 1). Chylomicrons and very low density lipoproteins (VLDL) are the lipoproteins that carry triglycerides from sites of absorption and synthesis to sites of storage and utilization. Low density lipoproteins (LDL), a degradation product of VLDL (2), is the major cholesterol-carrying lipoprotein in human plasma. Thus, it is the only known atherogenic lipoprotein. The biochemical pathway of LDL uptake by cells and its deposition on the arterial wall was elucidated by Goldstein and Brown. The reader interested in details is referred to review articles (3-5).

In 1975, Miller and Miller (6) showed a negative correlation between plasma high density lipoproteins (HDL) concentrations and the risk of ischaemic heart disease. In spite of much effort causality has not been shown. There is general agreement that HDL could serve two functions (7). Firstly, it is involved in "reverse cholesterol transport", i.e. the transport of cholesterol from the peripheral tissues to the liver, the main organ of cholesterol utilization. Secondly, it plays a central role in the catabolism of chylomicrons and VLDL and thus is involved in fat transport (8). During the catabolism of triglyceride-rich proteins HDL acts as an acceptor of apo A

TABLE 1

Protein and Lipid Composition of Major Lipoprotein Classes[A]

	HDL_3	HDL_2	LDL	VLDL	Chylomicron
[1]Protein	55	40	22	8	2
[1]Phospholipids	25	33	22	18	7
[1]Cholesterol	4	5	8	7	2
[1]Cholesteryl Esters	13	17	42	12	3
[1]Triglyceride	3	5	6	55	86
Density (g/cc)	1.125-1.21	1.063-1.125	1.019-1.063	0.95-1.006	<0.95
Radius (nm)	3.9	5.1	9.6	20	>60

[1]Weight percent composition.

[A]From reference (24).

proteins (see Table 2) phospholipids and free cholesterol (9). In both of the above functions an enzyme Lecithin: Cholesteryl Acyl Transferase (LCAT) is involved (10). The exchangeable cholesterol in HDL is esterified to cholesteryl ester by LCAT. Thus, HDL is a site of plasma cholesterol esterification (11). The cholesteryl ester is then transferred to other lipoproteins, VLDL and LDL, which delivers it to cells (12-17).

In order to understand the involvement of HDL in cholesterol homeostasis, we have studied the structure and dynamics of cholesteryl esters and phospholipids in HDL by NMR methods.

I Structure of High Density Lipoprotein

High density lipoprotein is a "quasi" spherical particle with a radius of 30-50 Å (18-23). The protein part of HDL (apoprotein) is embedded in the micellar structure formed by the phospholipids. The hydrophobic core of the micelle is filled with neutral lipids such as triglycerides and cholesteryl esters (24), (Figure 1).

A. Apoprotein

The major proteins of HDL are apo A-I and apo A-II (see Table 2). Apo A-I is the most abundant peptide (M.W. ~28,000 Daltons) having nearly twice the number of molecules as apo A-II per HDL particle. The latter peptide is a dimer whose molecular weight is ~17,000 Daltons (25-28).

Figure 1. The structural model of HDL_3. The sketch is half of the cross-section through spherical particle. Figure taken from reference (22).

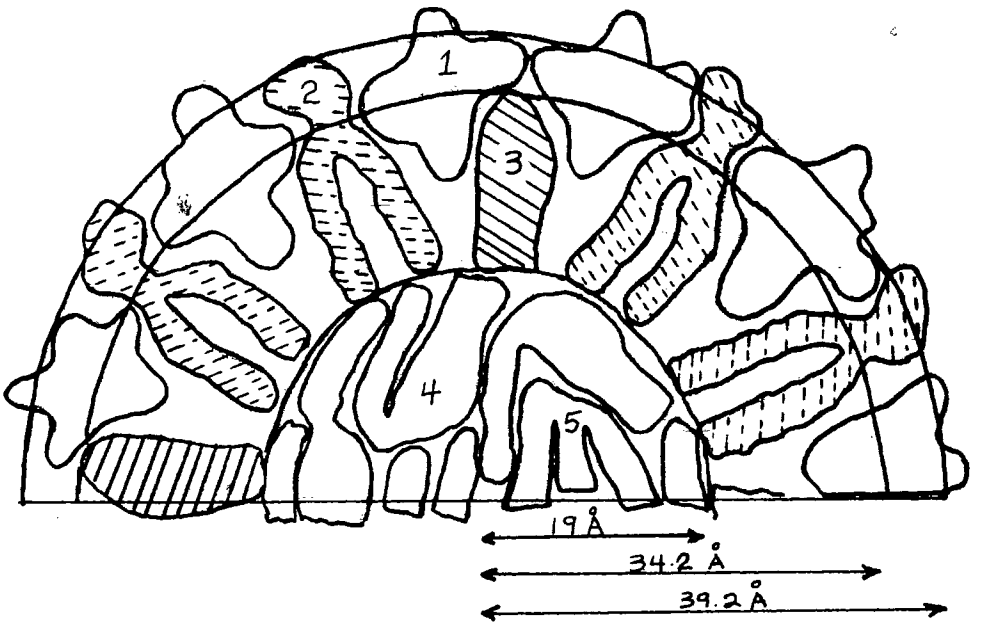

1. Protein
2. Phospholipid
3. Cholesterol
4. Cholesteryl Ester
5. Triglyceride

TABLE 2

Chemical Composition of Human Plasma Lipoprotein

Apoproteins	Chylomicrons	VLDL	LDL	HDL_2	HDL_3
	Percent Composition of Apoproteins				
A-I	<1	-	-		65
A-II	-	-	-	{>90	25
B		40	>95	-	-
C-I		10	-	1-2	
C-II	>90	10	-	1-3	5
C-III		30	trace	4-6	
D	?	-	-	<1	<1
E	<1	5-10	-	<1	<1

Table taken from reference 20.

The HDL apoproteins are believed to be located on the surface of HDL. Small angle x-ray scattering revealed a radial electron density suggesting surface location of the apoproteins (29,30). The chemical modification of the proteins revealed that more than 90% of the free amino groups are accessible to modification by succinic anhydride (31). Peptic digestion of HDL also supports the above hypothesis (32).

In another study the enzymes trypsin and chymotrypsin were bound to agarose gels. The bound enzymes were allowed to digest whole HDL. In all cases apo A-II was cleaved more rapidly than Apo A-I. This difference in apo A-I and apo A-II was also shown by the immunological reactivity, as only 10-20% of apo A-I in HDL reacts with its specific antibody. In contrast, essentially all of the apo A-II reacted with anti-apo A-II (33). When HDL particles are incubated with varying amounts of radioiodinated apo A-I, the radiactive A-I was found to bind to HDL and displace apo A-I to a maximum of 2 mol of apo A-I per mol of HDL. The rest was not displaceable even in the presence of large excess of apo A-I in the medium (34). This suggests that there are at least two pools of apo A-I on the HDL particle. The cross-linking reaction of 16-N_3,16-phosphatidylcholine incorporated in HDL is 40% greater with apo A-I than apo A-II. It was concluded that apo A-I is buried deeper in the HDL particle than apo A-II (35). The bifunctional cross-linking reagent 1,5-difluoro-2-4-diritrobenzene, was used to find the distribution of the proteins on HDL. Results showed apo A-I and apo A-II to be cross-linked. But no cross-linking was observed between the same apoproteins.

Hence it was concluded that apo A-I and apo A-II are adjacent to each other and neither A-I nor A-II self-associates (36, 37).

Upon heating the HDL particle above 60°C a broad, double-peaked endotherm is observed by differential scanning calorimetry. The first component (peak temperature = 71°C) corresponds to a selective release of apo A-I from the HDL particle. The second component (peak temperature = 90°C) corresponds to a general disruption of the HDL particle with release of cholesteryl ester and apo A-II. It was suggested that apo A-I is less important than apo A-II in maintaining the HDL apolar lipids in the form of a stable microemulsion (38).

The conformation of the apoproteins in HDL is not known. Based upon the primary sequence, Segrest et al. (39, 40) proposed that the apoproteins form an amphipathic helical structure such that the charged amino acids are exposed to the polar (water) surface and the non polar amino acid residues interact with the acyl chains of the phosphatidylcholine. These helical segments are oriented parallel to the curved surface of HDL.

B. Phospholipids

The major polar lipids (phosphatidylcholine: sphingomyelin, 4:1, wt/wt) are believed to be located such that their head groups are exposed to the aqueous medium (41). As stated earlier, low angle x-ray diffraction has shown that the electron

dense region of the HDL particle is located in a 12Å shell at the surface of the particle (29,30). Studies with paramagnetic quenching reagents Mn^{+2}/EDTA and Eu^{+3} have shown that more than 85% of the ^{31}P NMR signal is affected by these reagents (42,43).

More recently, HDL particles were exposed to phospholipase A_2. The enzyme hydrolysed all of the phosphatidylcholine to lysophosphatidylcholine (44). Therefore, it can be concluded that most of the phospholipid head groups are located at the surface of HDL.

The amphipathic helical structure of the apoprotein model (39,40) also suggests that zwitterionic phospholipid head groups interact with the charged amino acid residues. If this interaction were to occur then the conformation and/or the mobility of the head groups are expected to be different in the presence and absence of apoproteins. Brewer and Assman (45) and Stoffel et al. (46) have determined ^{13}C T_1s of the quaternary ammonium methyl group of the choline moiety in recombined HDL particles and phospholipid vesicles. Similar values of T_1 were found in both systems. This was taken as evidence that the protein and the phospholipid head group do not interact in HDL. Andrews et al. (47) reached similar conclusions for the reconstituted porcine apo A-I phosphatidylcholine complex. In these studies similar ^1H T_1s were obtained for the choline moiety phosphatidylcholine vesicles, phosphatidylcholine Apo A-I complex, and native porcine HDL.

We believe the above is insufficient evidence to rule out any electrostatic interaction of the head group and the protein because T_1 measurements are sensitive to fast motions. In addition, the above authors examined the quaternary methyl group which is relatively insensitive to changes in motion.

There has been very little information presented on the acyl chains of phospholipids. ^1H NMR of native HDL revealed narrow line widths for the methylene segments of the phospholipid acyl chains (48). Hence it was suggested that the acyl chains of phospholipids possess significant mobility. In contrast, 5-doxylstearate incorporated into HDL_3 exhibited a nearly immobilized electron spin resonance spectrum with $S_{mol} = 0.7$.

C. Cholesteryl Esters

Cholesteryl esters comprise about 15% of the particle. The major fatty acids of cholesteryl esters are linoleic acid (52%), oleic acid (19%) and palmitic acid (11%) (49).

Most models of HDL structure (Figure 1) do not address the arrangement of cholesteryl esters. It is generally assumed that the ester exists in the core of HDL in an oil-like fluid which is separate from the surface monolayer (50). It is also proposed that much of the stability of the HDL particle depends upon the hydrophobic boundary between the core and the inner surface of the phospholipid monolayer (51, 52). The model of Verdery and

Nichols (53) addresses itself to differences in the arrangement of cholesteryl esters in HDL_2 and HDL_3. HDL_3 is a smaller particle (<80 Å diameter) and the ester acyl chain is folded over the steroid nucleus, whereas in HDL_2 (~100Å diameter) the ester acyl chain extended. Based on x-ray scattering Laggner and Muller (54) have proposed that cholesteryl esters are extended and are arranged in a radially symmetric manner in HDL. In addition, the esters interdigitate with the acyl chains of the surface phospholipids. The size differences in HDL_2 and HDL_3 simply reflect the extent of interdigitation. Our results are consistent with the latter model (58) (see Section D.I. pp. 150-163).

Since the majority of the HDL cholesteryl esters can be readily exchanged into other lipoproteins such as VLDL and LDL, it is hypothesized that some ester must be dissolved in the phospholipid monolayer so that it becomes available to the plasma exchange protein. Cushley and co-workers (55-58) have demonstrated that cholesteryl esters can be dissolved in lamellar bilayers up to 5 mol %. Therefore, by analogy, it is possible some ester may be dissolved in the monolayer of HDL, although no evidence has yet been made available to support this conjecture.

Fluorescence depolarization, experiments with of pyrene excimer have shown that the lipids of HDL are more viscous than the lipids extracted from HDL (59, 60), and no thermal transition has been detected (59). It was therefore concluded that apoproteins may restrict the mobility of some of the HDL lipids.

This finding is supported by differential scanning calorimetry. The absence of any transition between 0°C-60°C in native HDL is in contrast to the extracted lipids from HDL which show a reversible liquid crystalline transition 20°C-40°C). Based upon these observations, Tall et al. (40) postulated that the absence of a cholesteryl ester phase transition in intact HDL may indicate an interaction of cholesteryl ester molecules with the protein phospholipid surface that prevents the formation of an organized lipid phase.

NMR studies have shown that cholesteryl esters possess significant mobility. Hamilton et al. (65-68), using ^{13}C NMR have shown that the cholesteryl moiety of cholesteryl esters undergoes anisotropic motions inside the HDL particle. The motion of the cholesteryl esters in HDL was compared to triglyceride/cholesteryl esters mixture (67-68). ^{13}C NMR spectra similar to native HDL were obtained. Hence, it was concluded that the motion(s) of cholesteryl esters in HDL was due to the presence of triglycerides in HDL. We challenge this explanation as we have shown that the ester present in reconstituted HDL has significant mobility even in the absence of triglycerides (see Section D.I. pp. 150-163).

D. Cholesterol

The unesterified cholesterol comprises about 5% by weight of the HDL particle. The location of cholesterol in the lipoprotein is controversial issue. It is believed that cholesterol has two

locations: surface monolayer and the core of HDL. The latter location is controversial because the polar hydroxyl group of cholesterol would probably prefer to be near the aqueous phase. The amount of cholesterol in HDL corresponds ~30 mol % with respect to phospholipids. Therefore, the HDL monolayer could easily accommodate all of the cholesterol. It is possible to incorporate as much as 50 mol % cholesterol in phospholipid bilayers (69). Nevertheless, cholesterol has finite solubility in the core components, i.e. cholesteryl esters and triglyceride (70).

Evidence in favour of the core location of cholesterol comes from ^{13}C NMR studies (71,72). In natural abundance ^{13}C NMR spectra of native HDL at 35°C, the C5 position of free and esterified cholesterol occur at 141.2 ppm and 139.7 ppm respectively. The ratio of the integrated intensity of the C5 resonance of cholesteryl ester to that of cholesterol (5:1) was found to be significantly different from the molar ratio of these species (3:1) as determined by chemical analysis. Hence it was concluded that cholesterol exists in more than one pool in HDL.

In another study cholesterol selectively enriched in ^{13}C at the C4 position was incorporated into reconstituted HDL, both in the absence and the presence of neutral lipids (73, 74). HDL reconstituted without neutral lipids yielded a single resonance at 41.7 ppm from the labelled cholesterol as in the case of egg phosphatidylcholine/cholesterol vesicles. However, in the

presence of neutral lipids an additional resonance at 42.2 ppm was also observed. It was concluded that 40% of the cholesterol is located in the core and the remaining was associated with surface monolayer.

Recently, Cowburn and co-workers (75), using 2-dimensional ^{13}C-^{1}H correlation spectroscopy showed that at a resolution of ~0.5 ppm, none of the HDL lipids exhibit partitioning between different structural environments, i.e. between the surface and the core.

From the above paragraphs it is clear that the details of lipid dynamics in HDL are not known. The acyl chains of phospholipids and cholesteryl esters are inaccessible to ^{1}H & ^{13}C NMR spectroscopy because the acyl chain resonances are found to overlap. In addition, HDL has complex composition which makes it difficult to extract meaningful results from the native systems. We have overcome these problems in the following ways. Firstly, we have employed ^{2}H NMR which is superior to ^{13}C and ^{1}H NMR because ^{2}H NMR relaxation affects are dominated by quadrupolar interaction (see Theory sections, A & B pp.17-24). Secondly, we used selectively deuterated lipids, hence the assigmemnt of peaks was unambiguous. Thirdly, in studying cholesterol esters we employed reconstituted HDL which was devoid of any cholesterol and triglycerides. Fourthly, we studied phospholipid unilamellar vesicles as models of the HDL phospholipd surface monolayer.

Phospholipids are amphiphilic molecules composed of non-polar fatty acids esterified to the polar head group (76, 77). The most common phospholipid is phosphatidylcholine. Under anhydrous conditions, phosphatidylcholine exhibits thermotropic mesomorphism with an isotropic melt of approximately 230°C. Upon the addition of water phosphatidylcholine has additional transitions, exibiting lyotropic mesomorphism (77-80). The structure formed in the presence of water is the lamellar phase, characterized by the occurrence of domains of phospholipid bilayers separated by water. The polar head groups are exposed to the aqueous phase, while the acyl chains form the inner part of the bilayer. When the water content is increased (lipid: water, 1:1, wt/wt), concentric bilayers of 100-1000 nm diameters are formed. These structures are called multilamellar liposomes. An important feature of many phospholipids in water is the reversible temperature dependent gel-liquid crystalline phase transition. This transition is markedly dependent upon the type of acyl chain. For example, for distearoyl phosphatidylcholine the melting transition occurs at 58°C while for the corresponding mono-unsaturated compound dioleyl phosphatidylcholine, the transition temperature is -20°C. The acyl chains adopt nearly all-trans parallel structures in the gel phase while in the liquid-crystalline phase they exist in a highly disordered or fluid-like state (77). The degree of anisotropic motion in the liquid crystalline state has been studied by several techniques (76, 81, 82, 90). The most reliable information regarding acyl chain dynamics has

been obtained by ^2H NMR. These studies have shown that the average alignment of phospholipid acyl chains above the gel-liquid crystalline transition is perpendicular to the bilayer surface (95,99), with the exception of the C2 segment of the sn-2 chain which is parallel to the bilayer surface. The orientational order of the phospholipid acyl chains exhibit a characteristic profile in the liquid crystalline phase. The region encompassing C2-C9 segments possess almost constant orientational order (S_{CD} ~0.20) called the "ordering plateau". There is a progressive decrease in the orientational order from C10 onwards to the terminal methyl where a minimum is observed.

Ultrasonic irradiation of multilamellar dispersions results in spherical structures of <50 nm (83-86). These structures are formed by a single closed bilayer which separates an inner aqueous compartment from bulk water. Unilamellar vesicles also undergo a reversible gel-liquid crystaline phase transition. But this transition is broader and occurs at a lower temperature than the corresponding multilamellar liposomes (82). There is much controversy regarding whether fatty acyl chain order and mobility are different in these highly curved vesicles as compared to multilamellar liposomes (103, 82, 87, 88, 89). The controversy stems from the fact that the unilamellar vesicles exhibit nearly high resolution ^1H NMR spectra whereas multilamellar liposomes exhibit broad spectra. Chan and co-workers (82,100) claim that NMR lines observed for unilamellar vesicles are largely due to an increase in structural disorder. Bloom et al. (103) and Stockton

et al. (106) have demonstrated that the unilamellar vesicle spectra can be explained largely by the isotropic tumbling and the lateral diffusion of phospholipid molecules around the curved vesicles (89,117). We have also shown that indeed the ^2H NMR spectra of vesicles can be explained in large part by the above mentioned isotropic motions. However, the presence of some structural disorder must be invoked to account for the ^2H NMR line widths (see Sections D. II, VI, pp.167-175; 204-210).

THEORY

I Deuterium NMR

A. Introduction

Deuterium NMR is a valuable technique compared to other magnetic resonance methods when applied to biological membranes. The low natural abundance of a deuteron (0.0156%) together with the ease of selective deuteration yields resonances which can be assigned unambiguously. This may be compared with the carbon-13 and proton NMR of membranes where many resonances are found to overlap. Since the van der Waals radii of the two isotopes are similar, selective deuteration leaves the membrane sterically unperturbed. Other methods such as electron spin resonance and fluorescence spectroscopy utilize bulky probes which may distort the membrane structure such that inaccurate inference may be drawn (91,92). Furthermore, deuterium NMR relaxation times are dominated by a single relaxation mechanism (quadrupolar interaction), which enables one to interpret ^2H NMR spectra in a straightforward manner. However, the ^2H NMR technique has a serious disadvantage in that large amounts (milligram quantities) of the sample are required. Nevertheless, ^2H NMR is a powerful technique for studying molecular motion and conformation in biological systems (93-98).

B. The Powder Pattern

The deuterium nucleus possesses a spin quantum number I = 1. In the presence of an external magnetic field Ho, the magnetic energy of interaction results in 2 I + 1 energy levels. The magnetic energy levels are equally spaced (see Figure 2), and in the absence of any quadrupolar effects, the allowed transitions, $m = -1 \leftrightarrow m = 0$ and $m = 0 \leftrightarrow m = +1$, give rise to a single NMR signal. However, in addition to the magnetic moment, the ^2H nucleus also possesses an electric quadrupole moment, Q. This is due to the fact that nuclear charge distribution departs from spherical symmetry and may be viewed as an ellipsoid (Figures 2 and 3). The interaction of the electric quadrupole with the electric field gradient at the position of the nucleus modifies the magnetic energy levels and removes the degeneracy of the two transitions. The energy levels m = + 1 and m = - 1 are raised to the same extent, while the m = 0 level is lowered by a similar amount. Consequently, the deuterium signal splits into two resonances centered about the Larmour frequency, ν_o (see Figure 2).

The interaction energy depends on the orientation of the quadrupole with respect to the symmetry axis of the local electric field gradient. The direction of the local field gradient along X, Y, Z axes is given by V_{xx}, V_{yy} and V_{zz}. The largest component of the field gradient is $V_{zz} = eq$. It is convenient to define an asymmetry parameter, η:

Figure 2: The left hand side of the figure contains the energy levels for a spin I = 1 system with and without quadrupolar interactions. The insert describes, schematically, the interaction of a quadrupolar nucleus of ellipsoidal charge distribution with an array of four point charges for the three different spin orientations. Figure from reference 93.

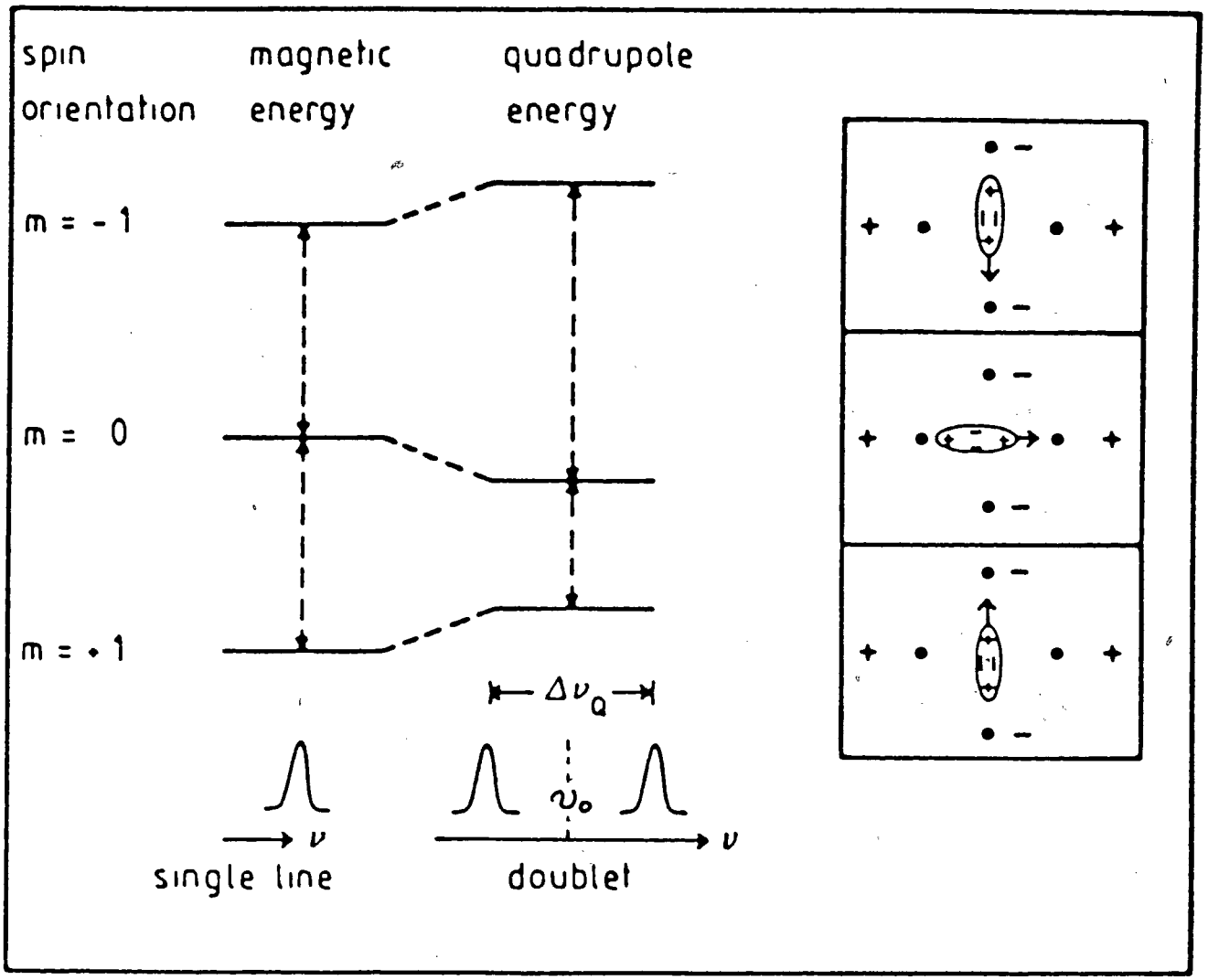
spin orientation
magnetic energy
quadrupole energy
m = - 1
m = 0
m = + 1
$\Delta\nu_Q$
ν_0
ν
single line
doublet
ν

$$\eta = \frac{V_{xx} - V_{YY}}{V_{zz}} \qquad (1)$$

For a C-D bond, where the electric field gradient is approximately axially symmetric, the resonance frequencies, (V_1 and V_2) for the two signals are given by

$$\upsilon_1 = \frac{\gamma H_o}{2\pi} + \frac{3}{4}\left(\frac{e^2 q Q}{h}\right)\left(\frac{3\cos^2\theta - 1}{2}\right) \qquad (2)$$

$$\upsilon_2 = \frac{\gamma H_o}{2\pi} - \frac{3}{4}\left(\frac{e^2 q Q}{h}\right)\left(\frac{3\cos^2\theta - 1}{2}\right) \qquad (3)$$

where γ is the magnetogyric ratio of the deuteron, h is Planck's constant, eq is the value of the electric field gradient along the C-D bond axis and θ is the angle between the axis of symmetry of the electric field gradient and the applied magnetic field. The frequency separation $\Delta\upsilon_Q(\theta) = (\upsilon_1 - \upsilon_2)$ of the two signals has an angular dependence given by

$$\Delta\upsilon_Q(\theta) = \frac{3}{2}\left(\frac{e^2 q Q}{h}\right)\left(\frac{3\cos^2\theta - 1}{2}\right) \qquad (4)$$

For a polycrystalline sample, where the C-D bonds are randomly oriented, the angle θ has all possible values. The summation of $\Delta\upsilon_Q(\theta)$ over all angles in a sphere yields the so-called powder pattern (see Figure 3). The probability maximum occurs when $\theta = 90^\circ$ and vanishes at $\theta = 0^\circ$ and $\theta = 180^\circ$. The frequency separ-

Figure 3: Deuterium NMR spectra of a single crystal oriented at various angles Θ with respect to the magnetic field (lower tracings). The different shadings refer to the two different transitions $m = -1 \leftrightarrow m = 0$ and $m = 0 \leftrightarrow m = +1$. The upper tracing is the power-pattern obtained from a polycrystalline sample. Figure taken from reference 98.

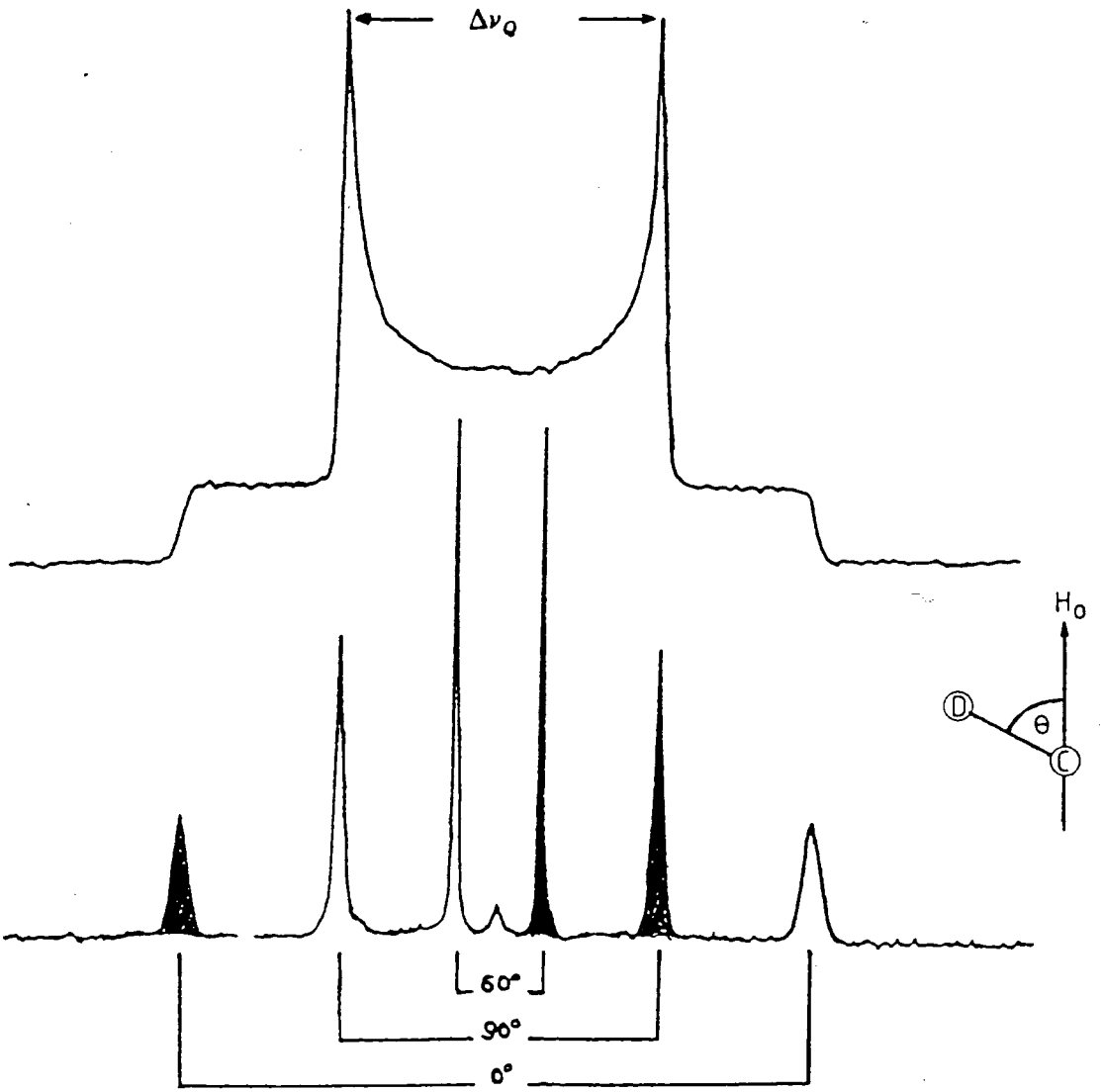
$\Delta\nu_Q$
H_0
D
θ
C
60°
90°
0°

ation between the two maxima ($\theta = 90^{o}$) is called the quadrupolar splitting, $\Delta\upsilon_Q$; hence,

$$\Delta\upsilon_Q = 3/4 \frac{(e^2qQ)}{h} \quad (5)$$

where $\frac{(e^2qQ)}{h}$ is called the quadrupolar coupling constant.

C. Anisotropic Motions

For a C-D bond of methylene type present in a polycrystalline sample $\Delta\upsilon_Q$ has the value of 126 kHz. The quadrupolar splittings observed for the deuterated acyl chains of multilamellar dispersions of phospholipids in the liquid-crystalline phase are <30 kHz suggesting that the quadrupolar interaction is averaged out by motions. The anisotropic motions responsible for the reduction of $\Delta\upsilon_Q$ are the fast anisotropic rotational diffusion of the acyl chains about their long molecular axis. The presence of rotational diffusion averages out the static electric field gradient such that the new effective field gradient is axially symmetric with respect to the axis of rotation. In addition, $\Delta\upsilon_Q$ is further reduced by the fluctuations of the C-D bond with respect to the director axis of the membrane bilayer. The director is the axis about which the molecules perform cylindrically symmetric motions. To describe the fluctuations of the C-D bond in the X, Y, Z direction, we introduce the orientational order parameter, S.

$$S = S_{ZZ} + 1/3\,\eta\,(S_{XX} + S_{YY}) \qquad (6)$$

The order parameters, S_{XX}, S_{YY}, and S_{ZZ} measure the angular fluctuations of the C-D bond about the director, where the Z axis is defined as parallel to the director. Given that $S_{XX} + S_{YY} + S_{ZZ} = 0$; two order parameters are needed to describe the motions of a single deuterated molecule. However, for a C-D bond $\eta < 0.05$, hence $S = S_{ZZ}$. Also, the dominant axis of the field gradient is identical with the C-D bond vector, therefore, $S_{ZZ} = S_{CD}$. The angular excursions of the C-D bond about the director is given by the carbon-deuterium bond order parameter S_{CD}:

$$S_{CD} = 1/2\,\langle 3\cos^2\beta - 1\rangle \qquad (7)$$

where β is the angle between the C-D bond and the director axis (Figure 4), and the angular brackets denote an average over the range of angles that the C-D bond traverses on the timescale of the NMR experiment. Hence, the quadrupolar splitting in equation 5 is modified by a factor S_{CD}

$$\Delta\nu_Q = 3/4\,\frac{(e^2qQ)}{h}\,|S_{CD}| \qquad (8)$$

The use of the carbon-deuterium bond order parameter, S_{CD}, to describe the mean orientation of flexible molecules can be much more involved. An assumption made in obtaining equation (8) is that the phospholipid molecules undergo cylindrically symmetric motion about the bilayer normal, i.e. the director axis

Figure 4: Illustrations of the vectors and angles relevant to the lipid chain motions. Ho is the direction of the applied magnetic field. The director, $\bar{d}$, is normal to the bilayer surface. The molecular interaction vector is the C-D bond. Figure taken from reference 100.

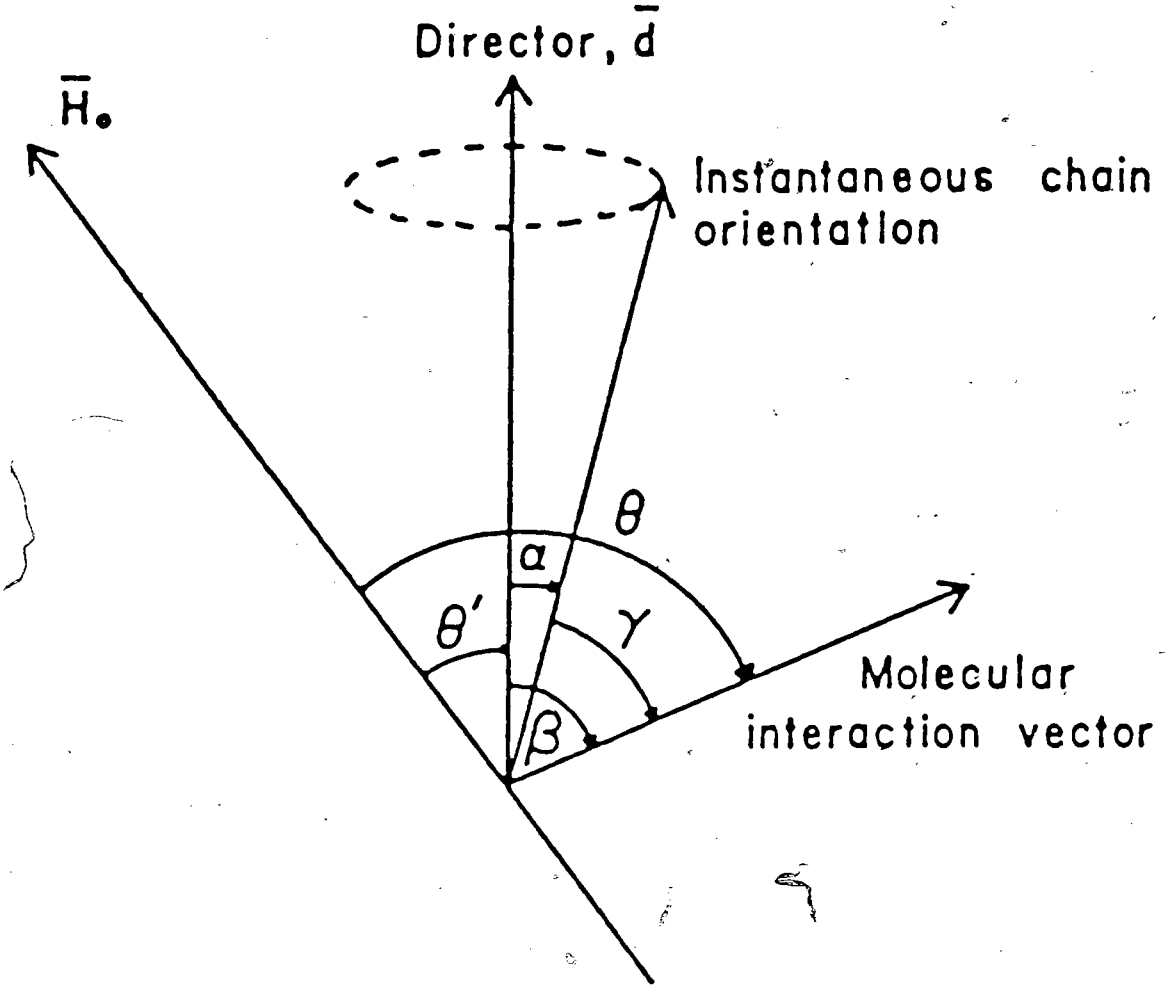
Director, $\bar{d}$
$\bar{H}_o$
Instantaneous chain orientation
θ
α
θ'
γ
β
Molecular interaction vector

is parallel to the bilayer normal. Seelig and Seelig (99) has shown this to be the case for phospholipid acyl chains, at least on the deuterium NMR time scale. Studies with oriented bilayers have shown that the quadrupolar splitting of a C5 deuterated dipalmitoyl phosphatidylcholine collapses if the bilayer is inclined at the magic angle (54.7°) with respect to the magnetic field. However, in the case of phospholipid vesicles and lipoproteins the orientation of the director with respect to the particle surface is not known. There is, however, suggestive evidence that the axis of motional averaging in the large unilamellar vesicles is identical with the bilayer normal on the fluorescence time scale (101). For purposes of the present study we will assume that the director is perpendicular to surface of vesicles and lipoproteins.

There are situations where the molecules in liquid crystalline samples re-orient slowly about the director (102). Under these conditions, the molecular motions are no longer cylindrically symmetric and S_{CD} has contributions from both chain reorientation and chain isomerization (Fig. 4), viz:

$$S_{CD} = S_{mol.}\ S_{geom.} \qquad (9)$$

and $S_{mol.} = 1/2 \langle 3\ COS^2 \alpha \quad -1 \rangle$;

$S_{geom.} = 1/2 \langle 3\ COS^2 \gamma \quad -1 \rangle$

where $S_{mol.}$ is the molecular order parameter for the instant-

aneous chain orientation and $S_{geom.}$ is the intramolecular chain isomerization order parameter. The angles α and γ are shown in Figure 4.

D. Isotropic Motions

If the isotropic motions are very much faster than the quadrupolar coupling constant, i.e. $\tau_c << (e^2qQ/h)^{-1}$ averaging of the quadrupolar interaction occurs and the "powder-pattern" is reduced to a Lorentzian lineshape. For such lineshapes the order parameter, S_{CD}, cannot be measured directly. The absorption curve can be analysed by the method of moments to yield an order parameter.

The most important moment for structural studies it he second moment, M_2 (103-105).

$$M_2 = \frac{\int_0^\infty (w-w_o)^2 f(w)\, dw}{\int_0^\infty f(w)\, d\, w} \qquad (10)$$

where w_o is the central frequency and w is the frequency away from the centre and f(w) is the NMR lineshape function. It should be noted that the integration of the Lorentzian lineshape would give an infinite value for the second moment. But very far in the wings where the absorption is too weak the lineshape is truncated, hence, the experimental values for the second moment are finite. The second moment for a rigid C-D bond is given by (104).

$$M_2 = 4/5 \ \pi^2 \ \Delta\upsilon_Q^2 \ . \qquad (11)$$

Particle tumbling in solution and lateral diffusion of a molecule within the vesicle bilayer or the lipoprotein particle result in narrowing of the ^2H NMR resonance. In the absence of any other motions, the width at half height, W, of the Lorentzian line is given by (105)

$$\pi W = M_2 \ \tau_e \qquad (12)$$

where τ_e is the effective correlation time for the isotropic motions.

As stated earlier, phospholipid molecules undergo fast local anisotropic motions (chain isomerization) which lead to partial averaging of the static quadrupolar coupling constant by a factor, S_{CD}. Hence the rigid lattice value of M_2 is reduced to a residual second moment, M_{2r}. Combining equations 8 and 11 we have

$$M_{2r} = \frac{9\pi}{20}^2 \left(\frac{e^2qQ}{h}\right)^2 S_{CD}^2 \qquad (13)$$

If the local motions are very fast, i.e. $W^2 \ \tau_c^2 << 1$, where τ_c is the correlation time for the fast motions then the spinlattice relaxation time, T_1 and the spinspin relaxation time, T_2, are equal. The line width may then be expressed as

$$W = M_{2\hbar} \tau_e + \frac{1}{\pi T_1} \qquad (14)$$

Substitutions of equation 13 into 14 yields the following expression for the line width (106):

$$W = \frac{9\pi}{20} \frac{(e^2qQ)^2}{h} S_{CD}^2 \tau_e + \frac{1}{\pi T_1} \qquad (15)$$

It should be noted that only two types of motions, i.e. isotropic motions and fast local motions are considered to explain the observed line width. Thus, the possibility of other slow motions such as molecular chain reorientation is not considered (100).

The correlation times, τ_e, for the isotropic motions have contributions from the aggregate tumbling (τ_t) and the lateral diffusion (τ_D) of lipid molecules.

$$\frac{1}{\tau_e} \qquad \frac{1}{\tau_t} + \frac{1}{\tau_D} \qquad (16)$$

The term τ_t is given by the Stokes-Einstein relationship

$$\tau_t = \frac{4 \pi \eta R^3}{3 k T} \qquad (17)$$

where τ_D is the solvent viscosity, R is the radius of the particle, k is the Boltzman constant and T is the absolute temperature.

$$\tau_D = \frac{R^2}{6D} \qquad (18)$$

where D is the lateral diffusion coefficient of lipid molecule in the lipoprotein particle or the phospholipid vesicle bilayer.

The line shape for the phospholipid vesicles and other heterogeneous aggregates is not a single Lorentzian line but a superposition of Lorentzian lines. This is due to the heterogeneity in the particle size distribution in the sample. Nevertheless, by statistically weighting the size distribution, a line shape $S(\upsilon)$, can be generated which simulates the observed spectra (107).

$$S(\upsilon) = A \sum_{i=1}^{n} \frac{F_i \bar{R}_i^2}{W_i} \frac{1}{1+(4\upsilon^2/W_i^2)} \qquad (19)$$

where Fi is the fraction of vesicles in the size category i and Wi s the line width (equation 14) for the ith size. The term $\bar{R}_i^2$ compensates for the fact that larger vesicles have greater numbers of phospholipid molecules. The term A is a scaling factor. Equation 19 is thus a weighted line shape of n superimposed Lorentzian signals due to deuterons in small to large vesicle sizes. Fortunately, for the lipoproteins HDL and LDL the particle size is homogeneous enough to yield a single ^2H Lorentzian line shape.

E. Spin Lattice Relaxation

The measurement of the quadrupolar splittings and the line widths gives information about the time averaged orientations and the angular fluctuations of the segments involved. However, the rate of segmental motions is obtained from the measurements of the spin-lattice relaxation time, T_1.

Qualitatively, spin lattice relaxation time is a measure of the efficiency of attaining thermal equilibrium between the spin and its surroundings after applying a radio frequency pulse. The mechanism whereby the spins achieve thermal equilibrium is similar to the mechanism of resonance in an NMR experiment. The difference is that the transitions are the result of the fluctuating local fields instead of the radio frequency pulse used in a NMR experiment. For deuterium, relaxation is the result of the interaction of the nuclear quadrupolar moments with inhomogeneous electric field gradients at the site of nucleus.

The general expression for deuterium T_1 is given by (108)

$$\frac{1}{T_1} = \frac{3}{80}\left(\frac{e^2qQ}{\hbar}\right)^2 \left[J(\omega_o) + 4J(2\omega_o)\right] \qquad (20)$$

where $(e^2qQ/\hbar)^2$ is a measure of the quadrupolar interaction and J(W) is the spectral density function which describes the intensity of the field gradient at the frequency (w). For spin lattice relaxation only the intensity of the Larmor frequency (W_o) and twice the Larmor frequency ($2W_o$) are important.

The exact form of J(W) is quite complicated and is dependent upon the type of motion(s) involved. For a molecular segment undergoing fast isotropic motion, the correlation function is a single exponential, hence J(W) is given by:

$$J(\omega) = \frac{2\tau_c}{1+W_o^2\tau_c^2} \qquad (21)$$

where τ_c is the correlation time of the motion.

For small molecules τ_c is usually very short and the extreme narrowing approximation ($\omega_o^2\tau_c^2 << 1$) may be used. Equation 20 is then reduced to

$$\frac{1}{T_1} = \frac{3}{8}\left(\frac{e^2qQ}{\hbar}\right)^2\tau_c \qquad (22)$$

For macromolecules or molecular aggregates such as HOL_3, τ_c can be obtained from the Stokes-Einstein relationship equation (17). Then, by substituting equation 21 into 20 a T_1 can be calculated. The failure of the calculated T_1 to account for the observed T_1 indicates anisotropic and/or internal motion(s) of the segments within the macromolecule.

Deuterium spin lattice relaxation of a deuteron on the acyl chain of the phospholipid is predominantly due to molecular motions which cause fluctuations in the orientation of the C-D bond axis with respect to the magnetic field. In the liquid crystalline phase the C-D bond motions are restricted in

amplitude and are axially symmetric about the symmetry axis, i.e. the bilayer normal. Thus, the spin lattice relaxation is expected to depend upon the C-D bond ordering and the angle (θ') the bilayer normal makes with the static magnetic field vector. Assuming fast isotropic motion with a single correlation time, the T_1 then is given by (109)

$$\frac{1}{T_1} = 3/8 \left(\frac{e^2qQ}{\hbar}\right)^2 \left[1-\frac{(3\cos^2\theta'-1)}{2} S_{CD} - \left(1- \frac{(3\cos^2\theta'-1)}{2}\right) S_{CD}^2\right] \tau_c \qquad (23)$$

Experiments with perdeutero dipalmitoyl phosphilidylcholine show no angular dependence of T_1 in the fluid phase (109). This has been explained by the fact that lateral diffusion of phospholipid molecule leads to an averaging of the $(3\cos^2\theta'-1/2)$ term and the equation 23 becomes

$$\frac{1}{T_1} = 3/8 \left(\frac{e^2qQ}{\hbar}\right)^2 (1-S_{CD}^2)\ \tau_c \qquad (24)$$

A similar expression is obtained for vesicles or lipoproteins where the orientational averaging occurs via the tumbling of the particles.

The spin lattice relaxation of phospholipid bilayers is also found to have frequency dependence which suggests the presence of slow motions (111). The relaxation rate is then given by

$$\frac{1}{T_1} = \frac{1}{T_1\,(\text{fast})} + \frac{1}{T_1\,(\text{slow})} \qquad (25)$$

There have been several models proposed to explain the origin of the slow motions (100, 111, 112). Based upon the temperature and frequency dependence of proton and C-13 relaxation rate, Petersen and Chan (100) suggest that the spin-lattice relaxation rate can be explained by two different correlation times, τ_{11} and $\tau_{\perp}$. τ_{11} is approximately 10^{-9} to 2×10^{-10}s and $\tau_{\perp} > 10^{-7}$s so that $W_o^2\,\tau_{11}^2 << 1$ and $W_o^2\,\tau_{\perp}^2 >> 1$. The expression for the relaxation rate is given by

$$\frac{1}{T_1} = A\,\tau_{11} + B\,\frac{1}{W_o^2\,\tau_{\perp}} \qquad (26)$$

where the first term on the right hand side of the equation 26 follows a temperature dependence and the second term accounts for the frequency dependence. The slow motions are characterized by $\tau_{\perp}$, which reflects the rigid rod-type chain reorientations about the director.

Brown (111) has proposed that the phospholipid acyl chains are very flexible. Thus, certain segments of the hydrocarbon chains could have cooperative motions which would lead to a distribution of correlation times. This is in constant to the Petersen and Chan model where a single correlation time is used to characterize "rigid body" motions of the entire phospholipid molecule. The origins of the fast motions are similar in both

models, i.e. $W^2 \tau_c^2 << 1$ but the correlation time for the fast motions is $\sim 10^{-11}$s in Brown's model. The correlation time(s) of the collective slow motions in the Brown model are approximately 10^{-10} s.

The Brown model of a continuous distribution of correlation times predicts the relaxation rate to have $W_o^{1/2}$ dependence. T_1^{-1} is given by

$$\frac{1}{T_1} = A \tau_f + B \quad S_{CD}^2 \; W_o^{-1/2} \qquad (27)$$

Such an expression has also been proposed by Jeffrey et al. (113) to explain the T_1 behaviour of lamellar potassium palmitate bilayers.

The term "A" is the expression corresponding to local motions, e.g. trans-gauche isomerization and the "B" term describes the collective slow motions.

Bloom and Smith (110) have argued against the "collective motion" model. The introduction of proteins into the phospholipid bilayers is expected to disrupt the "collective motions", hence, T_1, of the phospholipid acyl chains. In contrast, similar T_1's are observed for the acyl chains of phospholipid bilayers both in the presence and absence of the proteins. Instead, Bloom and Smith (110) favour the "defect diffusion" model of Kimmich et al. (112), which also predicts $T_1 \propto W^{1/2}$ behaviour. This model

assumes that a defect is introduced in the all trans acyl chain by the trans-gauche isomerization. Such a defect diffuses along the phospholipid acyl chain. Furthermore, in analogy with the trans-gauche isomerization, "defect diffusion", is also not expected to be influenced by lipid-protein interactions.

II. ^{31}P - NMR

^{31}P NMR is a convenient tool for the investigation of phospholipid head groups in membranes as it is the only naturally occurring isotope of phosphorus. Since no spin labelling is required it is a completely non-perturbing probe. The phosphorus nucleus has a spin quantum number, I = 1/2, and a relative sensitivity of 0.06 compared to that of a proton (114, 115, 116).

The ^{31}P NMR spectra of membranes are dominated by chemical shift anisotropy (CSA) and dipolar broadening. The dipolar effects are due to the neighbouring protons which can be removed by proton noise-decoupling. Chemical shift anisotropy arises from the fact that electronegative oxygens shield the phosphorus nucleus from the external magnetic field. Furthermore, this shielding is not isotropic but is dependent on the orientation of the molecular axis with respect to the magnetic field. For an anhydrous phospholipid powder the spectrum of Figure 5a, is obtained. The discontinuities represent the three different chemical shielding tensors, σ_{11}, σ_{22} and σ_{33}. The principal values of σ_{11}, σ_{22} and σ_{33} for the crystalline phospholipid may range from ~-100 ppm to ~+100 ppm (115).

For the monohydrate of dipalmitoyl phosphatidycholine the principal values of the CSA are reduced suggesting that the binding of one water molecule increases phosphate symmetry. Upon the addition of excess water, the ^{31}P spectrum of

Figure 5A: ^{31}P NMR (118 MHz) proton-decoupled spectrum of anhydrous dipalmitoylphosphatidylcholine powder at 15°C. Both 5A and 5B figures taken from reference (115).

Figure 5B: The three different orientations of the chemical shielding tensors in the molecular frame of the phosphate. O(1) and O(2) are the esterified oxygens bonded to the head group residue and glycerol backbone respectively. While O(3) and O(4) are the non-esterified oxygens.

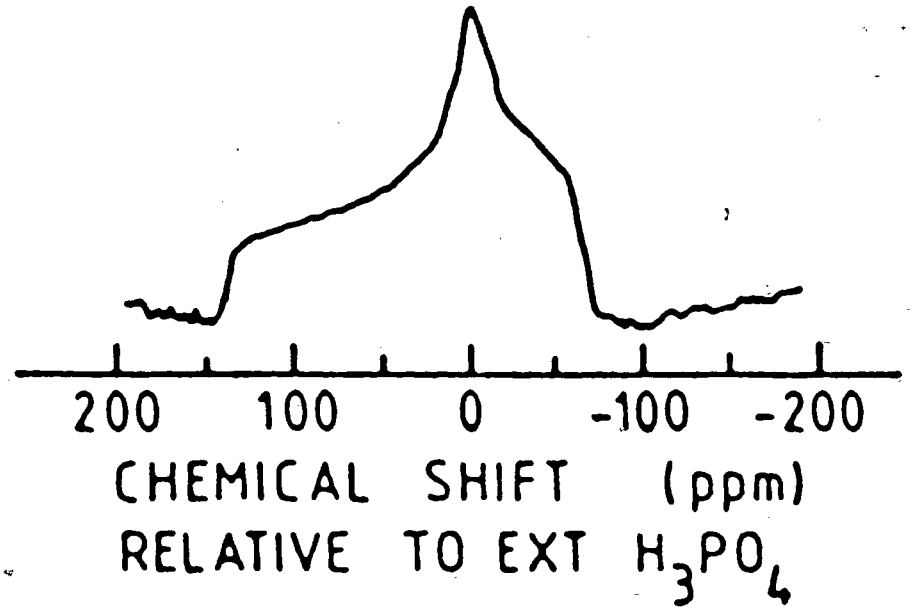
200
100
0
-100
-200
CHEMICAL SHIFT (ppm)
RELATIVE TO EXT H_3PO_4

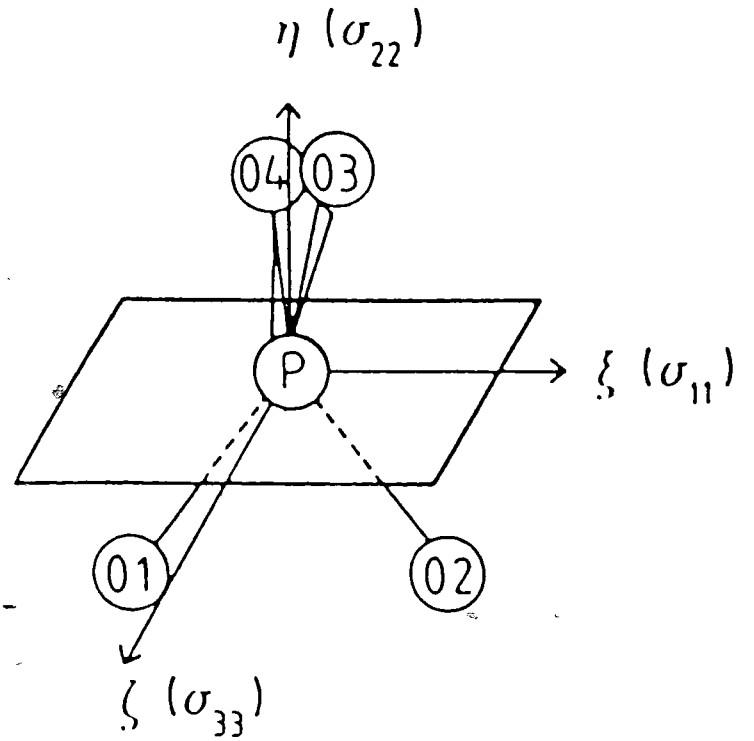
$\eta\ (\sigma_{22})$
04
03
P
$\xi\ (\sigma_{11})$
01
02
$\zeta\ (\sigma_{33})$

dipalmitoylphosphatidylcholine collapses from an asymmetric lineshape to an axially symmetric one at 18°C. This is not because the principal values of the CSA are changed by the addition of water as lowering the temperature to -10°C brings back the asymmetric lineshape as in the case of the monohydrate. Instead, it is due to the molecular motions, in particular the rotational diffusion of the phospholipid molecules about the bilayer normal, i.e. the director axis, which partially averages the CSA.

For planar oriented bilayers a single resonance is observed. The resonance frequency is dependent upon the angle (β) the director axis makes with the applied magnetic field. The resonance frequencies σ_{11} and $\sigma_{\perp}$ are obtained when $\beta = 0^{o}$ and $\beta = 90^{o}$ respectively. Figure 6a contains the spectrum of a randomly oriented multilamellar sample (powder spectrum) which consists of a superposition of spectra with all orientations of the bilayer.

A useful parameter for characterizing the powder pattern is the residual chemical shift anisotropy, $\Delta\sigma$, given by

$$\Delta\sigma = \sigma_{||} - \sigma_{\perp} \qquad (28)$$

For a fluid bilayer, $\Delta\sigma$ is of the order of 40-50 ppm. The quantitative relationship between $\Delta\sigma$ and the static CSA value

Figure 6: Proton-decoupled ^{31}P NMR spectra (36.4 MHz and 30°C) of polymorphic phases available to liquid crystalline phospholipids from reference (116).

A. Bilayer: egg phosphatidycholine

B. Hexagonal (H_{II}) soya bean phosphatidyl-ethanolamine.

C. Isotropic Motions: a mixture of 85 mol % soya bean phosphatidyl-ethanolamine and 15 mol % egg phosphatidyl-choline.

Phospholipid phases

Corresponding ^{31}P NMR spectra

Bilayer

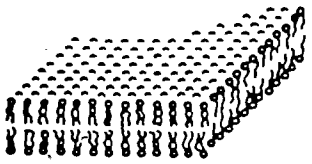

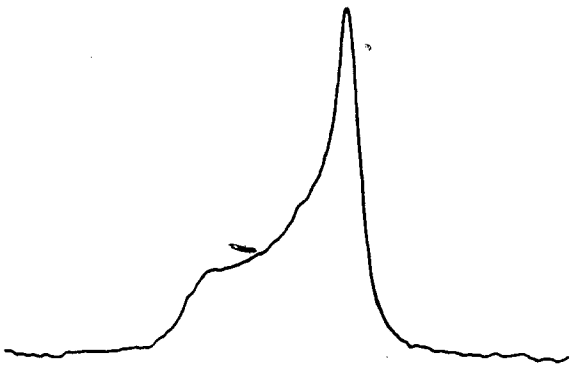

Hexagonal (H_{II})

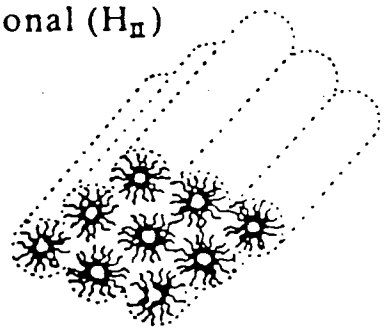

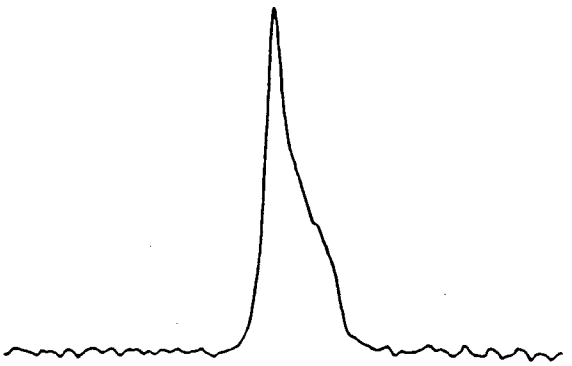

Phases where
isotropic motion occurs

a, Cubic
b, Rhombic
c, Micellar, inverted micellar
d, Vesicles

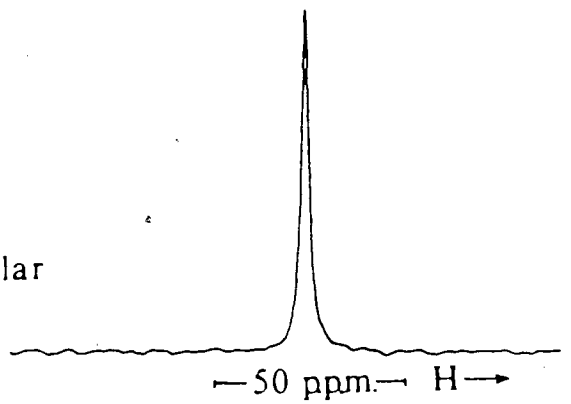

is

$$\Delta\sigma = S_{11} (\sigma_{11} - \sigma_{22}) + S_{33} (\sigma_{33} - \sigma_{22}) \quad (29)$$

where S_{11} is the order parameter of the axis connecting the esterified oxygens (ξ axis in Fig. 5b) of the phosphate group and S_{33} refers to the connecting axis of the non-esterified oxygens (ζ axis in Fig. 5b).

$\Delta\sigma$ is a measure of the orientation and the average fluctuation of the phosphate segment. It is comparable to the quadrupolar splittings in ^2H NMR. Unfortunately, $\Delta\sigma$ is determined by two independent order parameters which complicates the analysis of the ^{31}P NMR spectra.

In the normal and inverted hexagonal phases, the rotation of the long cylinders and/or lateral diffusion of the phospholipid molecules provide an additional averaging mechanism for the chemical shift anisotropy of the phosphate moiety. In the case of random distribution of cylinders, a proton noise decoupled ^{31}P NMR (Fig.6b) is obtained, whose residual chemical shift anisotropy is -1/2 that of lamellar phase spectrum.

The fast isotropic tumbling motions of unilamellar vesicles and the lipoprotein particles averages out the residual chemical shift anisotropy in a fashion similar to that of ^2H NMR

(see above). A single Lorentzian line is observed having width at half height, $\Delta\upsilon_{1/2}$, of

$$\Delta\upsilon_{1/2} = M_2 \tau_e + C \qquad (30)$$

where τ_e is defined as in equation 16. C is a constant which reflects line width contributions that are independent of particle tumbling such as very fast local motions and magnetic field inhomogeneities, and M_2 is the residual second moment of the ^{31}P NMR powder pattern (117, 118).

$$M_2 = \frac{4}{45} \Delta\sigma^2 \qquad (31)$$

It can be shown that the ^{31}P NMR line width for vesicles, as well as lipoproteins, varies as a function of the solvent viscosity. From such measurements, the value of M_2 and hence $\Delta\sigma$ can be obtained even for particles where the isotropic motion averages out the axially symmetric powder pattern.

EXPERIMENTAL PROCEDURES

Egg phosphatidylcholine was extracted from fresh hen egg yolks (121) and purified on a silica gel column (122). The purified egg phosphatidylcholine was dissolved at known concentration in chloroform and stored at -20°C until used.

Cholesteryl esters were prepared from the corresponding fatty acids and cholesterol by the method of Grover and Cushley (120).

[1-^{14}C] palmitic acid was purchased from New England Nuclear, Boston, Mass. Glycerol and cholesterol were obtained from Fisher Scientific Co. Cholesterol was recrystallized from benzene before being used. Deuterium depleted water, cholesteryl oleate, bovine brain sphingomyelin and egg albumin were purchased from Sigma Chemical Co. [5, 5, 6, 6-$^{2}H_4$] palmitic acid and [11, 11, 12, 12-$^{2}H_4$] palmitic acid were purchased from Merck, Sharp and Dohme, Canada Ltd. and [16, 16, 16-$^{2}H_3$] palmitic acid was obtained from Serdery Research Laboratories, London, Ontario. (4, 4-$^{2}H_2$] palmitic acid and [7, 7-$^{2}H_2$] stearic acid were generous gifts from Dr. A. P. Tulloch, Prairie Regional Laboratory, Saskatoon, Saskatchewan. [$^{2}H_2$] palmitic acid and selectively deuterated phospholipids were kindly provided by Dr. H. Gorrissen.

Fresh human blood (less than three days old) was obtained from the Canadian Red Cross, Vancouver Branch. HDL_2 and HDL_3

were isolated in the density range of 1.063-1.125 g/ml and 1.125-1.21 g/ml respectively as described previously by Havel et al. (123). The purity of HDL was checked by immunoelectrophoresiss using Ouchterlony cells (163).

The lipids from HDL_3 were removed from HDL_3 with $CHCl_3$: CH_3OH (2:2 V/V) to yield the apoproteins. The apoproteins were further washed (3-5 times) with diethyl ether to remove any residual lipids (125). The organic solvents were removed under vacuum to a yield solid white powder (apoproteins) which was stored at -20°C. The total lipids from the above fractions were pooled and dried to remove any water. The dried lipid was dissolved in $CHCl_3$: CH_3OH (1:4 V/V) and stored at -20°C under a layer of nitrogen.

I Preparation of Reconstituted HDL

Lipids, egg yolk phosphatidylcholine, cholesteryl oleate and the deuterated cholesteryl palmitate in the ratio of 3:1:1 (wt/wt) were codissolved in chloroform. The solvent was then removed by evaporation under a stream of nitrogen and subsequent overnight pumping under high vacuum. The dried lipid was incubated at 48°C for 10 minutes in $NaHCO_3/Na_2CO_3$ buffer pH 8.6 of density = 1.063 g/ml. The buffer was made in deuterium depleted water. Its density was adjusted with a NaCl/KBr in deuterium depleted water stock solution. The lipid dispersion was shaken periodically on a vortex mixer.

Dry apoprotein was added to the lipid dispersions (1:1; protein:total lipid) and allowed to incubate at 48°C for an additional ~10 minutes or until all of the solid protein particles appeared to have dissolved. The cloudy mixture was sonicated for five one minute pulses in a jacketed vessel using a Biosonic III probe sonicator. The temperature was maintained at approximately 40-48°C by allowing the sample to cool to ~40°C after each one minute pulse. The recombined particles were isolated in the density range of 1.063-1.21 g/ml (Hirz and Scanu, 126).

II Incorporation of Palmitic Acid into Native HDL

The concentrations of lipoprotein solutions were increased to levels suitable for NMR experiments using Amicon ultrafiltration membrane cones (CF25) or by Millipore immersible CX-30 membrane units. Exchanges with deuterium depleted water (typically 5) were performed to reduce the residual ^{2}HOH signal. Fatty acid was incorporated by incubating lipoprotein solutions with a thin film of selectively deuterated palmitic acid (~2-3 mg, representing an excess of 5 mol %) and a trace of [1-^{14}C] palmitic acid in a round bottom flask. The solution was gently agitated by hand during the period of incubation, which was up to 1 hour for ~5 mol % intercalation. The degree of incorporation was monitored by liquid scintillation counting of aliquots removed from the sample.

Selectively deuterated phosphatidylcholine was incorporated into native HDL_2 by mild sonication. HDL_2 solution was concentrated using Millipore CX-30 membrane units. Residual ^2HOH was exchanged with deuterium depleted water. Solid deuterated phospholipid (5 mol % with respect to phospholipid) was added to the HDL_2 solution. The sample was sonicated at 42°C for three one minute periods.

III Preparation of Multilamellar Liposomes and Unilamellar Vesicles

Lipids were mixed in sample tubes and co-dissolved in chloroform. The solvent was removed by evaporation under a stream of nitrogen and subsequent overnight pumping under high vacuum.

Multilamellar liposomes were prepared by adding an equal weight of deuterium depleted water and shaking vigorously with vortex mixer at a temperature above the gel to liquid-crystalline phase transition of the phospholipid until the sample appeared homogeneous.

Unilamellar vesicles were prepared by adding deuterium depleted water to the multilamellar dispersions and sonicating the resultant mixture for ~15 min. in a Biosonics III probe-type sonicator at a temperature above the gel to liquid-crystalline phase transition of the phospholipid. The vesicles were centrifuged for approximately one-half hour, on a small laboratory

centrifuge, in order to eliminate titanium fragments and undispersed lipids. The vesicles were used immediately for the experiments.

IV Analytical Methods

Purity of phospholipids and cholesteryl esters was checked by means of thin layer chromatography on Silica Gel G plates (Machrey-Nagel and Co., Duren, West Germany), eluting with chloroform/methanol/water (65:25:4 V/V) for phospholipids and chloroform for cholesteryl esters. The esters, cholesteryl palmitate and cholesteryl oleate were also characterized by their solid to isotropic liquid melting points.

The amount of phospholipids in the lipoprotein particles was quantified by phosphorus determination (127), while cholesteryl esters were determined either by the colorimetric method of Rudel and Moris (128) or by ^{2}H-NMR. The amount of protein present in the HDL solution was quantified according to the method of Lowry *et al.* (129) using egg albumin as a standard. Viscosity was measured using an Ostwald viscometer.

The association of the fatty acid was confirmed by gel-exclusion chromatography on Sepharose 4B with [1-^{14}C] palmitic acid. Typically, an aliquot of the labelled solution was applied to Sepharose 4B column (2.6 x 100 cm) and elution performed at 4°C, using a solution composed of 0.15 M sodium chloride plus

0.02% sodium azide pH 7.6. The void volume (141 mL) was determined using Blue Dextran (Pharmacia); average molecular weight equals 2.0 x 10^6 daltons. Total column volume (478 mls) was measured from the bed height under a constant head of pressure. The vesicles were monitored by following O.D. at 300 nm and the lipoproteins were monitored at O.D. 280 nm. The radioactivity was determined using a Beckman LS-8000 scintillation counter with liquifluor scintillation cocktail.

The scintillation cocktail was prepared by dissolving 60 g of naphthalene to 600 ml of dioxane. After dissolution, 42 ml of liquifluor, 20 ml of ethylene glycol and 100 ml of methanol were added. The final volume was adjusted to 1 litre with additional dioxane.

V Negative Staining Electron Microscopy

The size of vesicles and lipoproteins was determined by the negative staining method*.

Copper grids (200-400 mesh) were placed in a 100 ml beaker containing a detergent solution in doubly distilled water. The solution containing the grids was sonicated in a bath-type sonicator (Cole-Parmer Sonogen Automatic Cleaner) for approximately one-half hour. The detergent solution was decanted and replaced with doubly distilled water. Grids were sonicated for 1-2 min. prior to removing the water. This procedure was repeated approximately thirty times to yield very clean grids.

---

*Negative staining is a method of choice for visualizing subcellular particles as it has the ability to reveal subunit structure of macromolecules. It is superior to thin-sectioning as it avoids artifacts produced by fixing and embedding procedures. Forte and Nichols (18) attempted to section pelleted human LDL, but because of the thickness of the section (~600Å) and the granularity of the osmium particles, their results were uninterpretable. Negative staining is also superior to shadow casting as the accumulation of shadowing metal on small particles (e.g. unilamellar vesicles and lipoproteins) makes size determination inaccurate. Freeze-fracture is also a problem, because of the inability of locating the fracture plane of the lipoprotein particles. Hydrodynamic techniques, e.g. sedimentation, are inappropriate because they yield a mean size of the particles, whereas the negative staining method yields the distribution of sizes in the sample. In addition, negative staining technique is quite simple. Essentially all that is involved is to mix a suspension of the sample with an aqueous solution of the stain and then apply the solution onto a formvar-carbon coated grid which is left to air dry. The stain surrounds the particles on the support film as a result of surface tension interaction. The image produced by the negatively stained particles appears as light areas surrounded by a dark background.

Finally, the grids were rinsed with reagent grade acetone. The beaker containing the grids was left inverted on a Whatman filter paper overnight. The dried grids were stored under dessication until use.

Formvar was dissolved in reagent grade chloroform (BDH Chemicals) to yield a 2% wt/wt solution. Glass slides were coated with Formvar by lowering the slide into the Formvar-chloroform solution. The slide was then carefully raised out of the solution to avoid any ripples and held above the solution for approximately thirty seconds. Care was taken to execute this step so that slides with a uniform thickness of formvar coating can be obtained. The coated slides were air-dried for approximately 3-5 minutes.

The clean grids were placed (dull side up) on a filter paper immersed in a trough of doubly distilled water. The thin film of Formvar was floated off the slide onto the surface of water by gently immersing the Formvar coated slide into the trough. The water was removed from the trough in such a way that the Formvar film rests on the grids. The Formvar-coated grids were left to air dry in a Petri-dish.

The dried Formvar-coated grids were carbon coated using a Varian NRC 3115 vacuum evaporator. Carbon was shadowed using tapered one-eighth inch carbon rods. This procedure deposited <100 Å thin film of carbon onto the grids.

The vesicle or lipoprotein sample was diluted to approximately 300 ug/ml. Equal volumes of the diluted sample and 2% (wt/wt) ammonium molybdate pH 8.0 were mixed. The solution was applied on to the formvar-carbon coated grids. The excess sample was removed from the grid by touching the liquid with a piece of filter paper. The grids were then air dried, usually 2-3 hours and examined under a Philips electron microscope operating at 80 kV.

VI Deuterium NMR

Deuterium NMR of unilamellar vesicles and lipoproteins were obtained on a Nalorac 5.9T (38.8 MHz) superconducting magnet and home-built spectrometer. Collection and Fourier transformation of the free induction decays were performed on a Nicolet BNC-12 computer. All experiments were performed at temperatures between 15-40°C as indicated throughout the text, the temperature being controlled by means of a gas-flow system. Longitudinal relaxation times (T_1) were measured by the inversion-recovery method (159).

$[180°-\tau-90°$, sample and add, $\tau_R]_N$ where τ is the delay between the two pulses of the sequence and τ_R is the delay between subsequent pulses ($\tau_R > 5\ T_1$ to ensure complete return to equilibrium) and N is the number of acquisitions.

For multilamellar liposomes, a Nicolet Explorer IIIA digital

oscilloscope was used to acquire the NMR signals, which were subsequently transferred to a NIC BNC-12 computer where Fourier transforms were obtained. In order to minimize spectral distortions due to the receiver recovery time, a quadrupolar echo pulse sequence $(\pi/2|_{0^o} - \tau_1 - \pi/2|_{90^o} - \tau_R)_n$ was used (161). In all cases the time delay τ_1 between pulses was 75 us, the $\pi/2$ pulse length was 8 μs and the sequence of pulses was repeated after a time τ_R given in the text. A phase-alternating pulse sequence was used in order to cancel coherent receiver and pulse noise. Spectra were symmetrized by zeroing the "out of phase" channel and folding over, resulting in an increased signal to noise ratio of $\sqrt{2}$.

Quantification of Deuterated Cholesteryl Palmitate in Reconstituted HDL

The amount of deuterated cholesteryl palmitate present in reconstituted HDL was determined by recording a ^{2}H-NMR spectrum for reconstituted HDL containing cholesteryl [16,16,16-$^2H_3$] palmitate in which a capillary tube containing 3 μL of $CHCl_3$:C^2HCl_3 (9:1 v/v) was inserted coaxially into the sample tube. Sufficient time to ensure complete relaxation (>5 T_1) was left between successive r.f. pulses during data acquisition. Comparison of the integrated intensity of the C^2HCl_3 and cholesteryl ester signals, separated by 260 Hz, enabled quantitation of the ester.

VII ^{31}P NMR

Phosphorus-31 NMR spectra were acquired at 40.5 MHz on a Varian XL-100-15 spectrometer, operating in the Fourier transform mode and interfaced to a NIC 1080 computer. Magnet field stabilization was by means of an external ^{19}F field-frequency lock. Free induction decays were recorded in the presence of ^{1}H noise-decoupling having a 1 kHz bandwidth. In order to minimize sample heating due to the r.f. field (10 w) used for decoupling, either the decoupler was gated on only during acquisition of the free induction decay or, when decoupling was applied continuously, sample cooling by a gas flow system was employed. The temperature of the experiments was approximately 25°C. Chemical shifts were measured with respect to an external H_3PO_4 (85%) sample.

^{31}P NMR of lipoproteins were also acquired at 102.2 MHz, using a 5.9 Tesla superconducting Nalorac magnet and home-built spectrometer. Collection and Fourier transformation were performed on a Nicolet BNC-12 computer. The spectra were obtained without any decoupling. A phase-alternating pulse sequence was used in all experiments in order to minimize baseline aberrations.

RESULTS

I Selectively Deuterated Cholesteryl Palmitate in Reconstituted HDL.

Model HDL particles were prepared by sonication of a mixture containing apoproteins from HDL_3, cholesteryl oleate, deuterated cholesteryl palmitate and egg phosphatidylcholine (50:50 w/w of total lipids: apoproteins) in aqueous buffer. The sonicated mixture was then subject to ulracentrifugation and the reconstituted particles were isolated in the density range of 1.063-1.21 g/mL (Hirz and Scanu, 126).

The reconstituted HDL was characterized by chemical analysis, electron microscopy and ^{31}P NMR to establish the validity of the reconstituted HDL as a model of the native HDL particles. Table III shows the chemical composition of the reconstituted particles. This is in close agreement to the protein, phospholipid, cholesteryl esters found in native HDL's (Table I). Figure 7a shows the electron micrograph of the reconstituted HDL particles obtained by the negative staining method. For comparison, we have also obtained an electron micrograph of native HDL_3 (Figure 8). The HDL particles in both micrographs appear quite homogeneous, in agreement with Forte *et al.* (17). The mean diameter of the reconstituted HDL is given in Table III which compares very well with the value of 7.7 nm obtained for native HDL_3 particles.

TABLE III Physical parameters of HDL reconstituted using HDL_3 apoproteins, egg phosphatidylcholine, cholesteryl oleate, and deuterated cholesteryl palmitate.

Density (g/mL)	1.063-1.21
Mean Diameter[a] (nm)	7.8 (±1.2[b])
Composition (wt %)	
Protein	46 (±3)
Phospholipids	38 (±1)
Cholesteryl esters	16 (±1)
Cholesteryl oleate/cholesteryl palmitate (wt/wt)	2:1

(a) Approximately 200 particles were measured.

(b) Number in the parentheses represent standard deviation.

Fig. 7a Electron micrograph of reconstituted HDL. Magnification 195,100 times.

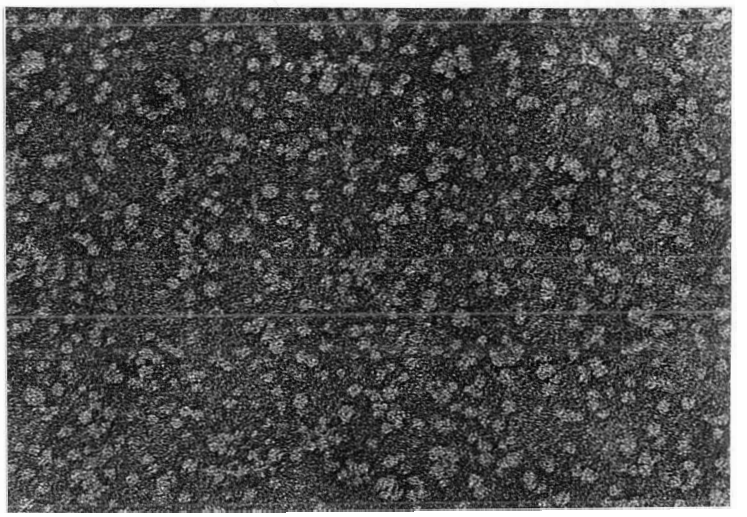

Fig. 8 Electron micrograph of native HDL_3. Magnification 363, 200 times.

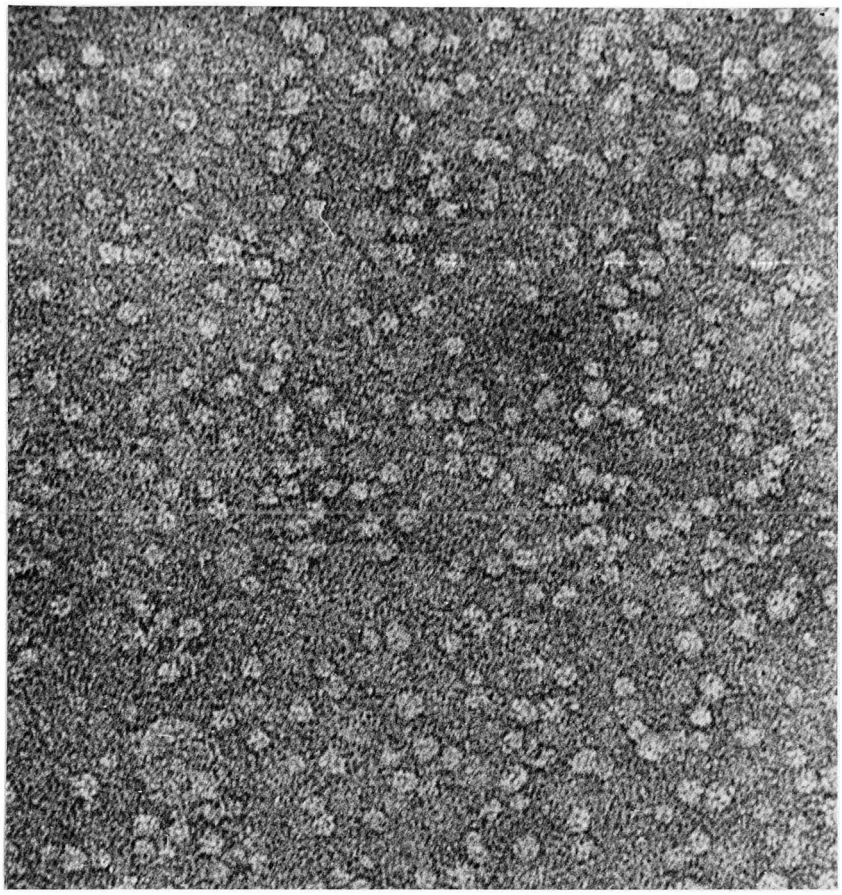

Phosphorous -31 NMR spectra of native HDL_3 as well as reconstituted HDL prepared with the total HDL_3 lipids and egg phosphotidylcholine, cholesteryl esters are shown in Figure 7b. The ^{31}P NMR of native HDL (Figure 7b) in practically identical to that published previously, Glonek et al., (130); and Henderson et al. (45). It consists of a strong resonance (~0.6 ppm upfield) having a width at half height, $\Delta\upsilon_{1/2}$ = 6 Hz which is due to phosphatidylcholine in HDL_3 particles plus a weaker resonance, shifted downfield ~0.1 ppm due to sphingomyelin. The ^{31}P NMR of reconstituted HDL using egg phosphatidylcholine/cholesteryl oleate/cholesteryl palmitate has a single resonance shifted +0.6 ppm upfield due to phosphatidylcholine. Its line width is 5±1 Hz (Figure 7b). HDL reconstituted with total HDL_3 lipids under identical conditions that using egg phosphatidylcholine/cholesteryl oleate/cholesteryl palmitate yields virtually indistinguishable spectrum to that of native HDL_3 (Figure 7b) with $\Delta\upsilon_{1/2}$ = 6 Hz.

The ^2H-NMR spectrum of reconstituted HDL containing cholesteryl [$^2H_{31}$] palmitate, i.e. cholesteryl palmitate completely deuterated along the acyl chain, is shown in Figure 9. This spectrum consists of a resonance with rather broad "skirts" extending up to approximately ±1 kHz from the centre frequency, plus a sharp resonance, shifted downfield ~3.7 ppm which arises from residual deuterium in water. The ^2H-NMR absorption of cholesteryl [$^2H_{31}$] palmitate in reconstituted HDL is obviously not a single Lorentzian line but is rather a superposition of Lorentzian line but is rather a superposition of Lorentzian lines

Figure 7b: ^{31}P NMR spectra: a: native HDL_3, b: HDL reconstituted using egg phosphatidylcholine/cholesteryl oleate/cholesteryl palmitate, c: HDL reconstituted using total HDL_3 lipids. Spectra parameters: sweep width = 2,000 Hz; number of acquisitions = 1.024; pulse length = 10 μs (60° flip angle); delay between subsequent pulses = 2 s; size of data set = 2 048 zero filled to 4 096; line broadening = 1 Hz.

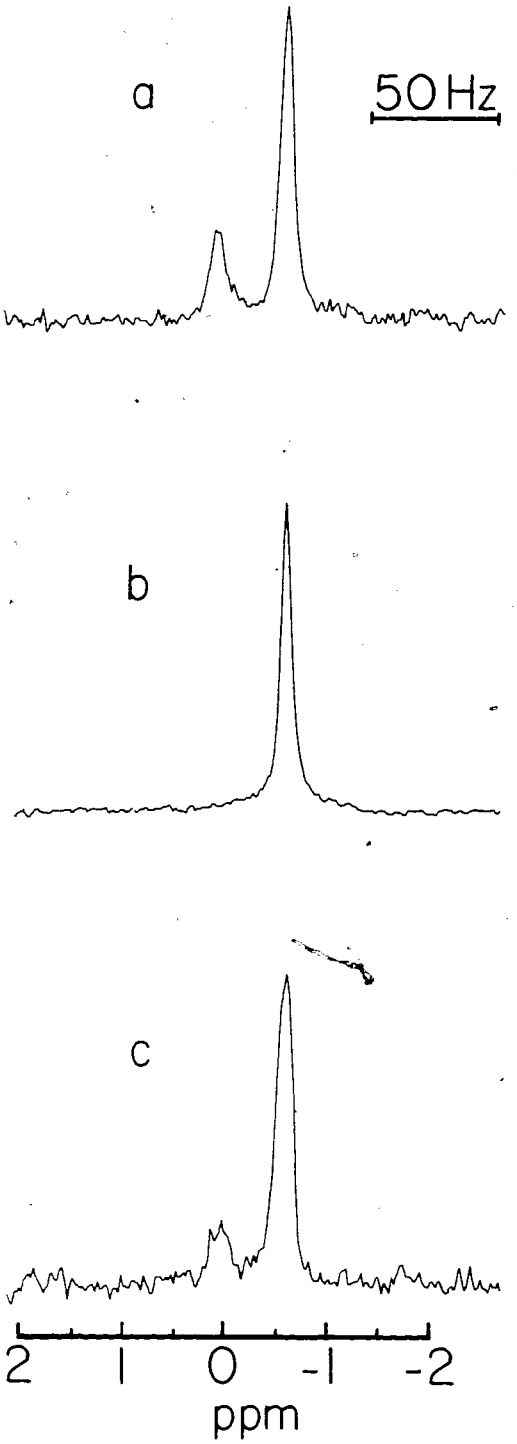
a
50 Hz
b
c
2
1
0
-1
-2
ppm

Figure 9: ^2H NMR of cholesteryl [$^2H_{31}$] palmitate in reconstituted HDL. Spectra parameters: sweep width = 5,000 Hz; number of acquisitions = 34,400; pulse length = 18 μs ($\pi/2$ pulse); delay between subsequent pulses = 1.8 s; size of data set = 8 K; line broadening = 1.5 Hz.

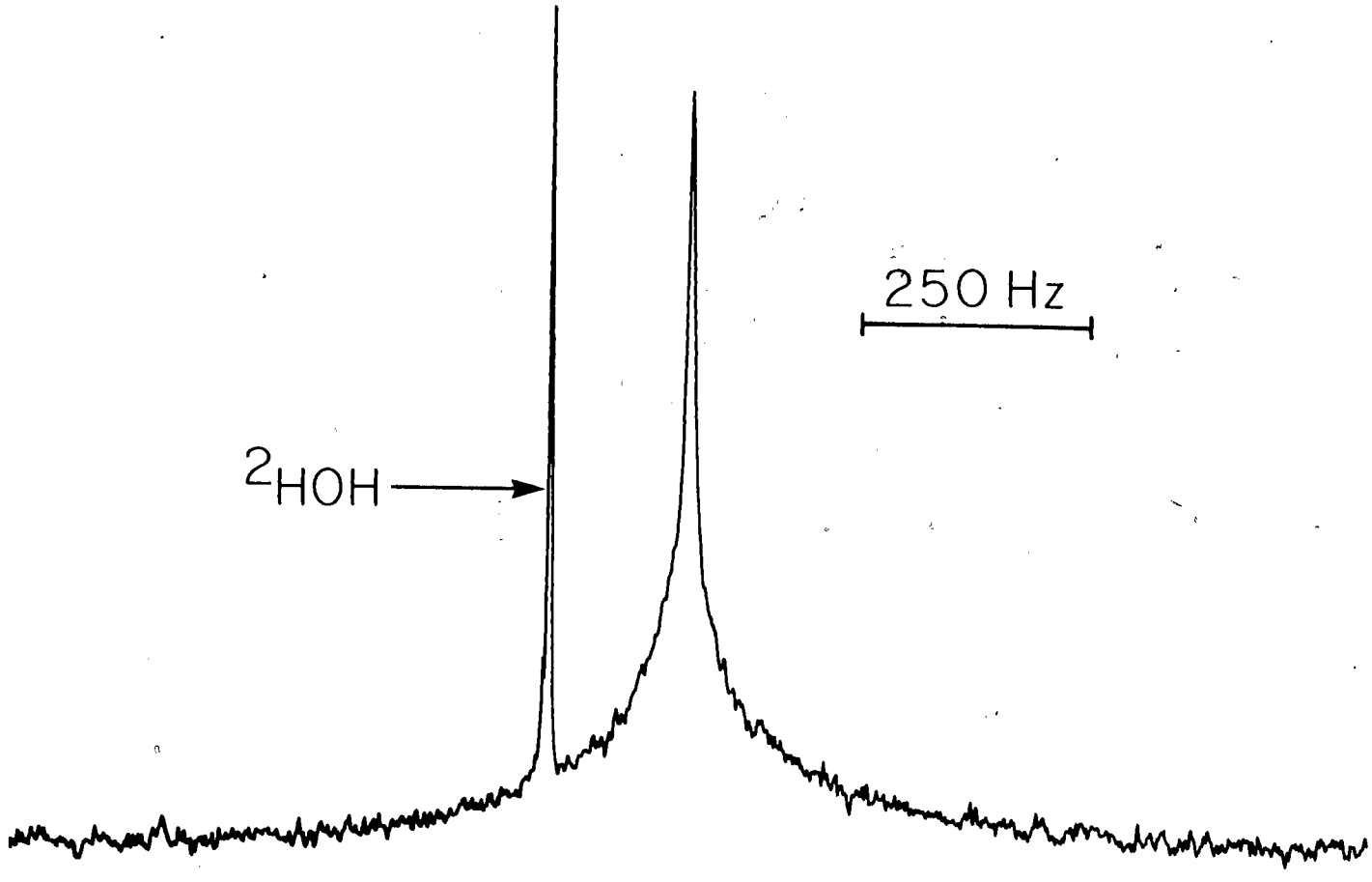
250 Hz
^{2}HOH

of different widths (see below). The information about the system that can be gathered from such an absorption is very limited; hence, we have obtained ^{2}H-NMR spectra of cholesteryl palmitate, selectively deuterated at different positions along the acyl chain, in reconstituted HDL.

Figure 10 depicts ^{2}H-NMR spectra of reconstituted HDL containing selectively deuterated cholesteryl palmitate. A single Lorentzian line gives a satisfactory fit to each of these spectra which, in addition to the absorption due to deuterated cholesteryl palmitate contains a narrow line from residual deuterium in water. Control experiments revealed that the line intensity and line width of the ^{2}H-NMR spectra of deuterated cholesteryl palmitate in reconstituted HDL are unchanged over the timespan of the NMR runs, indicating that no significant change in structure of the sample occurs over the length of the experiments (up to ~48 hours).

The reproducibility of reconstitution method was checked by preparing reconstituted HDL sample consisting of cholesteryl [16,16,16-$^2H_3$] palmitate three times. In all cases, identical line width, $\Delta\upsilon_{1/2}$ = 9 Hz (Table IV) were observed.

Table IV describes the ^{2}H NMR line width, $\Delta\upsilon_{1/2}$, profile versus chain position of selectively deuterated cholesteryl palmitate in reconstituted HDL. The value of $\Delta\upsilon_{1/2}$ in reconstituted HDL is approximately constant for deuterons chain position C2 - C6 then decreases sharply at C11 and C12 before

Figure 10: ^2H NMR spectra of cholesteryl palmitate, selectively deuterated along the acyl chain, in reconstituted HDL. A: [2-$^2H_2$]; b: [4-$^2H_2$]; c: [5,5,6,6-$^2H_4$]; d: [11,11,12,12-$^2H_4$]; e: [16-$^2H_3$]. Spectra parameters: sweep width = 5,000 Hz (a,c), 10 000 Hz (b), 2 500 Hz (d), 1 000 Hz (e); pulse length = 18 μs ($\pi/2$ pulse); number acquisitions = 300 000 (a), 100 000 (b,c), 50 000 (d), 5 700 (e); size of data set = 1 K (a,c), 1 K zero filled to 2 K (b), 2 K (d,e); delay between subsequent pulses = 0.1 s (b,c), 0.2 s (d), 1 s (e). For the spectrum in (a), a $\pi - \tau - \pi/2$ pulse sequence with τ = 0.11 s was used in order to minimize the deuterium in water with the peak from cholesteryl [2-$^2H_2$] palmitate. In this case the delay between subsequent pulses was 0.1 s. Line broadening = 20 Hz (a,c), 30 Hz (b), 10 Hz (d), 1.5 HZ (e).

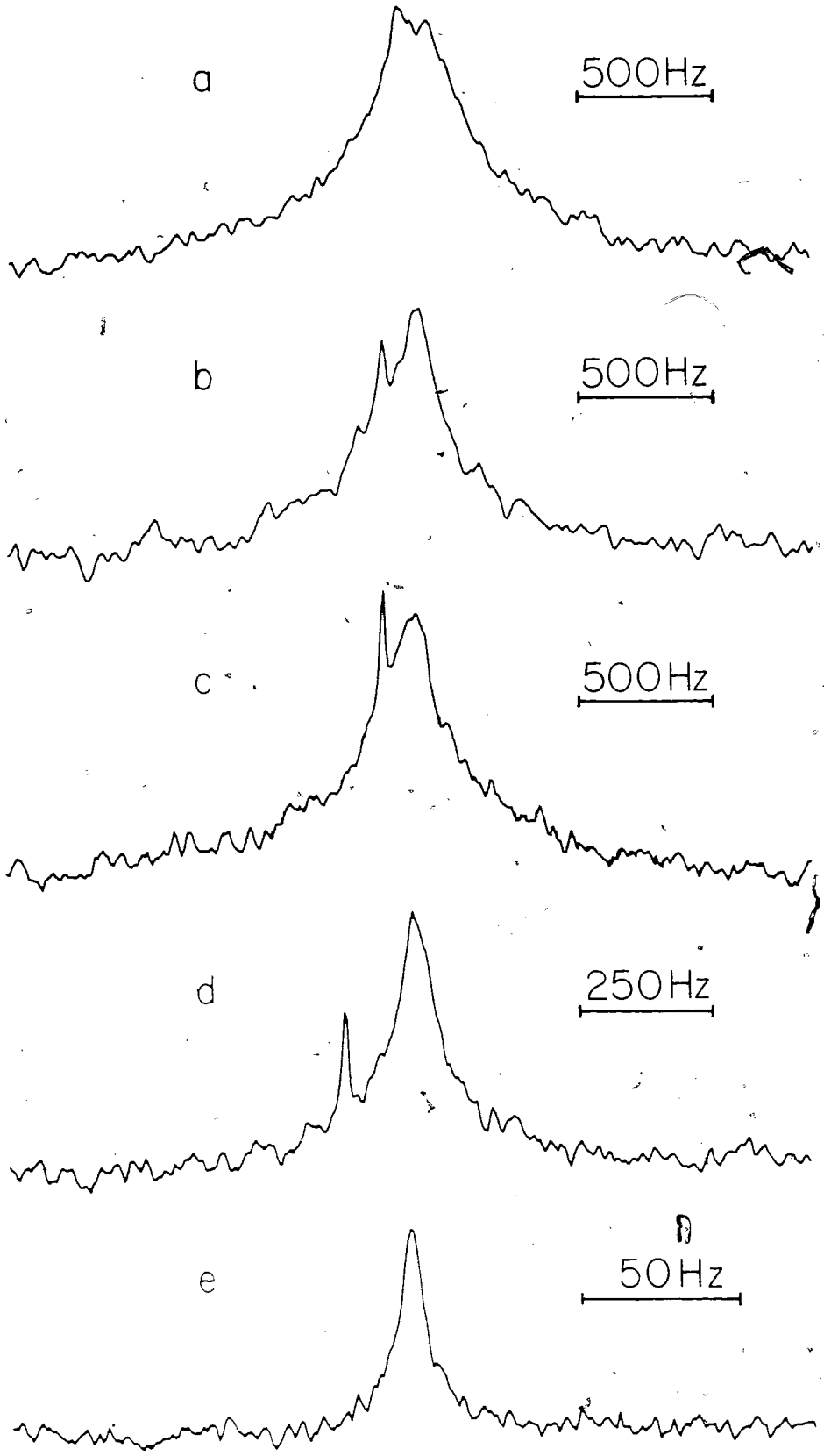
a
500Hz
b
500Hz
c
500Hz
d
250Hz
e
50Hz

reaching a minimum at C16.

Longitudinal relaxation times, T_1, measured for selectively deuterated cholesteryl palmitate in reconstituted HDL are listed in Table IV. They were obtained by a least squares fit of the data. Due to the low amplitude of the methylene signals for the ester, necessitating long periods of data collection, the T_1 values are subject to a relatively large uncertainty of $\pm$30%. On the other hand, for the narrow cholesteryl [16,16,16-$^2H_3$] palmitate resonance, the accuracy of the T_1 value is $\pm$10%.

TABLE IV ^2H NMR line widths at half height, $\Delta\upsilon_{1/2}$, and longitudinal relaxation times, T_1, at 38.8 MHz for cholesteryl palmitate, selectively deuterated along the acyl chain, in reconstituted HDL, at approximately 25°C.

Position	$\Delta\upsilon_{1/2}$(a) in Hz	T_1(b) in ms
2	430	14
4	340	12
5,6	350	17
11,12	110	14
16	9	155

(a) Uncertainty in these values is approximately ±10%.

(b) Uncertainty in these values is approximately ±30%, except for position 16 where it is approximately ±10%.

II Selectively Deuterated Palmitic Acid in Native HDL_3.

Selectively deuterated palmitic acid has been incorporated (up to ~5 mole % with respect to the phospholipid) into native HDL_3 by incubation of HDL_3 solution on solid fatty acid. The mol % incorporation of the deuterated fatty acid was monitored with the trace amount of [1-^{14}C] palmitic acid. The actual incorporation of the palmitic acid into HDL_3 was demonstrated with the use of gel-excursion chromatography. In Figure 11 we show the results of gel permeation chromatography at 4°C of HDL_3 which had been incubated with [5,5,6,6-$^2H_4$] palmitic acid containing a trace amount of [1-^{14}C] palmitic acid. The solid line is the protein as monitored by UV spectroscopy (optical density at 280 nm). The dashed line is the carbon -14 counts (85% of the total applied) which are coincident with the HDL_3 proteins. This suggests strongly that the palmitic acid is associated with the HDL_3 particles. The small peak to the right of the HDL_3 peak in Figure 11 contains ~4.5% (optical density) and ~6% (radioactivity) of the total eluted intensity. Part of the small peak intensity is no doubt due to "tailing" of HDL_3 component plus possible contamination due to serum albumin. However, assuming all of this peak is due to albumin, any fatty acid bound to so small an amount of this protein will contribute negligibly to the NMR signal. It is believed that the fatty acid is located in the surface monolayer of the lipoprotein particle on the basis of its amphiphilic nature. Earlier experiments on the ascorbate reduction of the ESR spin label 12- doxylstearic acid (131) and energy transfer experiments with fluorescent fatty acids

Figure 11: Elution profile of HDL_3 containing ~5 mol % [5,5,6,6-$^2H_4$] palmitic acid in Sepharose 4B at 4°C. Elution solvent was 0.15 M sodium chloride plus 0.02% sodium oxide and fractions were ~5.2 mL each (._____.). UV absorbance of HDL_3 apoprotein at 280 nm (x--x) [1-^{14}C] palmitic acid 56, 410 cpm). The arrow indicates the total volume.

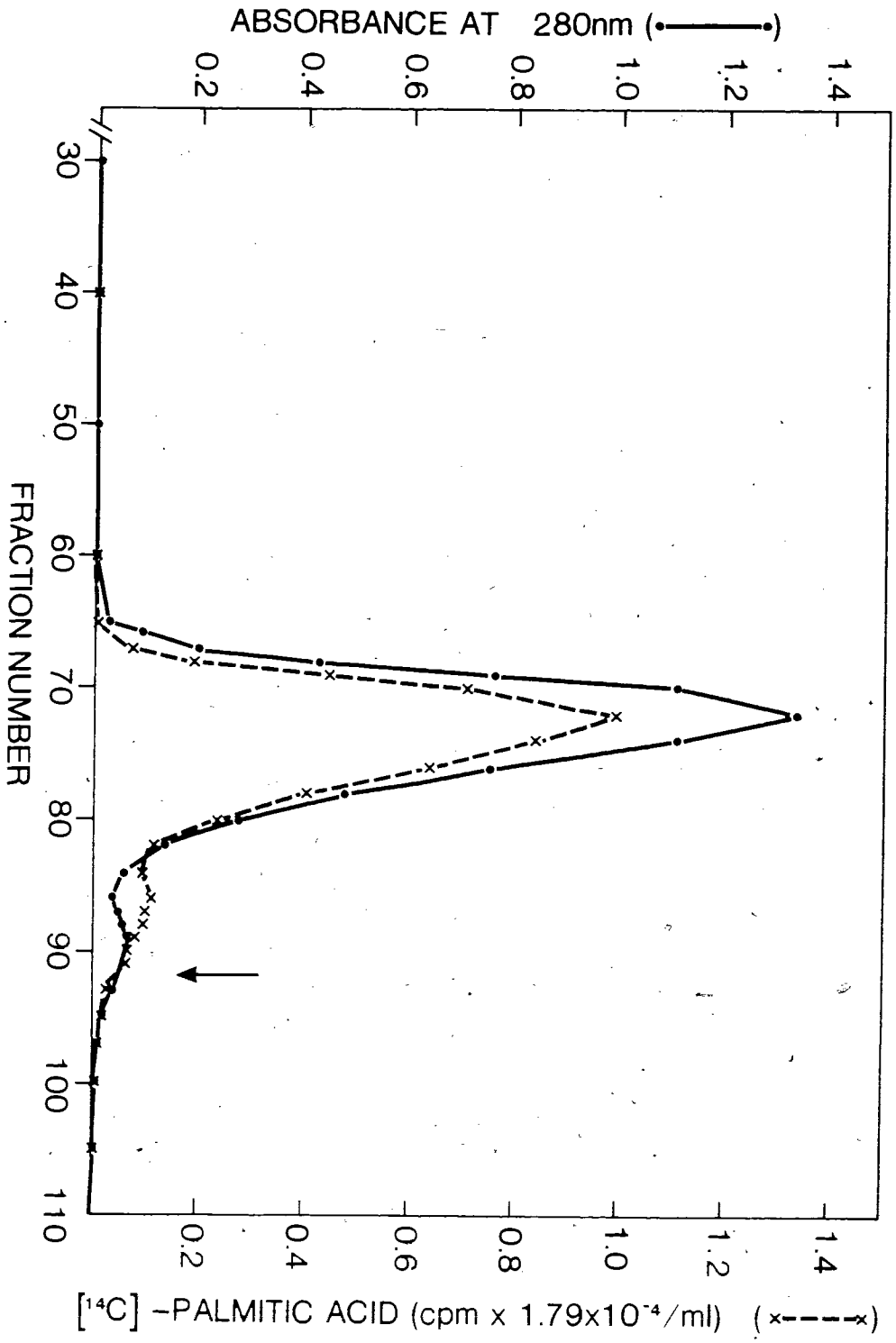
ABSORBANCE AT 280nm (•——•)
0.2
0.4
0.6
0.8
1.0
1.2
1.4
FRACTION NUMBER
30
40
50
60
70
80
90
100
110
[14C] –PALMITIC ACID (cpm x 1.79x10-4/ml) (×- - -×)

(132,133) support this conclusion.

Deuterium NMR spectra of selectively deuterated palmitic acid incorporated into HDL_3 are depicted in Figure 12. Single Lorentzian lines provide a good fit to all of these spectra. It is apparent that the widths at half height $\Delta\upsilon_{1/2}$ of the ^2H resonances in Figure 12 depend on the position of the deuteration. The line widths, $\Delta\upsilon_{1/2}$ are shown in Table V. Clearly, the line widths are highest and nearly constant between C_2 and C_6 of the acyl chain, then decrease progressively until reaching a minimum value at C_{16}. Such a behaviour is similar to that observed for deuterated fatty acids incorporated into phospholipid unilamellar vesicles (106).

Longitudinal relaxation times, T_1, at 38.8 MHz for selectively deuterated palmitic acids in HDL_3 are shown in Table VI. T_1's are short (<18 ms) for all the C^2H_2 segments, while at the terminal C^2H_3 segment a much longer T_1 of approximately 170 ms is measured. In addition, T_1's were measured at 61.4 MHz for [5,5,6,6-$^2H_4$]- and [16,16,16-$^2H_3$] palmitic acids in HDL_3. The results of the high field relaxation measurements are included in Table VI.

In order to interpret the ^2H NMR line widths of deuterated probes incorporated into small structures such as lipoproteins and unilamellar vesicles a knowledge of the size of these structures is necessary (105). Therefore, we have employed electron microscopy (negative staining method) to determine the size

Figure 12: Deuterium NMR spectra for selectively deuterated palmitic acids in HDL_3. The position of the deuterium substitution is given to the left of each spectrum. The plotted width of the top three spectra is the same. Spectral parameters: 2,2-: sweep width = 5 kHz; plot width = 4 kHz; pulse width = 19 μs (90° flip angle); number of acquisitions = 4×10^5; data points = 1,024; delay before acquisition = 50 μs; line broadening (LB) = 30 Hz. A $(180°-\tau-90°-T)_n$ sequence was used with τ = 110 ms and T = 210 ms in order to minimize interference due residual ^2HOH. The FID was left shifted one data point to remove spectral abberations due to pulse breakthrough. 4,4-: same as 2,2- except LB = 20 Hz. 5,5,6,6-: same as 2,2- except LB = 20 Hz. 11,11,12,12-: same as 2,2- except sweep width = 2.5 kHz; plot width = 2 kHz; number of acquisitions = 1×10^5; τ = 120 ms; T = 320 ms; LB = 8.0 Hz. 16,16,16-: same as 2,2- except sweep width = 500 Hz; plotted width = 200 Hz; number of acquisitions = 8×10^3; T = 2.20 s; LB = 0.5 Hz.

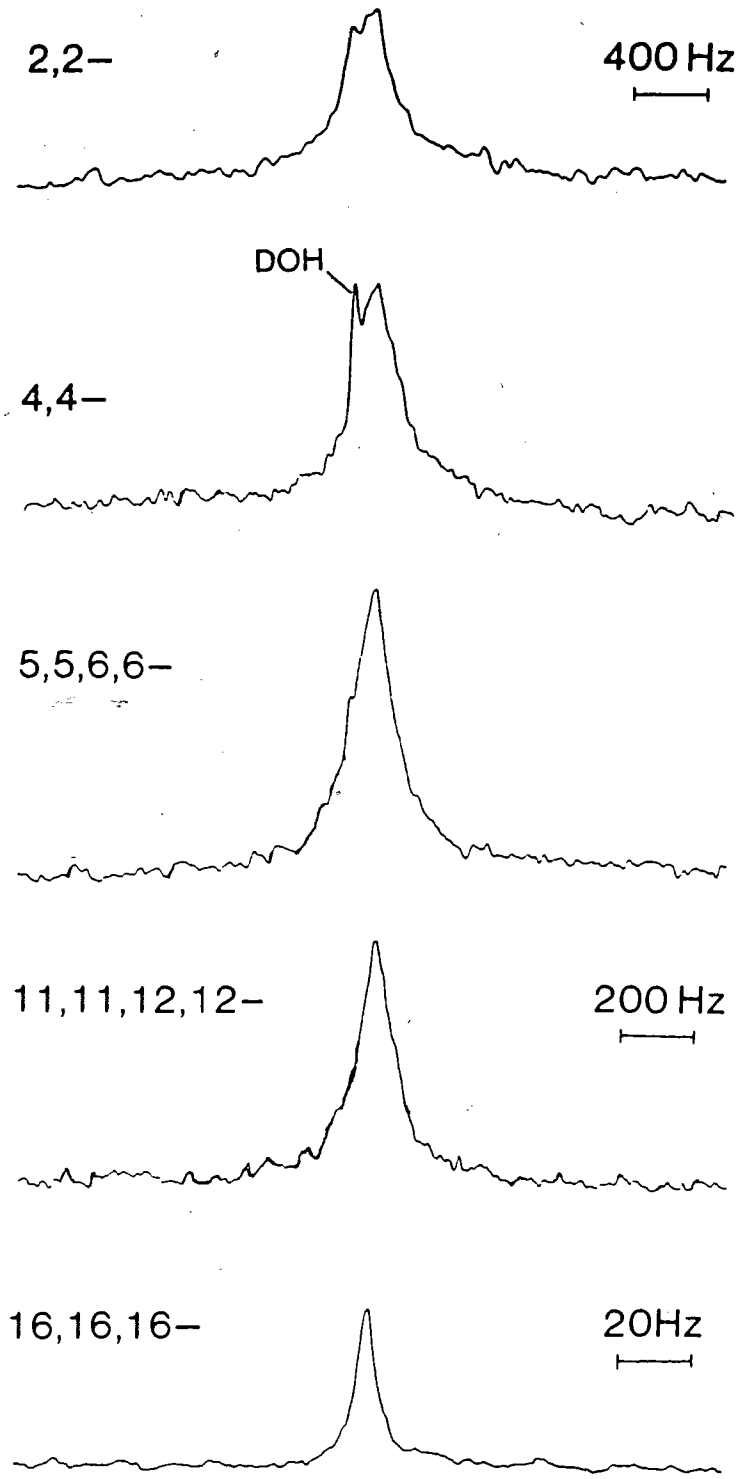
2,2–
400 Hz
DOH
4,4–
5,5,6,6–
11,11,12,12–
200 Hz
16,16,16–
20Hz

TABLE V: ^2H NMR line widths, $\Delta\upsilon_{1/2}$, for selectively deuterated palmitic acid in HDL_3 (Temperature 25-27°C).

Chain Position	$\Delta\upsilon_{1/2}$ (Hz)[a]
2-	300
4-	300
5,6-	280
11,12-	120
16-	6

[a]Uncertainty in the line widths $\Delta\upsilon_{1/2}$ is approximately $\pm$10%.

TABLE VI: Longitudinal relaxation times, T_1, for selectively deuterated palmitic acid in HDL_3 at 38.8 MHz and 61.4 MHz (Temperature 25-27°C).

Chain Position	T_1 in ms(a)	
	38.8 MHz	61.4 MHz
2	14	-
4	14	-
5,6-	16	23
11,12-	18	-
16-	170	190

(a) Uncertainty in T_1 is approximately $\pm$10%.

distribution of HDL_3 containing fatty acid probes. An example is shown in Figure 13 which is the electron microscope photograph of HDL_3 particles containing [5,5,6,6-$^2H_4$] palmitic acid. From electron micrographs of HDL_3 containing [16,16,16-$^2H_3$] palmitic acid, and HDL_3 containing [5,5,6,6-$^2H_4$] palmitic acid, mean diameter of 7.4 $\pm$ 1.2 nm and 7.5 $\pm$ 1.4 nm, respectively, were measured. Native HDL_3 yielded mean diameters of 7.7 $\pm$ 1.2 nm, hence incorporation of fatty acid does not appreciably change of the HDL particle. In each case, approximately 200 particles were counted and the results are in agreement with the previously published work (17,18).

^{31}P NMR spectra of HDL_3 containing palmitic acid are indistinguishable from those of native HDL_3, further indicating no significant change in either size, nor head group conformation occurs upon the incorporation of ~5 mol % palmitic acid into native HDL_3.

III Selectively Deuterated Palmitic Acid in Native HDL_2

Figure 14 depicts ^2H NMR spectra of ~5 mol % selectively deuterated palmitic acid incorporated into native HDL_2. In addition to the signal from the deuterated palmitic acid, the spectra sometimes contain a narrow resonance (~135 Hz downfield) due to the residual deuterium in water. Single Lorentzians provide good fits to the spectra. The line widths obtained from these spectra are presented in Table VII. It is apparent that the widths at half height are dependent upon the position of

Fig. 13 Electron micrograph of native HDL_3 containing 5,5,6,6-[$^2H_4$] palmitic acid. Magnification 190,700 times.

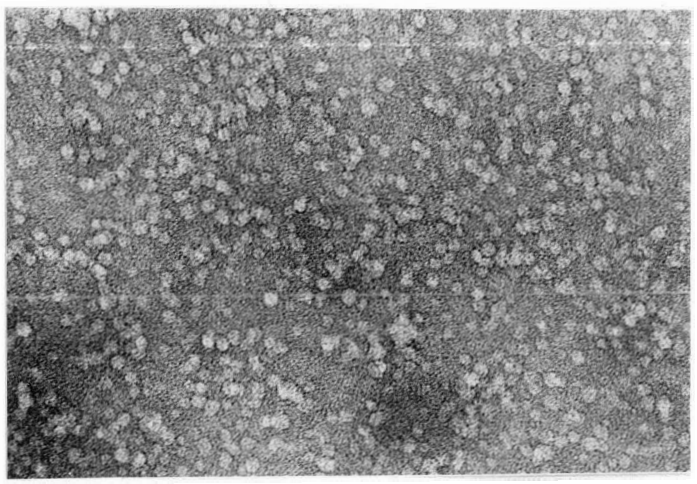

Figure 14: ^2H NMR spectra of native HDL_2 containing ~5 mol % selectively deuterated palmitic acid at ambient temperatures (20-25°C). The position of deuteration is given to the left of each spectra. The resonance shifted approximately 135 Hz downfield from the main peaks is due to residual deuterium in water. Spectral parameters: 2,2 position; sweep width = 5,000 Hz; data size = 2048 points delay before data acquisition = 50 μs; delay between subsequent pulses = 205 ms; number of acquisitions = 1.95 x 10^5; line broadening = 30 Hz. A 180° - τ -90° pulse sequence with pulse length = 18 μs (for 90° flip angle and τ = 0.12 s was used to minimize residual deuterium in water. 4,4 position same as 2,2 except NA = 1.80 x 10^5; 5,5,6,6 position; same as 2,2 except data size 1 K zero filled to 4 K; number of acquisitions = 2.0 x 10^5; line broadening = 40 Hz; delay between subsequent pulses = 0.10 s; the τ in 180°τ-90° pulse sequence was 0.1 s. The FID was left shifted 1 point to reduce the spectral abberations. 11,11,12,12 position; sweep width = 2500 Hz; delay before acquisition = 250 s; delay between subsequent pulses = 0.41 s; number of acquisition = 8.0 x 10^4; line broadening = 25 Hz. A 180°- τ -90° pulse sequence with pulse length = 16 μs (90° flip angle) and τ = 0.15 s was used; 16,16,16 position; the spectra was obtained with a one pulse experiment; pulse length = 18 s for 90° flip angle; number of acquisitions = 1.0 x 10^4; delay before data acquisition =250 μs; delay between pulses = 1.02 s; data size 2 K zero filled to 4 K; line broadening = 1.0 Hz.

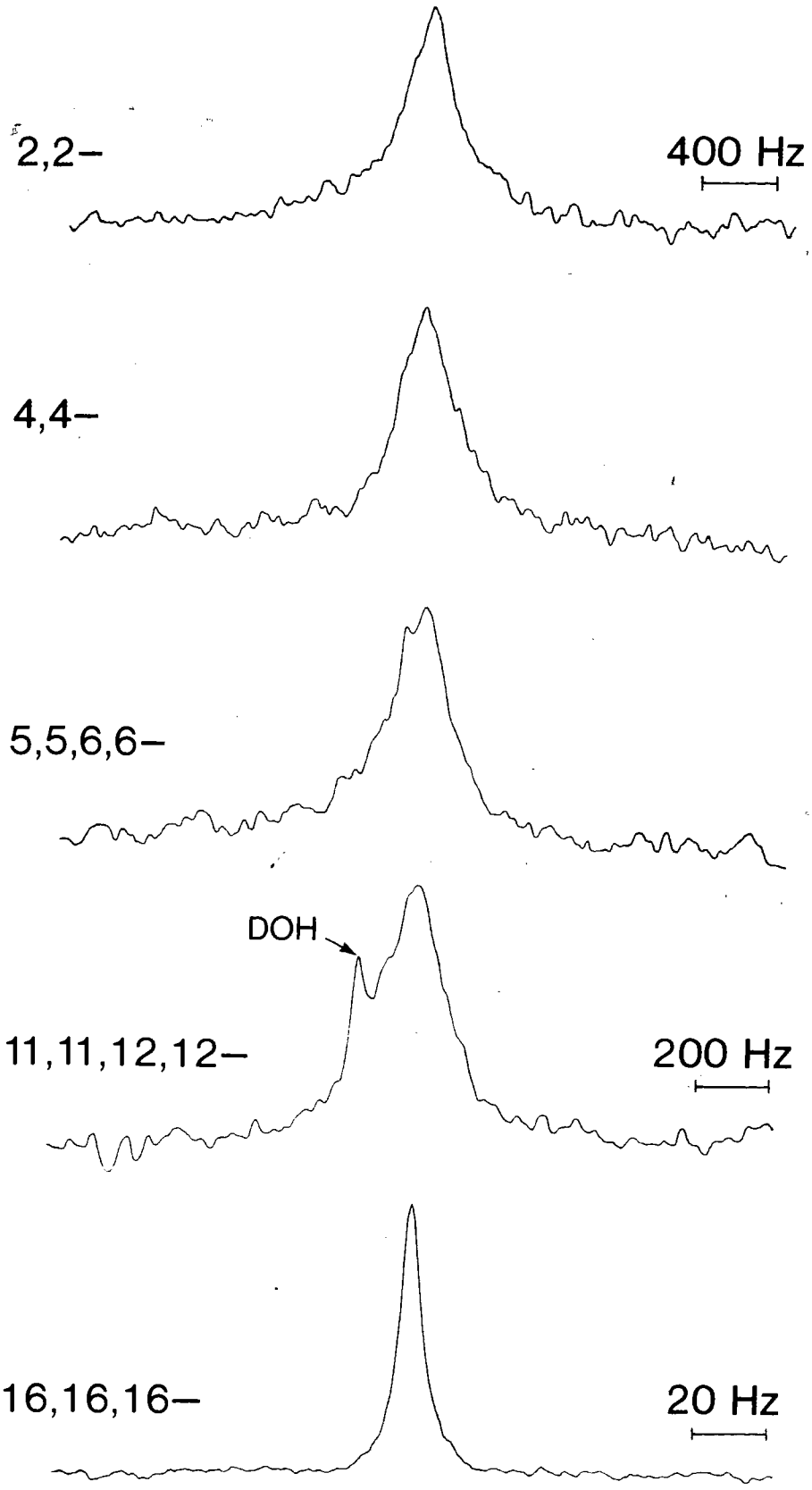
2,2–
400 Hz
4,4–
5,5,6,6–
DOH
11,11,12,12–
200 Hz
16,16,16–
20 Hz

TABLE VII: ^2H longitudinal relaxation times and line widths for selectively deuterated palmitic acid in HDL_2 (20-25°C).

Chain Position	T_1 (ms)[a]	$\Delta\nu_{1/2}$ (Hz)[b]
2-	15	340
4-	13	405
5(6)-	15	395
11(12)-	21	240
16-	194	7

(a) Uncertainty in these values is ±20% except for the 16 position, where it is approximately ±10%.

(b) Uncertainty in these values is approximately ±10%.

selective deuteration. A constant plateau is observed from C_2 - C_6 which progressively decreases until reaching a minimum value at the terminal methyl.

The longitudinal relaxation times, T_1, of selectively deuterated palmitic acid in HDL_2 measured at 38.8 MHz are shown in Table VII. These relaxation times are short (<21 ms) for all of the C^2H_2 segments studied, while at the terminal C^2H_3 segment a much longer T_1 of approximately 194 ms is obtained. Due to the low amplitude of the broad methylene signals, necessitating long periods of data collection, the T_1 values are subject to a relatively large uncertainty of $\pm$20%. On the other hand, for the narrow terminal methyl, the uncertainty of the T_1 value is only $\pm$10%. Control experiments revealed that the native HDL_2 was not as stable as native HDL_3 at ambient temperatures (25°C-27°C). In some cases, there was a loss of signal intensity over the time-span of the NMR experiment (~36 hours). Visual inspection of the sample revealed white flocculent precipitate. The reason(s) for this are not known. However, it was found that spinning of the HDL_2 sample during the NMR run facilitated the precipitation.

In order to interpret the ^2H NMR as with the HDL_3 particles, it is essential to know the particle size of HDL_2. We have attempted to know the particle size of HDL_2. We have attempted several times to size the HDL_2 particles by negative staining method but were unsuccessful. The images showed the HDL_2 particles to be severely aggregated. In order to disperse the particles, the following conditions were employed: (a) the pH

of the HDL_2 solution was varied from pH 4.0 to pH 12.0, (b) HDL_2 solution was mildly sonicated, (c) the concentration of salt in HDL_2 solution was varied from 0.15 M NaCl and 2.0 M NaCl. In all cases good spreading of the stain was not observed. We have also used 2% sodium phosphotungstate pH 7.0 instead of 2% ammonium molybdate pH 8.0. Even under this condition, individual particles imbedded in the stain such as those observed for HDL_3 and phospholipid vesicles (see below) were never observed. Attempts to size HDL_2 by the sedimentation velocity method were also unsuccessful as non-Gaussian Schlieren patterns with broad wings were observed. This is expected since there are two molecular weight species having similar size but different protein content per particle are present in the density range of 1.063-1.125 g/mL (134). We have therefore used the literature value of 100Å as the diameter of native HDL_2 particle in our calculation.

Since ^{31}P NMR is sensitive to both the size of the particles in solution and the conformation of the phospholipid head group, it was employed to monitor the changes induced in the HDL_2 structure by the added fatty acid. Figure 15 shows the ^1H decoupled spectrum of native HDL_2 containing ~4 mol % [$^2H_{31}$] palmitic acid. The spectrum obtained is similar to the previously published spectra of native HDL_2 (162). The spectrum shows a strong resonance at -0.8±1 ppm due to phosphatidylcholine, while the downfield resonance at -0.2±1 ppm is assigned to sphingomyelin. The line widths of both the phosphatidylcholine and sphingomyelin resonances are identical 6±1 Hz and are similar to the native

Figure 15: ^{1}H decoupled ^{31}P NMR spectra of native HDL_2 containing 4 mol % [$^{2}H_{31}$] palmitic acid. Spectral parameters: sweep width = 2 kHz; data size = 2 K zero filled to 4 K; line broadening = 1 Hz; number of acquisition = 1024. Chemical shifts are with respect to an external H_3PO_4 (85%) reference. Resonance frequency = 40.5 MHz.

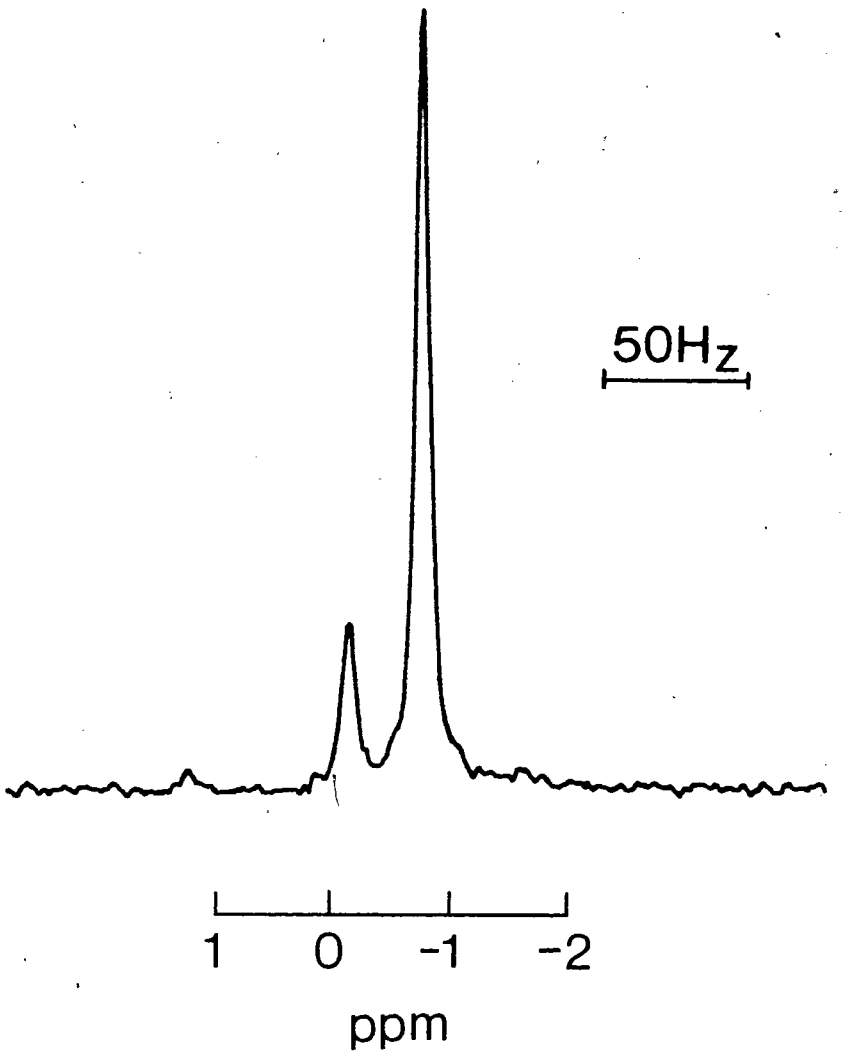
50Hz
1
0
-1
-2
ppm

HDL_2 without fatty acid. This indicates that neither the size of the lipoprotein particle nor the conformation of the phospholipid head group are appreciably altered by the addition of fatty acid. The association of deuterated palmitic acid with HDL_2 was established by Sepharose 4B gel permeation chromatography. In Figure 16 we show the results of gel exclusion chromatography at 4°C of HDL_2 which had been incubated with [$^2H_{31}$] palmitic acid containing a trace amount of 1-[^{14}C] palmitic acid. The HDL_2 solution was eluted from the Sepharose 4B column with a solution of 0.15 M NaCl plus 0.02% sodium azide pH 7.6. Approximately 78% of the carbon -14 counts in the original solution were eluted and all are found coincident with the O.D. 280 nm peak as monitored by UV spectroscopy. In addition to the main peak due to HDL_2, the figure also contains a smaller peak close to the total volume of the column. It comprises less than 4% of the main peaks. The origin of the small peak is not known. It could be due to the displaced apoprotein from HDL_2. But more probably it may be contamination due to serum albumin. Such a peak is also observed in HDL_3 sample (see above).

We assume that the fatty acid is located in the surface monolayer of HDL_2 on the basis of its amphiphilic nature. Earlier experiments on the ascorbate reduction of the ESR spin label 12-doxylstearic acid (135) and energy transfer experiments with fluorescent fatty acids (136,137) support this conclusion.

Figure 16: Elution profile of HDL_2 containing ~4 mol % [$^2H_{31}$] palmitic acid on Sepharose 4B column at 4°C. Elution solvent was 0.15 M NaCl plus 0.02% sodium azide; (•–•) absorbance of HDL_2 apoproteins at 280 nm, (o–o) 1-[^{14}C] palmitic acid. The volume of each faction was 8.0 ml. The arrow indicates the total volume of the column.

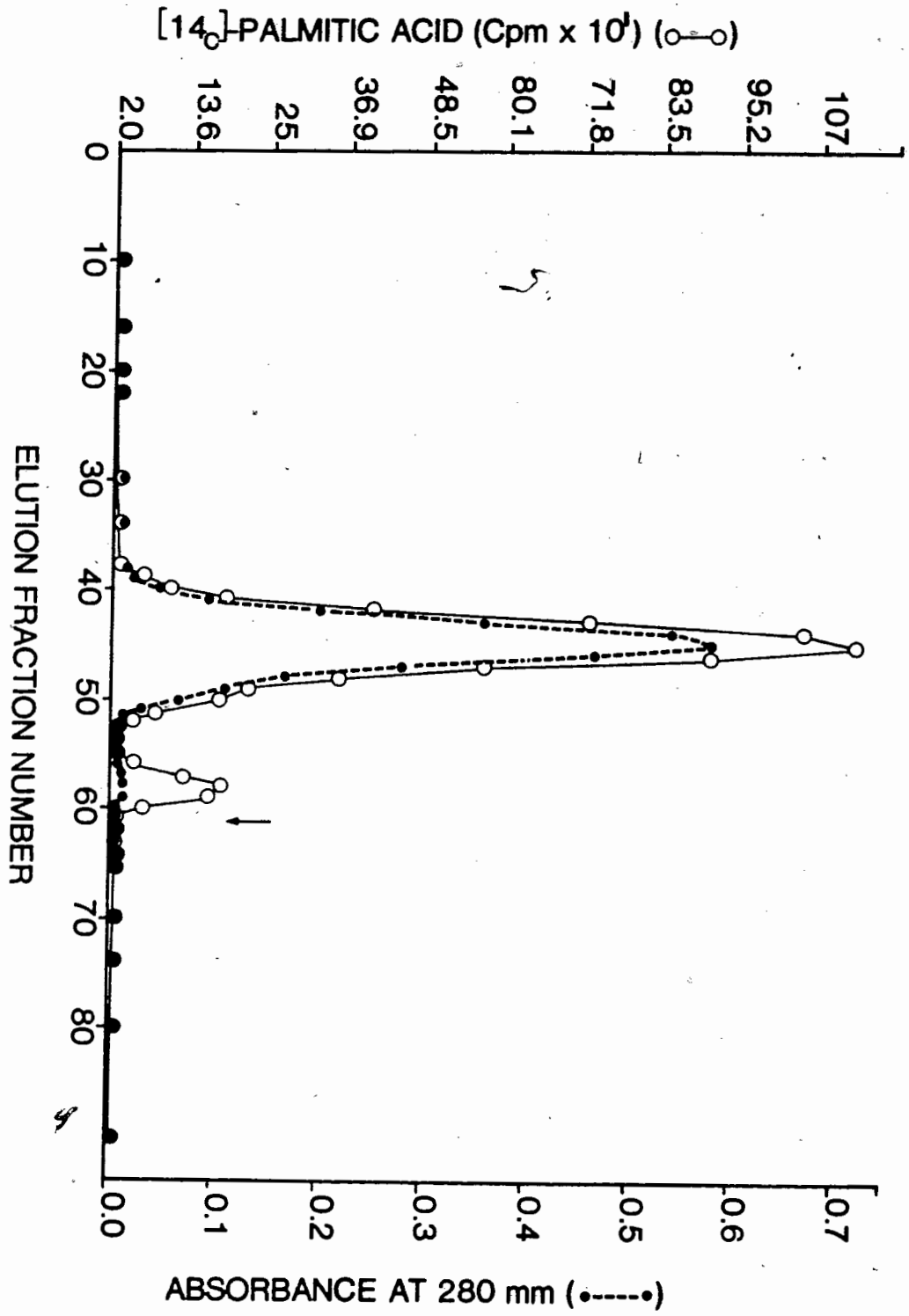
[14C]-PALMITIC ACID (Cpm x 10³) (o—o)
2.0
13.6
25
36.9
48.5
80.1
71.8
83.5
95.2
107
0
10
20
30
40
50
60
70
80
ELUTION FRACTION NUMBER
0.0
0.1
0.2
0.3
0.4
0.5
0.6
0.7
ABSORBANCE AT 280 mm (•-----•)

IV Selectively Deuterated Palmitic Acid in Unilamellar Vesicles

We have studied selectively deuterated palmitic acid in unilamellar vesicles. Unilamellar vesicles were made from egg phosphatidylcholine/sphingomyelin/selectively deuterated palmitic acid 80/14/6 mol % in deuterium depleted water. The mixed sphingomyelin/egg phosphatidylcholine system was chosen since this is the composition of phospholipids found in the outer monolayer of HDL (47, 130).

Deuterium NMR spectra of selectively deuterated palmitic acids in unilamellar vesicles are depicted in Figure 17. Single Lorentzians do not provide an excellent fit to the spectra obtained for the [2,2-$^2H_2$], [4,4-$^2H_2$]-, and [5,5,6,6-$^2H_4$] acids. Instead, the spectra appears to be a super-position of Lorentzian lines with "broad skirts" approximately $\pm$2 kHz wide. Whereas, a single Lorentzian does provide a satisfactory fit to the spectra obtained for [11,11,12,12-$^2H_4$]- and [16,16,16-$^2H_3$] acids. It is apparent that the widths at half-height, $\Delta\upsilon_{1/2}$, of the ^2H NMR resonances in Figure 17 depend upon the position of selective deuteration, the values measured are shown in Table VIII. Strictly speaking, it is not correct to use $\Delta\upsilon_{1/2}$ as a parameter of the resonance curve which cannot be described by a single Lorentzian. We have measured the line widths for qualitative purposes only.

As vesicles are heterogeneous with respect to size, it is imperative that their size distribution be determined. We have

Figure 17: Deuterium NMR spectra of (~5 mol %) selectively deuterated palmitic acids in 15% w/v egg phosphatidylcholine/bovine brain sphingomyelin (85:15) w/w unilamellar vesicles in deuterium depleted water. The position of deuterium substitution is given to the left of each spectrum. Spectral parameter: 2,2-: sweep width = 50,000 Hz; pulse width = 8 μs (90° flip angle); number of acquisitions = 50,000; data size = 8192; delay before acquisition = 10 μs; delay between subsequent pulses = 290 ms; line broadening = 20 Hz. 4,4-: same as 2,2-. 5,5,6,6-: same as 2,2- except number of acquisitions = 30,000. 11,11,12,12-: same as 2,2-. 16,16,16-: sweep width = 1 kHz; number of acquisitions: 5,000; data size = 2048; delay before data acquisition = 50 μs; delay between subsequent pulses = 500 ms; line broadening = 1.0 Hz.

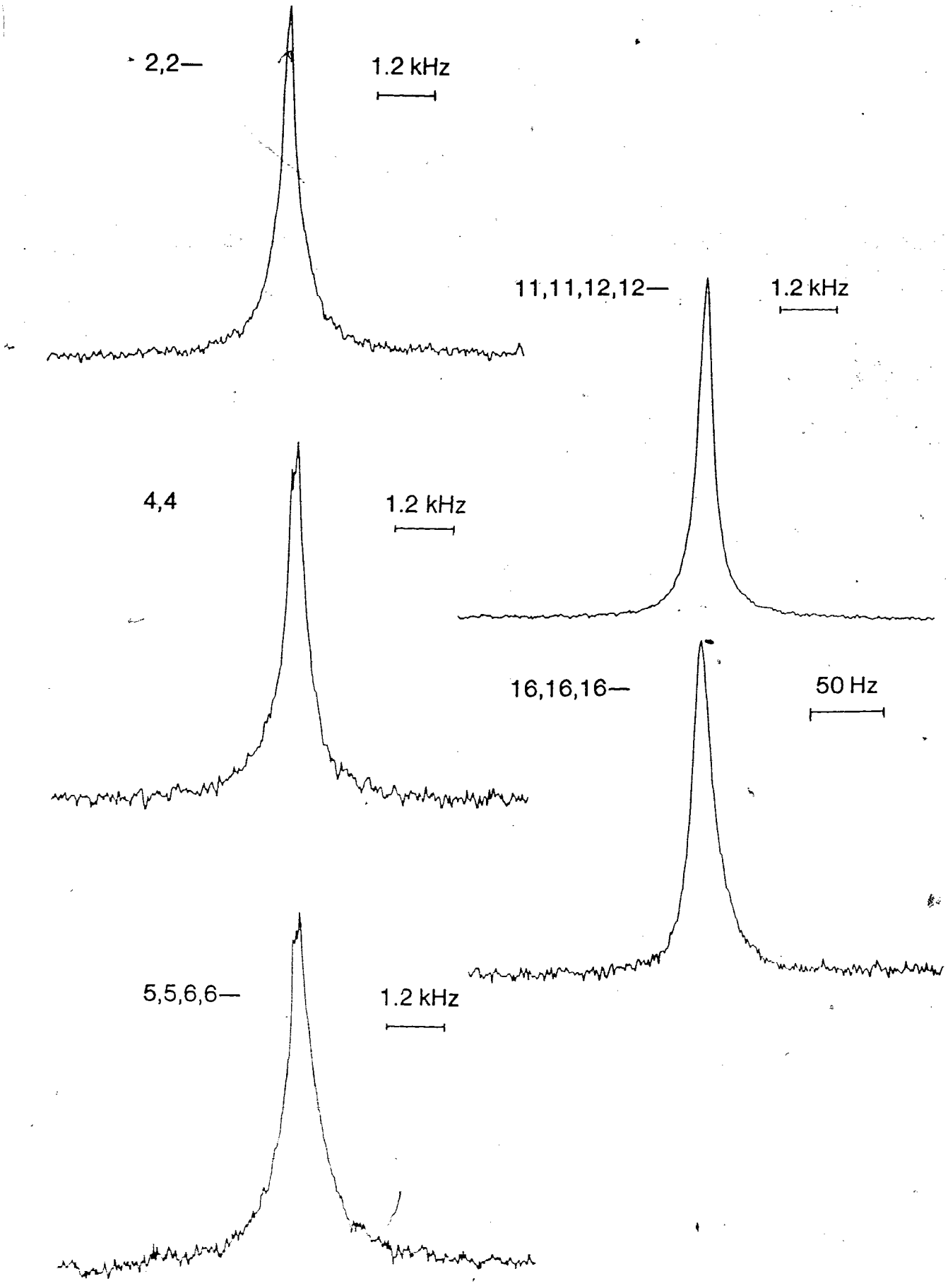
2,2—
1.2 kHz
11,11,12,12—
1.2 kHz
4,4
1.2 kHz
16,16,16—
50 Hz
5,5,6,6—
1.2 kHz

TABLE VIII: ^2H NMR line widths, $\Delta\upsilon_{1/2}$, of ~5 mol % selectively deuterated palmitic acid in unilamellar vesicles at 25°C.

Chain Position	Line Width (Hz)[1]
2-	386
4-	446
5,6-	612
11,12-	365
16-	15

[1]The uncertainty in these values is ±10%.

electron micrographs of unilamellar vesicles using the negative staining method. An example is shown in Figure 18, which is the micrograph of unilamellar vesicles containing [11,11,12,12-$^2H_4$] palmitic acid. The photograph shows a majority (>90%) of the vesicles are approximately spherical, although other shapes (flat discs) are also in the micrograph.

Vesicles having diameters <200 Å to >600 Å were found in the samples prepared in this study. The size distribution of vesicles containing [2,2-$^2H_2$]- and [11,11,12,12-$^2H_4$] palmitic acid were determined separately. Approximately 75% of the vesicles in the sample containing [2,2-$^2H_2$] palmitic acid and 80% of vesicles containing [11,11,12,12-$^2H_4$] palmitic acid were in the size range 215 Å - 345 Å. We have pooled the results from the two samples to reflect the size heterogeneity in all of the samples in our study. Vesicle diameters were divided into six size categories, each fraction having 40 Å range (Figure 19).

An important question which must be answered is whether palmitic acid actually incorporates into the unilamellar vesicles. In Figure 20 we show the results of gel permeation chromatrography at 4°C of vesicles containing [5,5,6,6-$^2H_4$] palmitic acid and a trace amount of [1-^{14}C]. palmitic id. All of the radioactivity (92.5% of the initial counts) was eluted coincident with the OD 300 nm peaks. No other radioctivity peakwas subsequently eluted, indicating the absence of smaller structures.

Fig. 18 Electron micrograph of egg phosphatidylcholine / sphingomyelin vesicles containing 11,11,12,12-$[^2H_4]$ palmitic acid. Magnification 170,700 times.

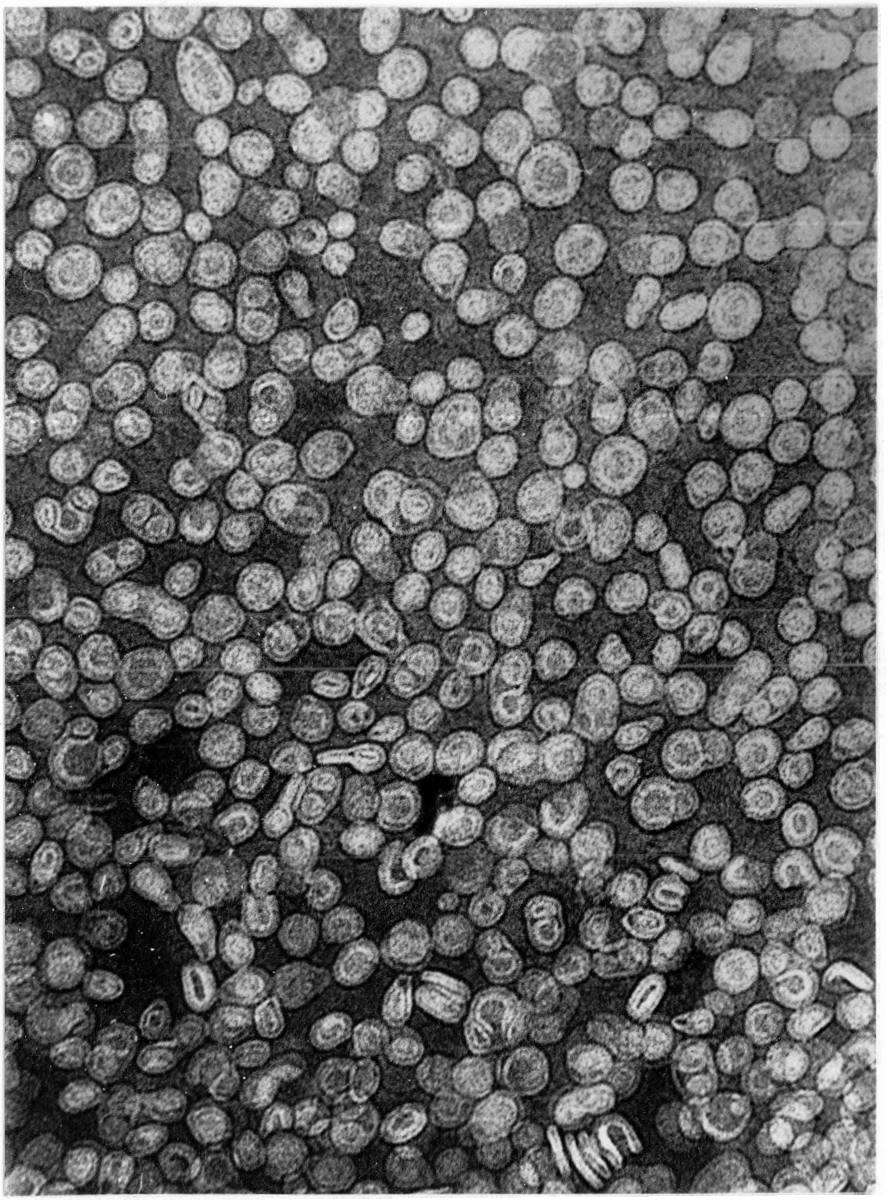

Figure 19: Histogram of unilamellar vesicle sizes containing selectively deuterated palmitic acid.

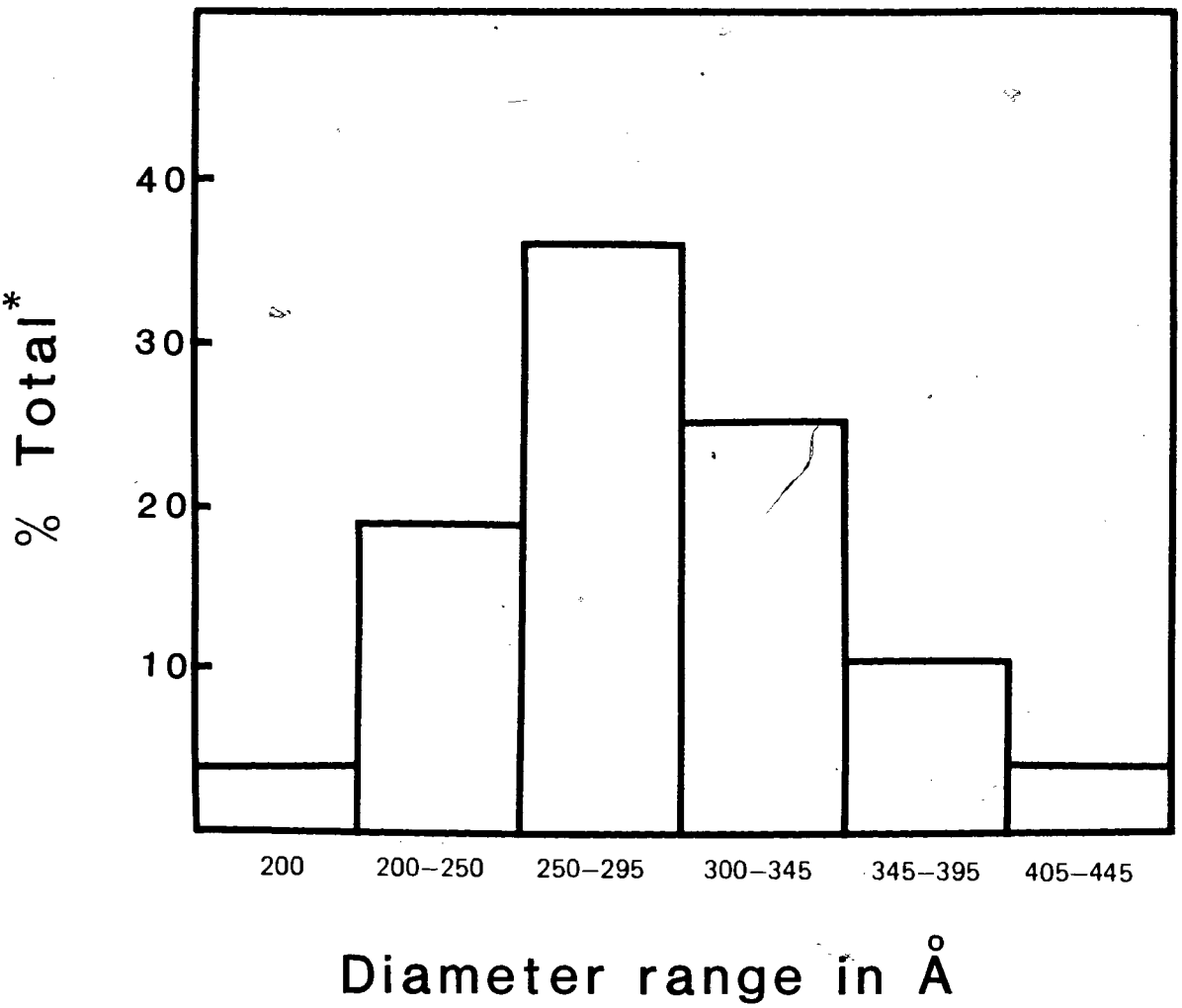

*Total of 1346 vesicles were measured.

Figure 20: Elution profile of unilamellar vesicles containing 5 mol % 5,5,6,6-[$^{2}H^{4}$] palmitic acid on Sepharose 4B at 4°C. Elution solvent was 0.15 M NaCl plus 0.02% sodium azide; (●—●) is the optical density at 300 nm, (o–o) 1-[^{14}C] palmitic acid. The volume of each fraction is 5.2 mLs. The column dimensions are given in the Materials and Methods section.

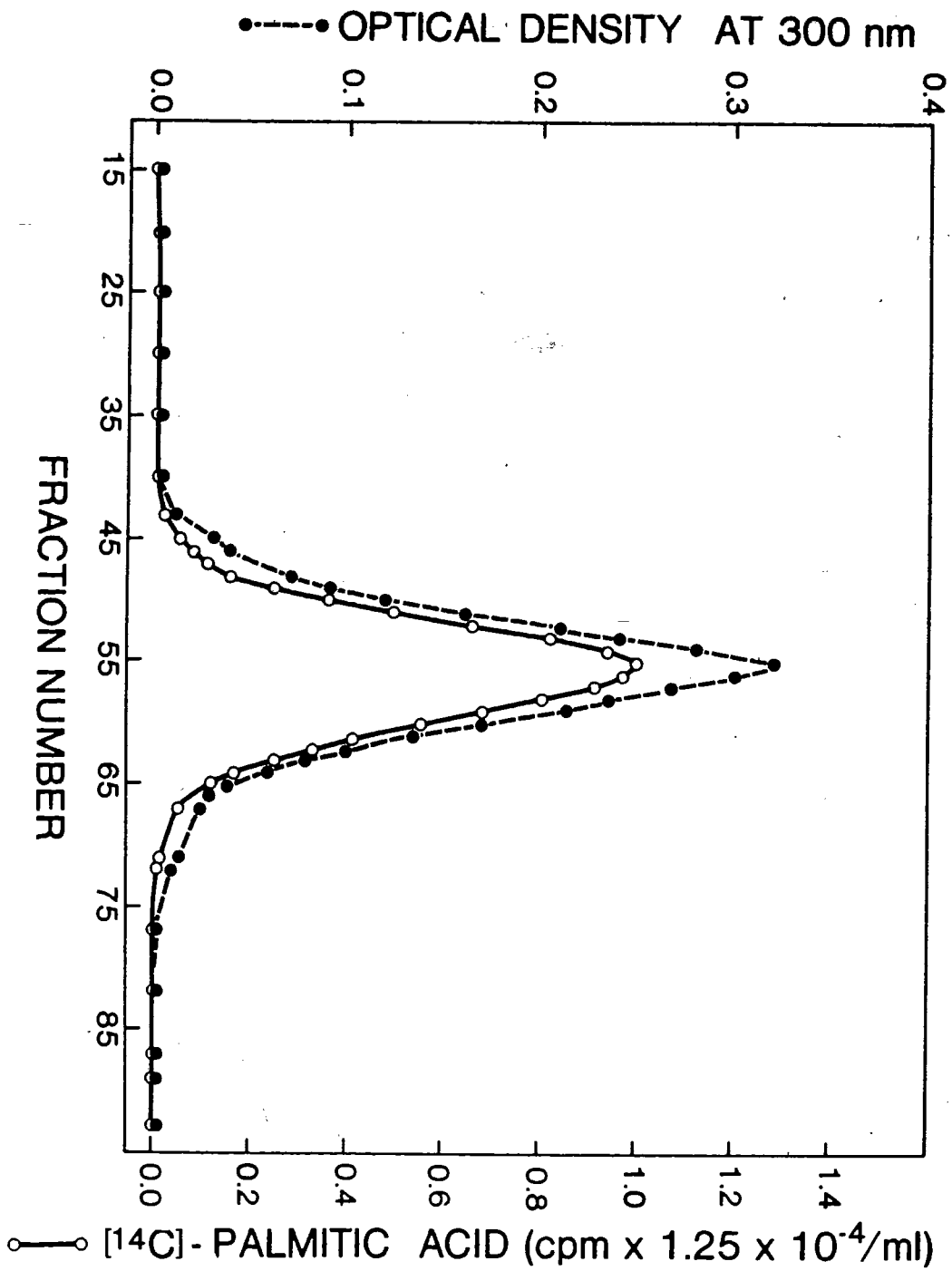
OPTICAL DENSITY AT 300 nm
0.0
0.1
0.2
0.3
0.4
FRACTION NUMBER
15
25
35
45
55
65
75
85
0.0
0.2
0.4
0.6
0.8
1.0
1.2
1.4
[14C] - PALMITIC ACID (cpm x 1.25 x 10-4/ml)

V Phospholipid in Native HDL_2

We have incorporated 5 ~mole % of selectively deuterated phosphatidylcholine into native HDL_2 particles by mild sonication at 40°C. Figure 21 shows an undecoupled phosphorus -31 NMR of HDL_2 containing PC-d3 as well as that of native HDL_2. It consists of a strong resonance due to phosphatidylcholine and a weaker resonance shifted ~69 Hz downfield due to sphingomyelin. The width at half height, $\Delta\upsilon 1/2 = 32 \pm 3$ Hz for native HDL_2 compares with $\Delta\upsilon 1/2 = 31 \pm 3$ Hz in the case of HDL_2/PC-d3. Thus, it appears that the size of HDL_2 particle is not significantly altered with addition of ~5 mole % phosphatidylcholine.

To discount the possible existence of unilamellar phospholipid vesicles in the HDL_2/PC sample, the solution density was adjusted to 1.06 gm/ml. The sample was centrifuged for 6 hours. The unilamellar vesicles have a hydrated density = 1.02 gm/ml compared with 1.09 gm/ml for HDL_2, Table I (85,86). Therefore, vesicles are expected to float to the top of the tube and HDL_2 to the bottom. The spectra obtained for the bottom half of the sample containing 4,4.PC-d_2 in HDL_2 had ~94% of the original signal intensity. The line width at half-height at 25°C ± 1°C, $\Delta\upsilon 1/2 = 310$ Hz compared with the original unspun sample whose $\Delta\upsilon 1/2 = 320$ Hz at 25°C ± 1°C. Hence we conclude that approximately 94% of the added phospholipid is in association with HDL_2.

Figure 21: An (undecoupled) ^{1}P NMR (102.2 MHz) spectra of native HDL_2 and of HDL_2 containing ~5 mol % 16-[2H3] phosphatidylcholine.

Spectral parameters: pulse length = 16 μs (~60° flip angle); data size = 2048 points; delay before acquisition = 250 μs; delay between subsequent pulses = 1.51 s; sweep width = 2000 Hz; line broadening = 2.0 Hz; number of acquisitions = 35,329 (native HDL_2) and 7,140 (HDL_2 + PC-d_3).

NATIVE HDL_2

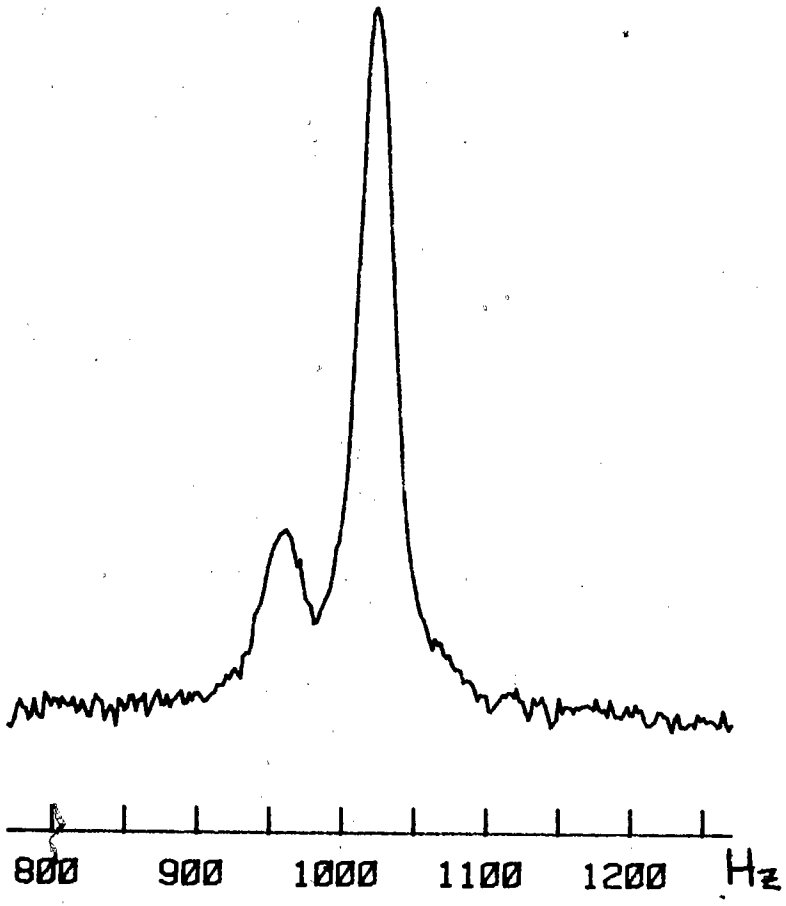

NATIVE HDL_2 + 5 MOLE% PC-D3

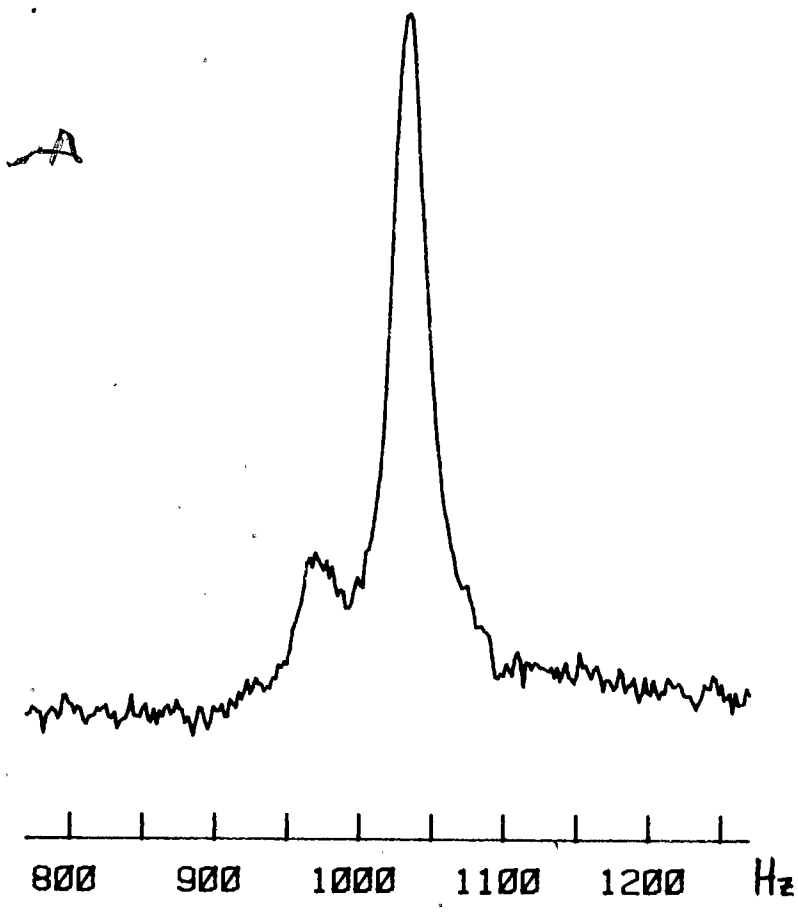

Figures 22a-c depict ^2H NMR spectra of selectively deuterated phosphatidylcholine in HDL_2 as a function of temperature. In addition to absorption to the deuterated phospholipid in HDL_2, the spectra also contain signal due to residual deuterium in water. This is minimized for the positions [2,2]; [4,4]; [7,7]; and [11,11,12,12] by an inversion recovery method when appropriate values for τ are used to obtain the M_∞ value (see spectral parameters). However, for the 16,16,16 position, ^2HOH absorption is pronounced.

A single Lorentzian gives a satisfactory fit to each of these spectra. Control experiments revealed that the intensity of the signal and the line width at half height for the HDL_2/PC sample remains unchanged over the time span of the NMR run (up to 36 hours). Hence no significant changes in structure of the sample occur over the length of the experiment.

The line widths for selectively deuterated phosphatidylcholine in HDL_2 as a function of temperature are presented in Table IX. The values 470-420 Hz of line widths, $\Delta\nu 1/2$, are approximately constant for C4 to C7 positions, then decrease sharply at C11 and C12 before reaching a minimum at C16. The line widths for the [2, 2-^2H_2] position of the <u>sn</u>-2 chain of phosphatidylcholine in HDL_2 are noticeably higher at all temperatures than [4,4-^2H_2] and [7,7^2H_2] position. This contrasts with the results obtained for the same probe in egg-phosphatidylcholine multilamellar liposomes and unilamellar vesicles (see Section R.VIII, pp.142-149).

Figure 22a: Deuterium NMR spectra of selectively deuterated phosphatidylcholine in native HDL_2 as a function of temperature. The deuterated position is given at the top of the page and the temperature at which spectra were taken is in the centre of the page.

Spectral parameters for 2,2-: sweep width = 5000 Hz a (180° -τ -90°-T) pulse sequence was used to obtain these spectra. τ = 0.10 s (15°C); τ = 0.125 (25°); τ = 0.16 s (40°C). T = 0.1 s (15°C and 25°C); T = 0.16 s (40°C); data size = 1024; delay before acquisition = 50 μs; line broadening = 30 Hz (15°C and 25°C); line broadening = 25 Hz (40°C); number of acquisitions = 1.12 x 10^5 (15°C); 7.5 x 10^4 (25°C); 7.92 x 10^4 (40°C). All spectra were left shifted 1 point to reduce the baseline abberations; pulse length = 6.5 μs (90° flip angle). Spectra parameters for 4,4-: same as 2,2- except τ = 0.11 s; and T = 0.1 s for all temperatures; line broadening = 20 Hz (15°C and 25°C) and 25 HZ (40°C); number of acquisitions = 1.2 x 10^5 (15°C and 25°C) and 6.0 x 10^4 (40°C). The spectra for 15°C was left shifted 2 points.

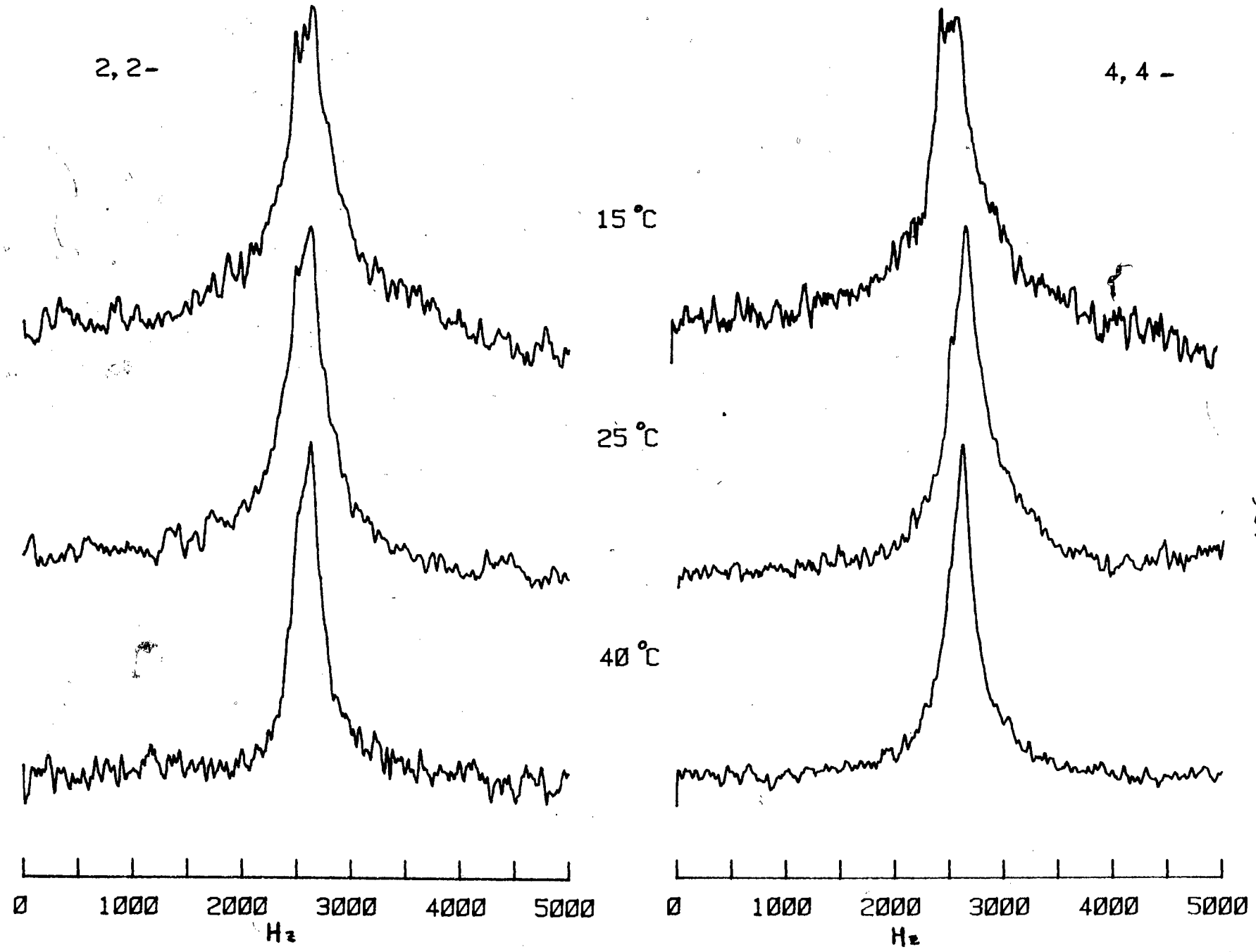
2, 2-
4, 4 -
15 °C
25 °C
40 °C
0
1000
2000
3000
4000
5000
Hz
0
1000
2000
3000
4000
5000
Hz

Figure 22b: Deuterium NMR spectra of selectively deuterated phosphatidylcholine in native HDL_2 as a function of temperature. The deuterated position is given at the top of the page and the temperature at which spectra were taken is in the centre of the page. Spectral parameters for 7,7- same as 2,2- in Figure 22a except τ = 0.11 s and T = 0.1 s for all three temperatures; number of acquisitions = 1.2 x 10^5 (15°C); 8.4 x 10^4 (25°C); line broadening = 20 Hz (15°C and 25°C); 25 Hz (40°C).

Spectra parameters 11,12- same as 2,2- in Figure 22a except τ = 0.12 s (15°C, 25°C); 0.20 s (40°C); T = 0.2 s for all three temperatures; number of acquisitions = 6.9 x 104 (15°C); 8.0 x 104 (25°C); 4.5 x 104 (40°C); line broadening = 15 Hz (15°C); 10 Hz (25°C and 40°C).

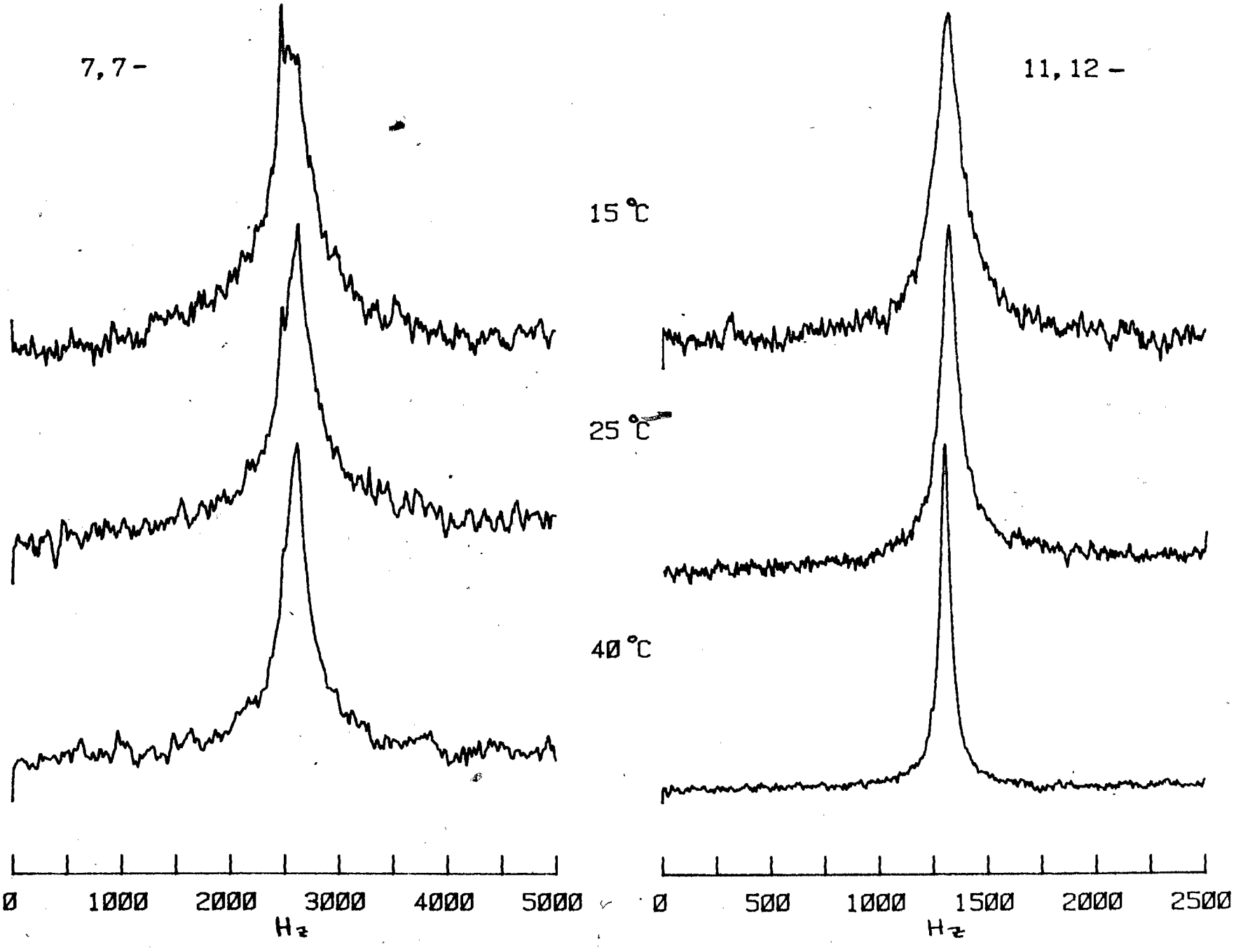
7,7 -
11,12 -
15 °C
25 °C
40 °C
0
1000
2000
3000
4000
5000
Hz
0
500
1000
1500
2000
2500
Hz

Figure 22c: Deuterium NMR spectra of 16,16,16-[$^2H_3$] phosphatidylcholine (5 mol %) in native HDL_2 as a function of temperature. The spectra exhibit two resonances, the methyl [$^2H_3$] signal and ^2HOH resonance shifted 150 Hz downfield (to the left) due to residual deuterium in water. Spectral parameters: sweep width = 2000 Hz; pulse length 19 μs (90° flip angle); number of acquisitions = 3010; delay before acquisition = 150 μs; delay between subsequent pulses = 1.0 s (15°C and 25°C); 1.2 s (40°C) line broadening = 1.0 Hz, data size = 2048.

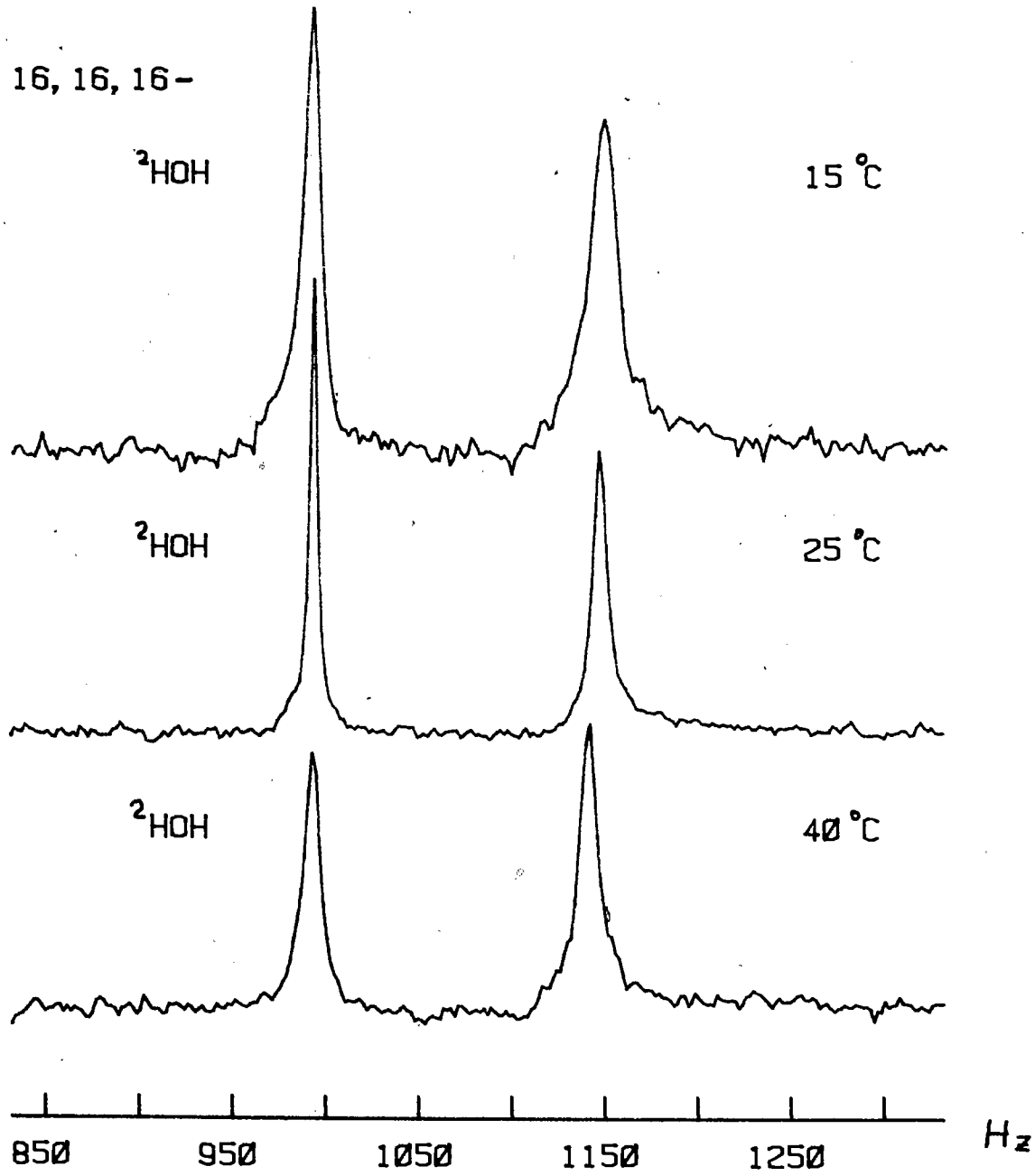
16, 16, 16-
^{2}HOH
15 °C
^{2}HOH
25 °C
^{2}HOH
40 °C
850
950
1050
1150
1250
Hz

TABLE IX ^2H NMR line widths ($\Delta\upsilon_{1/2}$) of a phosphatidylcholine selectively labelled at the sn-2 chain incorporated into native HDL_2 as a function of temperature.

Chain Position	Line Width (Hz)(a)		
	15°C	25°C	40°C
2-	470	400	330
4-	420	330	260
7-	420	330	260
11,12-	290	195	90
16-	18	12	9

(a) Uncertainty in the line width measurements in approximately ±10%.

Longitudinal relaxation times, T_1, were measured by inversion-recovery method (Vold et al., 159). Figures 23a-e are plots of ln ($M_\infty - M_\tau$) vs τ for various positions as a function of temperature. M_∞ is the magnetization in the Z direction obtained when $\tau > 5\ T_1$ where τ is time in second after 180° pulse. The straight lines drawn are the least squares fit to the experimental points. In this analysis the last point, i.e. the highest τ value was ignored as it is subject to large error. The correlation coefficients for all of the fits were greater than 0.95. Due to low amplitude of the signal of methylenes, C2, C4 and C7 at 15°C, the intensity measurements had an uncertainty of ± 20%, whereas for the spectra obtained for C11 and C12 methylenes and methyl, the error in intensity measurements was reduced to ± 10%.

The spin-lattice relaxation times, T_1, are presented in Table X. The T_1 values are approximately constant for C1-C12 methylenes while the methyl T_1 is much larger. It is noteworthy that the T_1 remain essentially unchanged over the temperature interval of 25°C (15°C-40°C) for C2-C12. This contrasts with dipalmitoylphosphatidylcholine bilayers where T_1 increases 50-100%, for the C2-C12 positions when the temperature is increased from 50°C-80°C (Brown et al., 152).

Figure 23a: Deuterium longitudinal relaxation time(s) measurements of [2,2-$^2H_2$] phosphatidylcholine incorporated into native HDL_2 as a function of temperature. The spin lattice relaxation times were measured by inversion recovery method, (180°-τ-90°) where τ is in seconds. The figure is a plot of $\ln(M_\infty - M_\tau)$ vs. τ. M_∞ is the magnetization after waiting τ, following a 180° pulse. As there is large error, $\pm$20%, in the peak height measurements, integrated areas were used to calculate the magnetization.

Spectral parameters same as in 2,2- of Figure 22a except τ was varied from 0.001 s to 0.0225 (15°C): 0.001 s to 0.025 s (25°C); 0.02 s to 0.036 s (40°C). Number of acquisitions = 3.3×10^4 (15°C); 2.5×10^4 (25°C); 7.2×10^3 (40°C). M_∞ is when τ = 0.1 s (15°C); 0.1 s (25°C); 0.16 s (40°C).

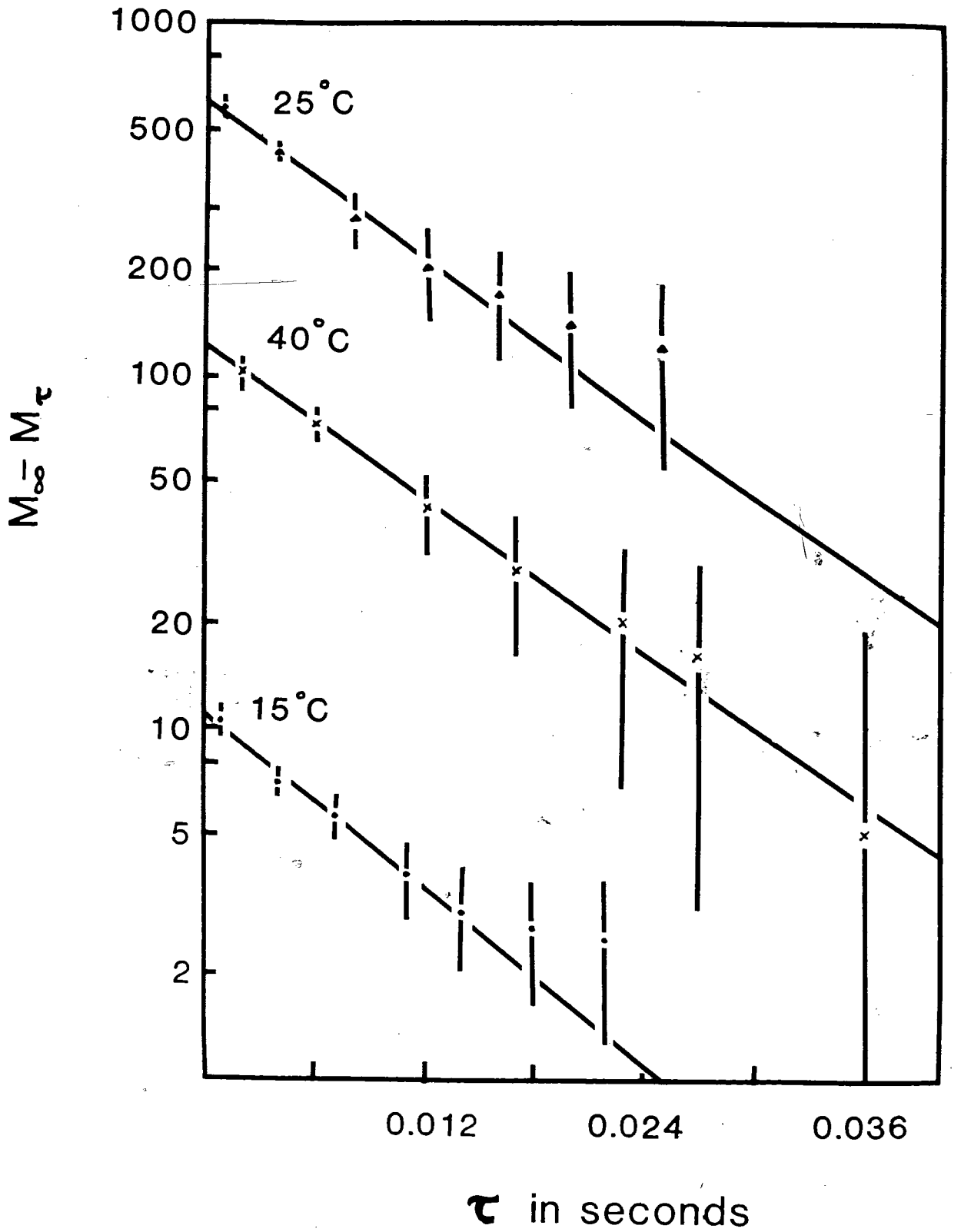
1000
500
200
100
50
20
10
5
2
25°C
40°C
15°C
$M_\infty - M_\tau$
0.012
0.024
0.036
τ in seconds

Figure 23b: Deuterium longitudinal relaxation time(s) measurements of [4,4-$^2H_2$]- phosphatidyl-choline incorporated into native HDL_2 as a function of temperature. T_1's were measured as described in the legend of Figure 22a. Spectral parameters were the same as in 2,2- of Figure 22a legend except τ was varied from 0.001 to 0.022 s for all three temperatures. Number of acquisitions = 4.0×10^4 (15°C and 25°C); 2.0×10^4 (40°C). M_∞ is when τ = 0.11 s for all temperatures.

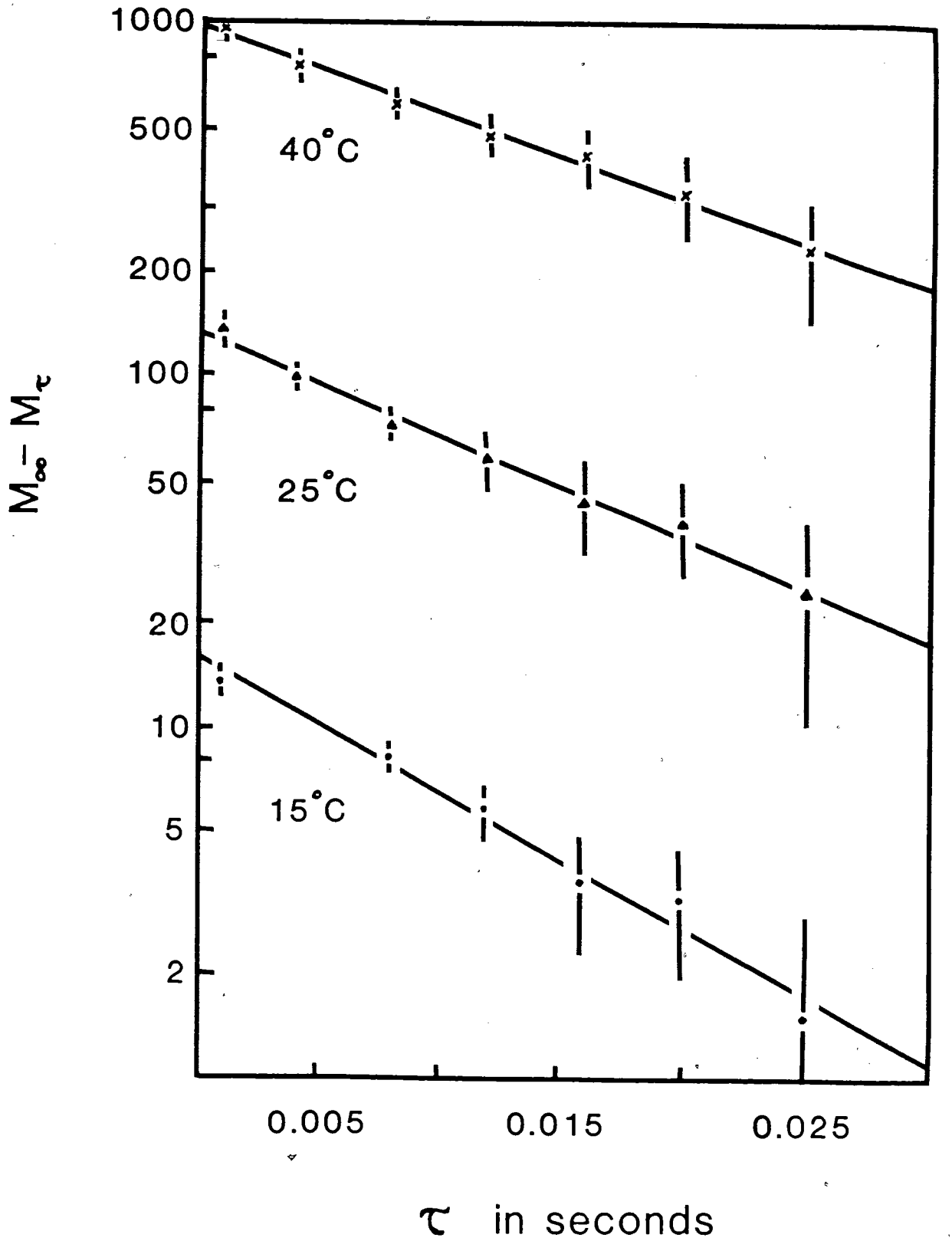
1000
500
200
100
50
20
10
5
2
40°C
25°C
15°C
$M_\infty - M_\tau$
0.005
0.015
0.025
τ in seconds

Figure 23c: Deuterium longitudinal relaxation time(s) measurements of [7,7-$^2H_2$]- phosphatidyl-choline incorporated into native HDL_2 as a function of temperature. T_1's were measured as described in the legend of Figure 23a. Spectral parameters were the same as in 2,2- of Figure 22a legend except τ was varied from 0.001 to 0.025 s for all three temperatures. Number of acquisitions = 3.5×10^4 (15°C); 2.1×10^4 (25°C); 1.0×10^4 (40°C). M_∞ is when τ = 0.11 s for all three temperatures.

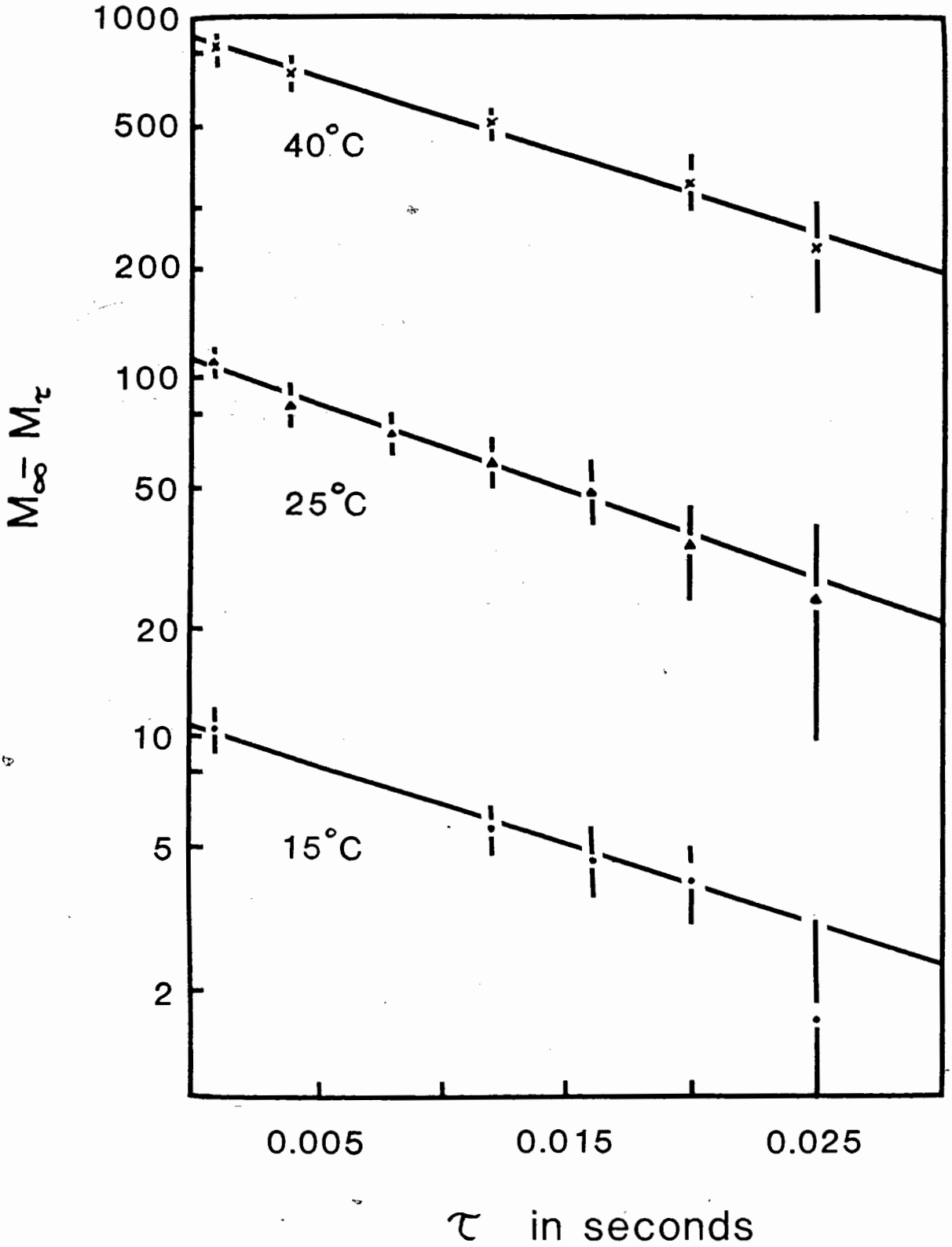
1000
500
200
100
50
20
10
5
2
$M_\infty - M_\tau$
40°C
25°C
15°C
0.005
0.015
0.025
τ in seconds

Figure 23d: Deuterium longitudinal relaxation time(s) measurements of [11,11,12,12-$^2H_2$]- phosphatidylcholine incorporated into native HDL_2 as a function of temperature. T_1's were measured as described in the legend of Figure 23a. Spectral parameters were the same as in 2,2- of Figure 22a legend except τ was varied from 0.001 to 0.035 s (15°C and 25°C); 0.002 s to 0.055 s (40°C). Number of acquisitions = 1.5×10^4 (15°C); 2.0×10^4 (25°C); 1.5×10^4 (40.0°C). M_∞ is when τ = 0.12 s (15°C and 25°C); 0.20 s (40°C).

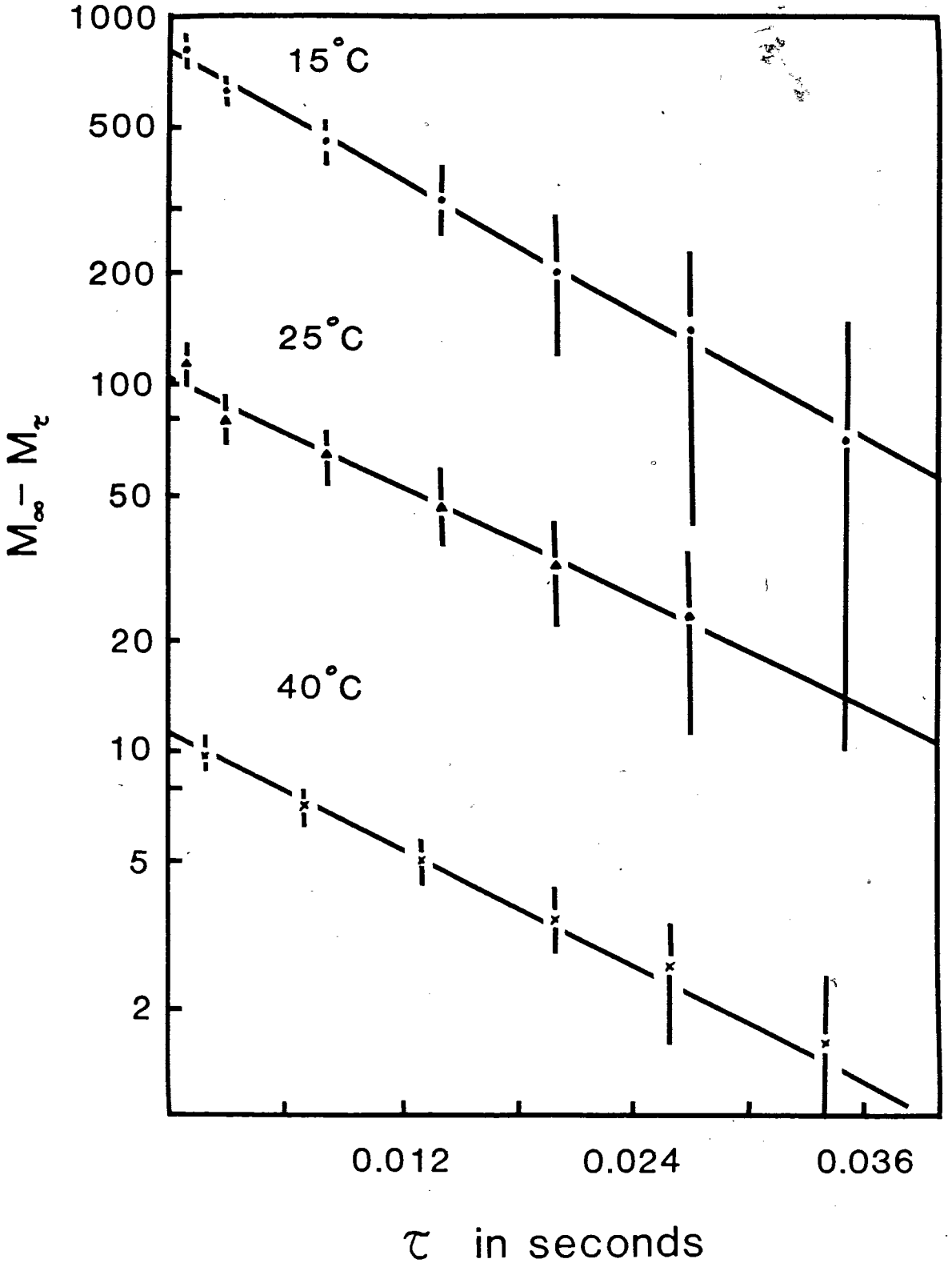
1000
500
200
100
50
20
10
5
2
15°C
25°C
40°C
$M_\infty - M_\tau$
0.012
0.024
0.036
τ in seconds

Figure 23e: Deuterium longitudinal relaxation time(s) measurements of [16,16,16-$^2H_2$]- phosphatidyl-choline incorporated into native HDL_2 as a function of temperature. T_1's were measured as described in the legend of Figure 23a. Magnetization (M_∞ or M_τ) was obtained from the peak height measurements. Spectral parameters sweep width = 2,000 Hz data size = 2048; pulse length = 38 μs (180° flip angle); delay after the 90° pulse = 1.0 (15°C and 25°C); 1.2 (40°C). Line broadening = 2 Hz; number of acquisitions = 1500 for all three temperatures. τ was varied from 0.1 s to 0.35 s for all three temperatures. M_∞ is when τ =1.0 s (15°C and 25°C); 1.2 s (40°C).

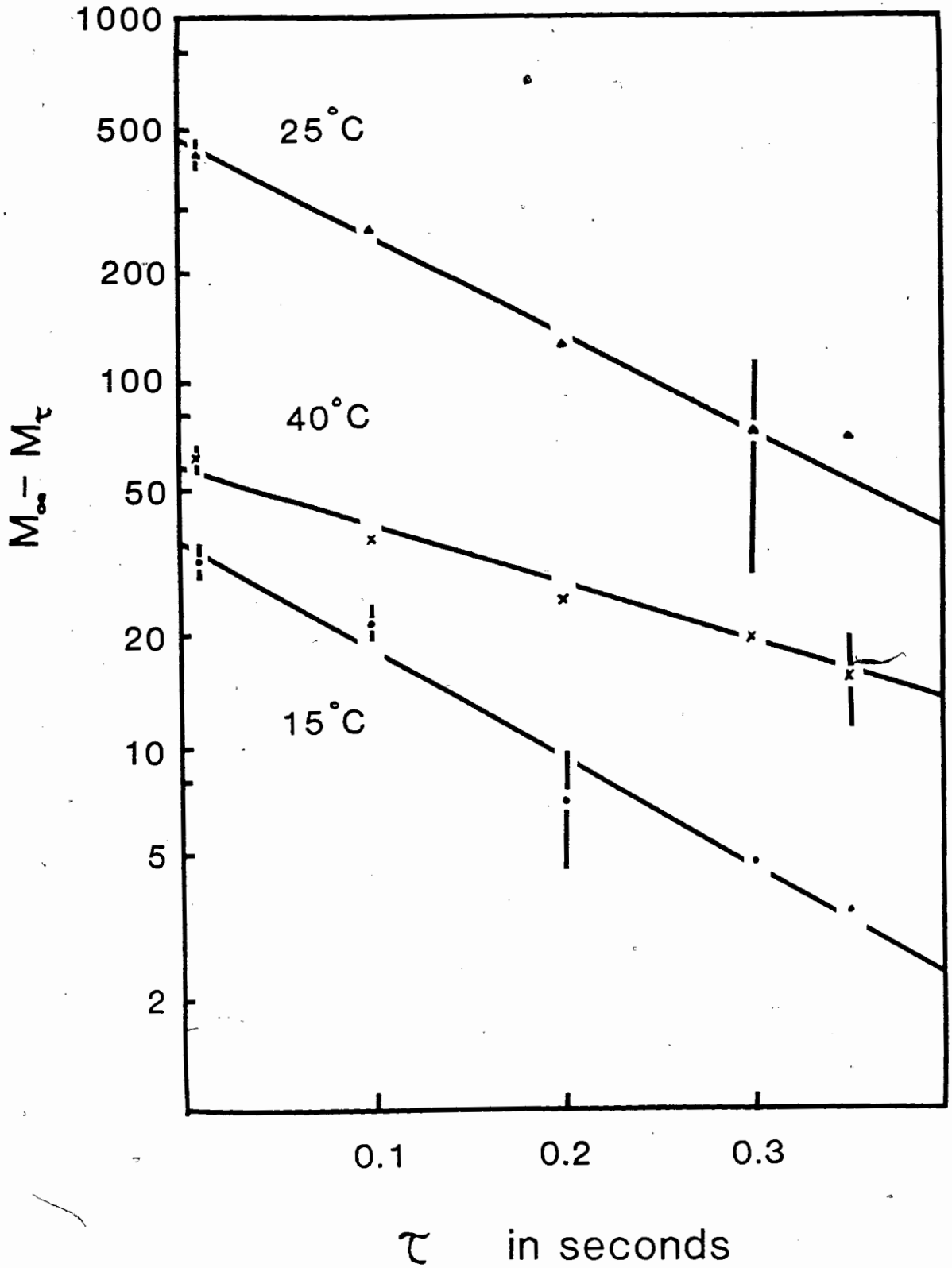
1000
500
200
100
50
20
10
5
2
25°C
40°C
15°C
$M_\infty - M_\tau$
0.1
0.2
0.3
τ in seconds

TABLE X ^{2}H longitudinal relaxation times T_1's of a phosphatidylcholine selectively deuterated at the sn-2 chain incorporated into native HDL_2 as a function of temperature.

Chain Position	T_1 (ms)[a]		
	15°C	25°C	40°C
2-	10	11	13
4-	13	14	14
7-	19	17	19
11,12-	15	18	18
16-	148	172	237

(a) Uncertainty for the positions 2-, 4-, 7- is approximately (±20%) and for the 16- position it is approximately (±10%).

VI The variation of ^{31}P NMR line with of HDL_2 containing 16-[$^2H_3$] phosphatidylcholine

Figure 24 shows the undecoupled ^{31}P NMR spectra of native HDL_2 containing ~5 mol % 16, 16, 16 -[$^2H_3$-] phosphatidylcholine as a function of the solvent viscosity. Only representative spectra are shown in this figure. The spectra contain two resonances, an intense phosphatidylcholine peak and a weaker resonance ~ 69 Hz downfield due to sphingomyelin. Although both of the resonances have the same line widths only those of phosphatidylcholine peak are measured as the sphingomyelin peak becomes less discernible at higher glycerol concentration. At high viscosities, the line widths are measured by drawing a perpendicular at the centre of the phosphatidycholine peak and doubling the half width at half height (see Figure 24). The line widths measured in this manner are presented in Table XI. For convenience the line widths are plotted as a function of the solvent viscosity in Figure 25. A smooth curve is drawn through the points. The error bars represent the $\pm$10% accuracy in the line width measurements.

From the Table XI and Figure 25 it is apparent that the line width of the phosphorus resonances in HDL_2 increases with increasing viscosity. However, it is important to note that the increase in the line width is not linear but instead gradually levels off. In fact, the line widths for η = 29.0 cp and η = 34.5 cp are virtually identical within the experimental error.

Figure 24: ^{31}P NMR spectra of native HDL_2 containing approximately 5 mol % [16,16,16-$^2H_3$] phosphatidylcholine as a function of the solvent viscosity. Only representative spectra are shown in this figure. The perpendicular dotted line is drawn through the centre of the phosphatidylcholine resonance (see text).

Spectra parameters: resonance frequency 102.2 MHz; sweep width = 2000 Hz; data size = 2048 points;delay before acquisition = 250 μs; delay between subsequent pulses = 1.51 s; pulse length = 16 μs (for a 60° flip angle); number of acquisitions = 3432 (η = 3.8 cp); 5024 (η = 11.7 cp); 6845 (η = 34.5 cp); line broadening = 3.0 Hz (η = 3.8 cp); 5.0 Hz (η = 11.7 cp); 8.0 Hz (η = 34.5 cp).

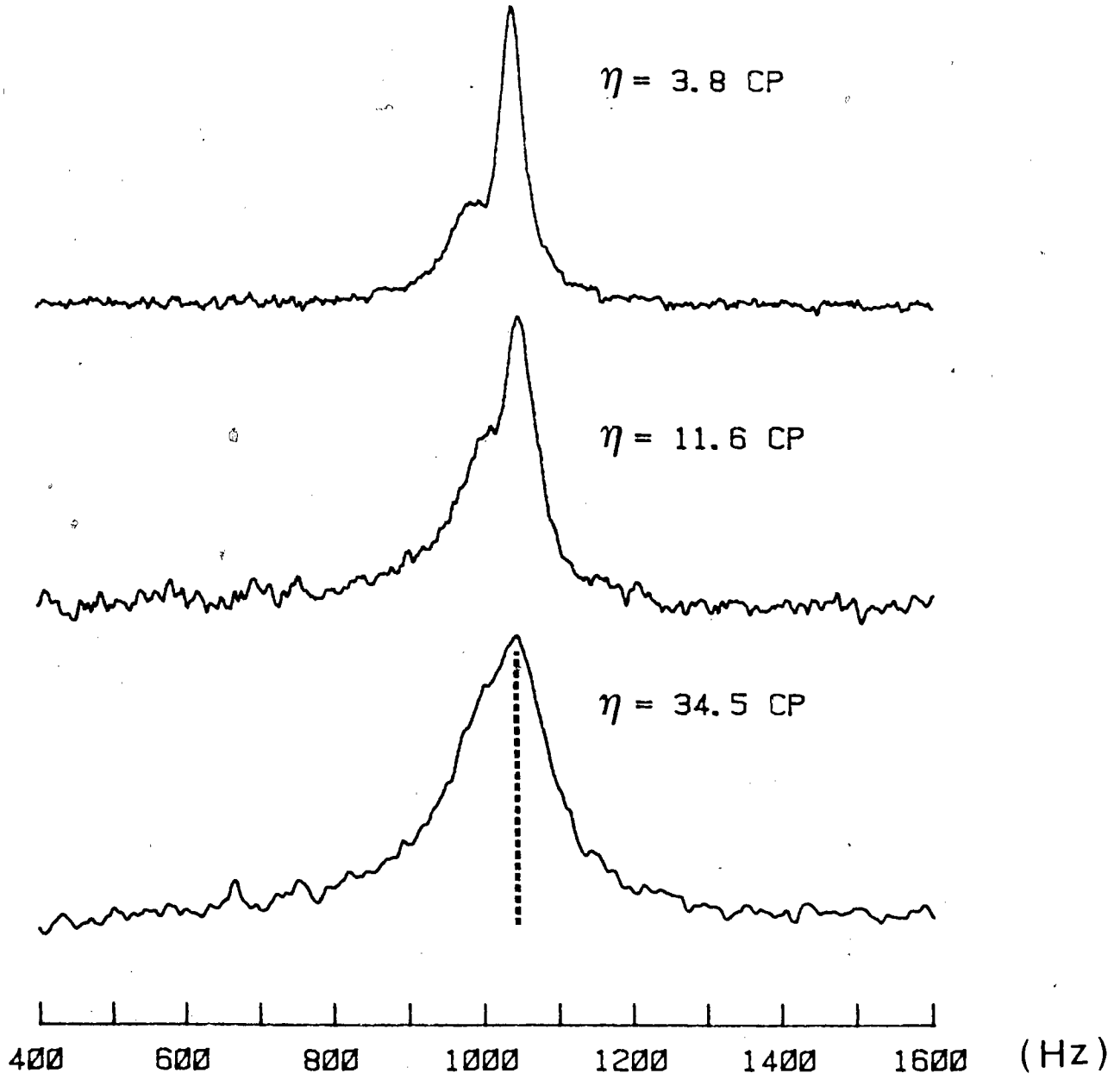
η = 3.8 CP
η = 11.6 CP
η = 34.5 CP
400
600
800
1000
1200
1400
1600
(Hz)

TABLE XI The ^{31}P NMR line width of native HDL_2 containing ~5 mole % [16,16,16-$^2H_3$] phosphatidylcholine as a function of the solvent viscosity.

Solvent Viscosity (cp)	Line Width (Hz)(a)
0.89	27
3.8	42
5	44
11.7	68
18.4	80
29	102
34.5	110

(a) Uncertainty in the line width measurements is approximately ±10%.

Fig 25: The variation of ^{31}P linewidth of HDL_2 as a function of solvent viscosity

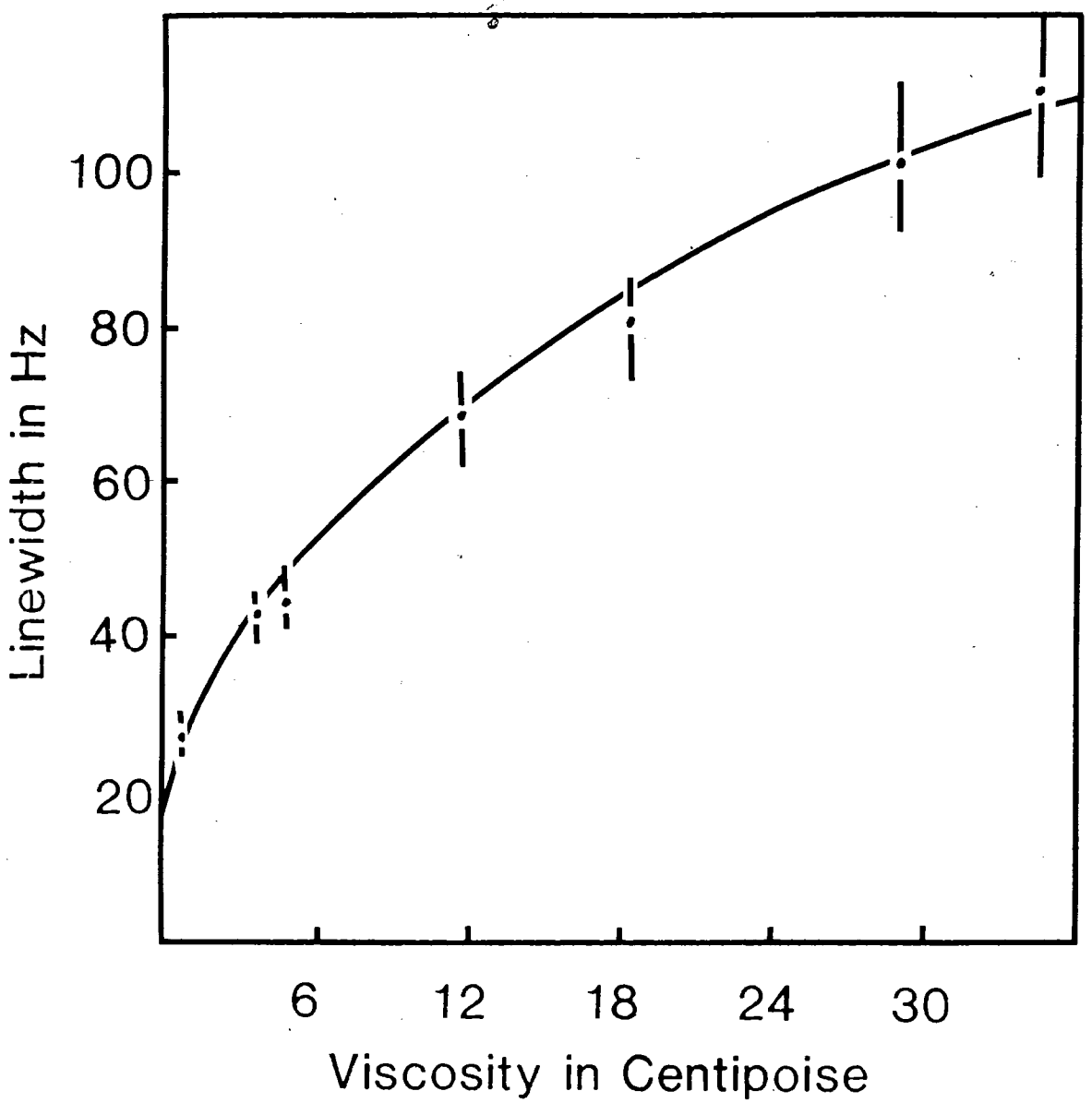

In order to analyze the line width variation as a function of the solvent viscosity results using equation 30, p.46, the value of the constant "C" is required. C is usually taken as the natural line width of the phospholipid in chloroform, which is the isotropic value. Figure 26 shows an undecoupled ^{31}P NMR spectrum of egg phosphatidycholine in chloroform/methanol (2:1 v/v) in 2 mM EDTA. The sample was prepared from sonicated vesicles containing 2mM EDTA, which were freeze dried and dissolved in chloroform/methanol. The spectrum is a quintuplet of 1:4:6:4:1 due to phosphorus coupling to the nearby methylenes. The coupling constant, $J \sim 6$ Hz (117). The isotropic line widths of phosphorus in egg phosphatidylcholine was obtained (15 Hz) from this spectrum as the line width at half height.

Thus using equation 16, p.31, and the above results, the value of M_2 can be approximated provided τ_e in equation 16 is also known. In ^{31}P NMR the value of M_2 can also be obtained from the line width measurements as a function of the resonance frequency (see pages 44-46). We have obtained the undecoupled ^{31}P NMR of HDL_2 at three difference resonance frequencies. The results are shown in Table XII.

Figure 26: The Undecoupled ^{31}P NMR Spectrum of Egg Phosphatidylcholine in Chloroform/Methanol.

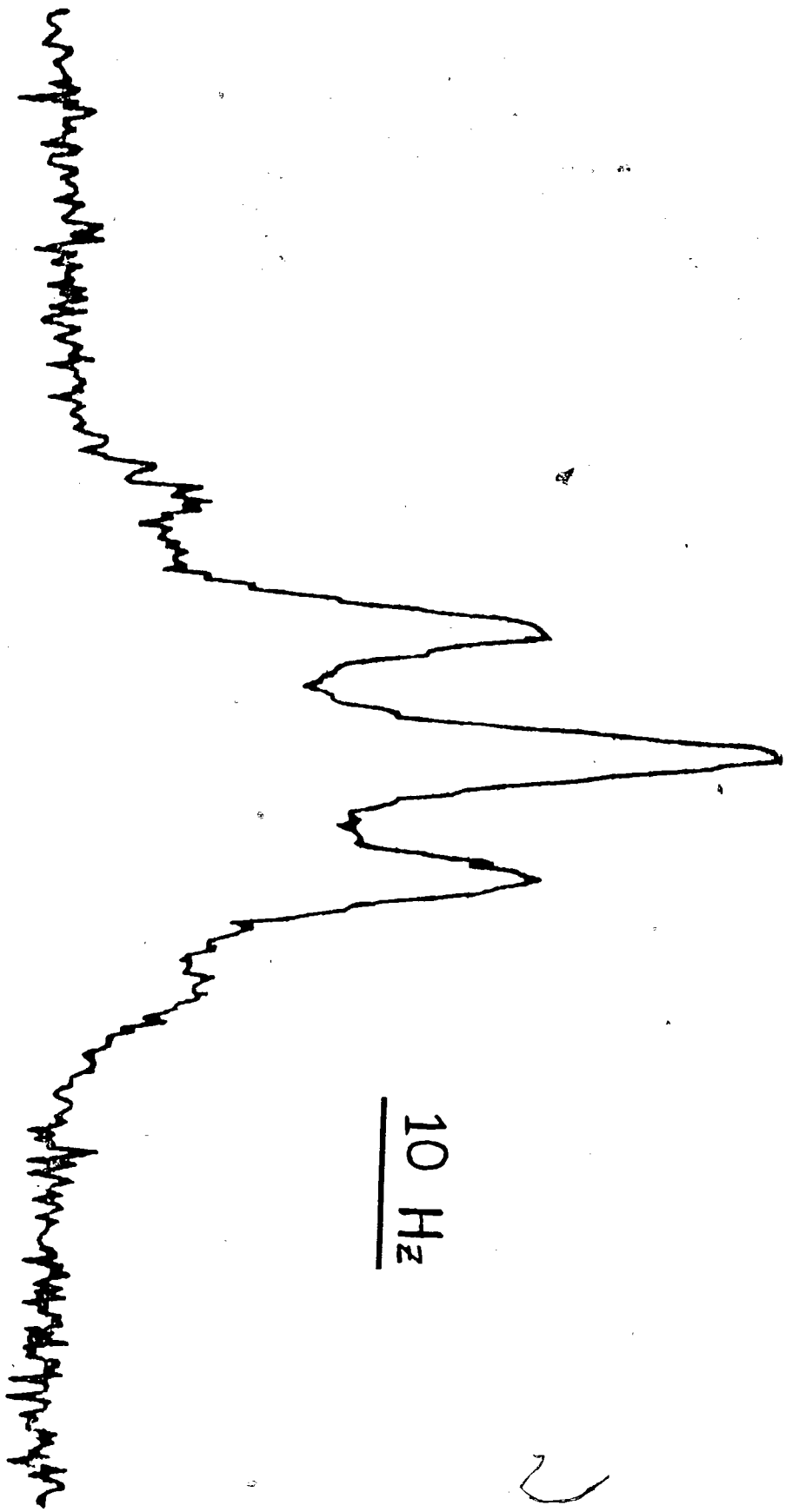
10 Hz

TABLE XII Undecoupled ^{31}P NMR line width of native HDL_2 as a function of resonance frequency.

Line width ($\Delta\upsilon_{1/2}$ in Hz)(a)	Frequency (MHz)
21	40.5
28	102.2
35	162

(a) Uncertainty in the line width is approximately $\pm$10%.

VII Viscosity dependence of ^2H NMR line width of methyl deuterated phospholipid in native HDL_2

Figure 27 shows the ^2H NMR spectra of ~5 mol % [16,16,16,-$^2H_3$] phosphatidylcholine incorporated into native HDL_2 as a function of the solvent viscosity. The line width of 6.5 Hz observed for η = 0.89 (0% glycerol) is in agreement with that of [16,16,16-$^2H_3$] palmitic acid incorporated into native HDL_2 (162). Figure 27 contains only the representative ^2H NMR spectra of [16,16,16-$^2H_3$] phosphatidylcholine in HDL_2 as a function of the solvent viscosity. The two resonances due to natural abundance deuterium in glycerol, 117 Hz and 184 Hz, downfield to the methyl resonance are not shown for the sake of brevity. The line widths as a function of solvent viscosity are presented in Table VIII. For convenience the line widths are plotted as a function of viscosity in Figure 28. A smooth curve is drawn through the points. The error bars represent the $\pm$ 10% accuracy in the line width measurements.

From Table VIII and Figure 28, it is readily apparent that the line width of the methyl resonance increases with increasing viscosity. However, it is noteworthy that the increase in the line width is not linear but instead gradually levels off. In particular, the line widths for η = 27; 29; 32 are virtually identical within the experimental error.

Figure 27: ^2H NMR line widths of [16,16,16-$^2H_3$]- phosphatidylcholine in native HDL_2 as a function of solvent viscosity (η). Only representative spectra are shown in this figure.
Spectral parameters for η = 0.89 are: pulse length = 12 μs (60° flip angle); sweep width = 1000 Hz; data size = 2048 points; delay between pulses = 1.12 s; delay before data acquisition = 250 μs; number of acquisitions = 4373; line broadening = 0.5 Hz.
Spectral parameters for η = 5.0 cp were the same as η = 0.89 except number of acquisitions = 30,000; delay between pulses = 1.22 s; line broadening = 2 Hz.
Spectral parameters for η = 29.0 cp were the same as η = 0.89 excpet number of acquisitions = 25,000; delay between subsequent pulses = 1.22 s; line broadening = 2.0 Hz.

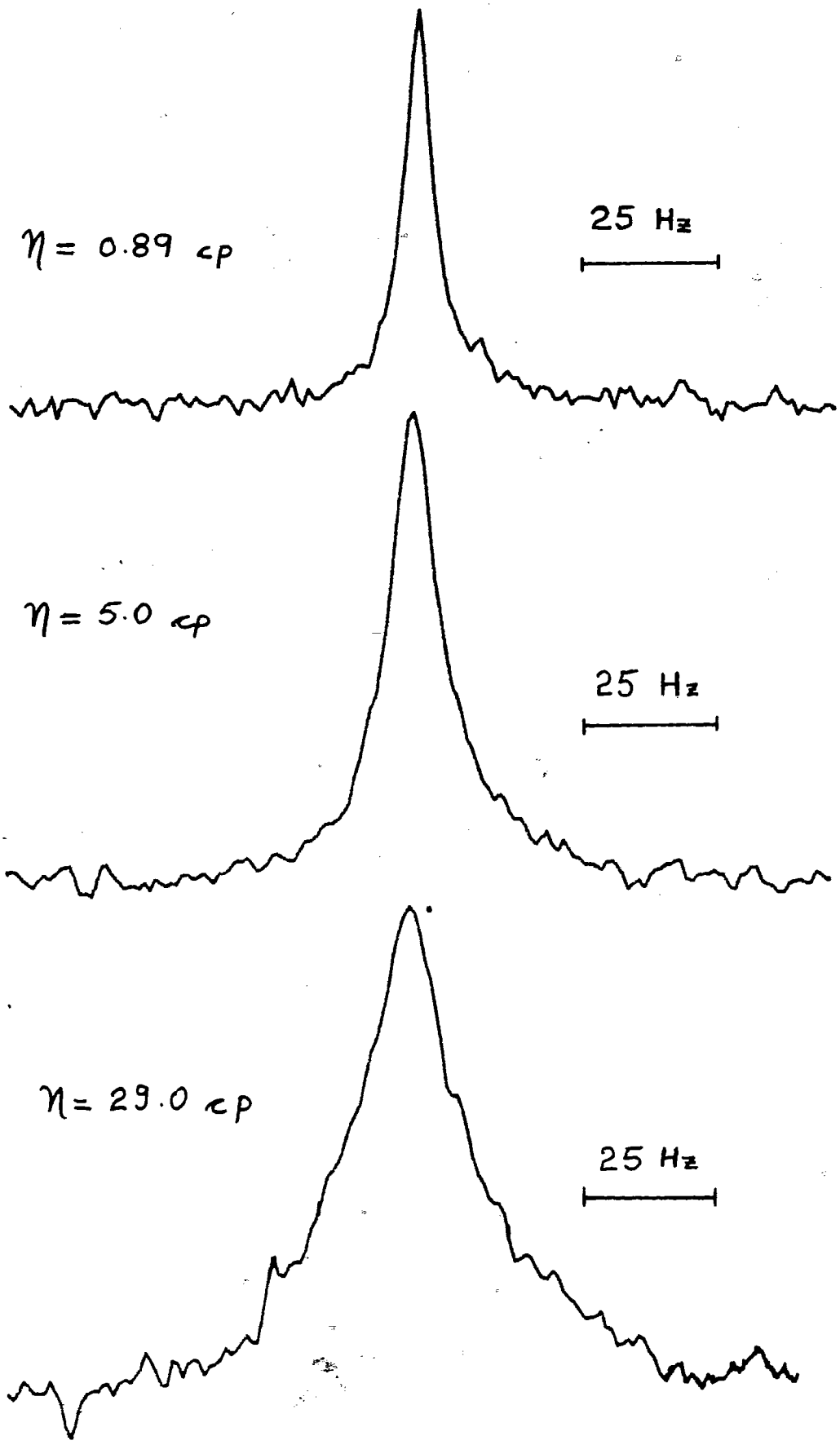
η = 0.89 cp
25 Hz
η = 5.0 cp
25 Hz
η = 29.0 cp
25 Hz

TABLE XIII ^2H NMR line width of [16,16,16-$^2H_3$]- phosphotidylcholine incorporated into native HDL_2 as a function of the solvent viscosity.

Solvent Viscosity Centipoise	Line Width[(a)] Hz
0.89	6.5
5.0	11.7
8.0	14.4
11.0	17.1
16.0	21.5
22.8	22.4
27.0	28.5
29.0	26.7
32.0	27.3

(a) Line width measurements had approximately $\pm$ 10% uncertainty.

Fig.28: The variation of ^2H linewidth of phosphatidyl-choline-D3 in HDL_2 with solvent viscosity

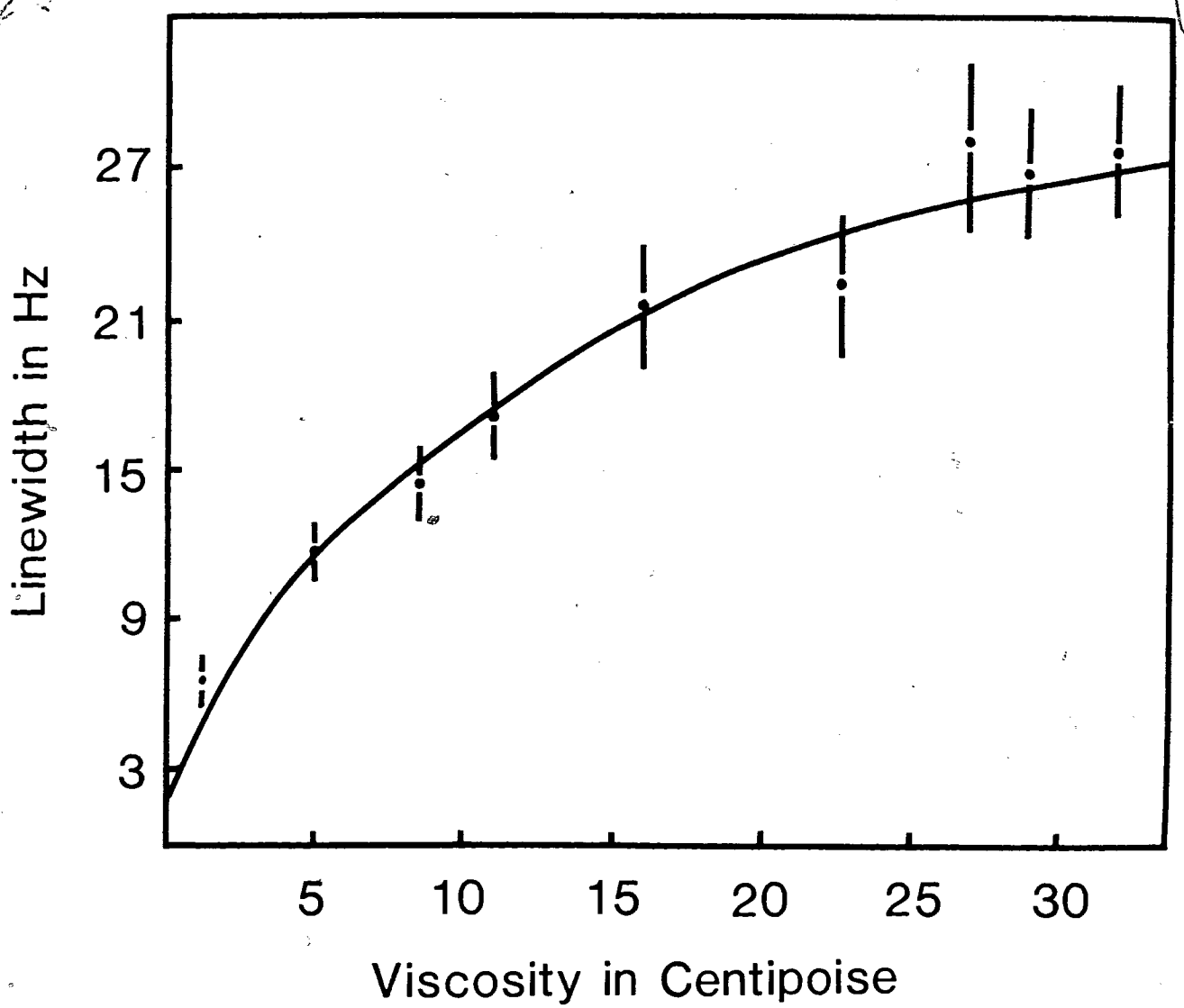

VIII Selectively Deuterated Phospholipids in Unilamellar Vesicles

Although fatty acids are considered to be reliable probes of the phospholipid acyl chains if multilamellar liposomes, the possibility still remains whether they adequately reflect the acyl chain ordering in the unilamellar vesicles. The fatty acids are also known to cause vesicle fusion (135). This is a serious problem as there may be time dependent changes in the vesicle diameters in our study. We did not observe this phenomenon, as both the signal intensity and the line widths remained unchanged over the period of 36 hours. Nevertheless, to alleviate such problems, we have examined the acyl chain order in unilamellar vesicles using selectively deuterated phospholipids.

For the initial part of the present work we determined using ^2H NMR, the acyl chain order in egg phosphatidylcholine multilamellar liposomes containing (~5 mol%) a saturated phosphatidylcholine selectively deuterated along the sn-2 acyl chain. Figure 29 contains ^2H NMR spectra of such liposomes ~50% w/v in deuterium depleted water at 25°C. The ^2H quadrupolar splittings obtained from each spectra are presented in Table XIV. The two deuterons at the 2-position of the sn-2 chain are inequivalent, hence two quadrupolar splitings are observed (137). These results, listed in Table XIV, are in substantial agreement with those egg phosphatidylcholine and dipalmitoyl phosphatidylcholine multilamellar liposomes (96,106).

TABLE XIV: ^2H quadrupolar splittings ~5 mol % selectively deuterated phosphatidylcholine in egg phosphatidylcholine multilamellar liposomes.

Chain Position	Quadrupolar Splittings in kHz
2-	11.62, 17.93
4-	27.53
7-	28.7
11,12-	20.30, 22.73
16	2.65

Figure 29: Deuterium NMR spectra of ~5 mol % selectively deuterated phosphatidylcholine along the sn-2 chain in egg phosphatidylcholine multilamellar liposomes in deuterium depleted water. Spectral parameters: 2,2-: sweep width 200 kHz; data set = 4 K; number of acqusitions (NA) = 2.2 x 10^5; line broadening (LB) = 200 Hz. 4,4-: same as 2,2- except NA = 1.0 x 10^5; LB = 300 Hz. 7,7-: same as 2,2- except NA = 2.0 x 10^5; LB = 100 Hz. 11,11,12,12-: same as 2,2- except NA = 1.0 x 10^5; LB = 50 Hz; τ_R = 260 ms. 16,16,16-: same as 2,2- except NA = 1.963 x 10^4; LB = 10 Hz; τ_R = 1.21 s. The number to the left of each spectrum indicates the position of deuterium substitution of the sn-2 palmitoyl chain of deuterated phosphotidylcholine.

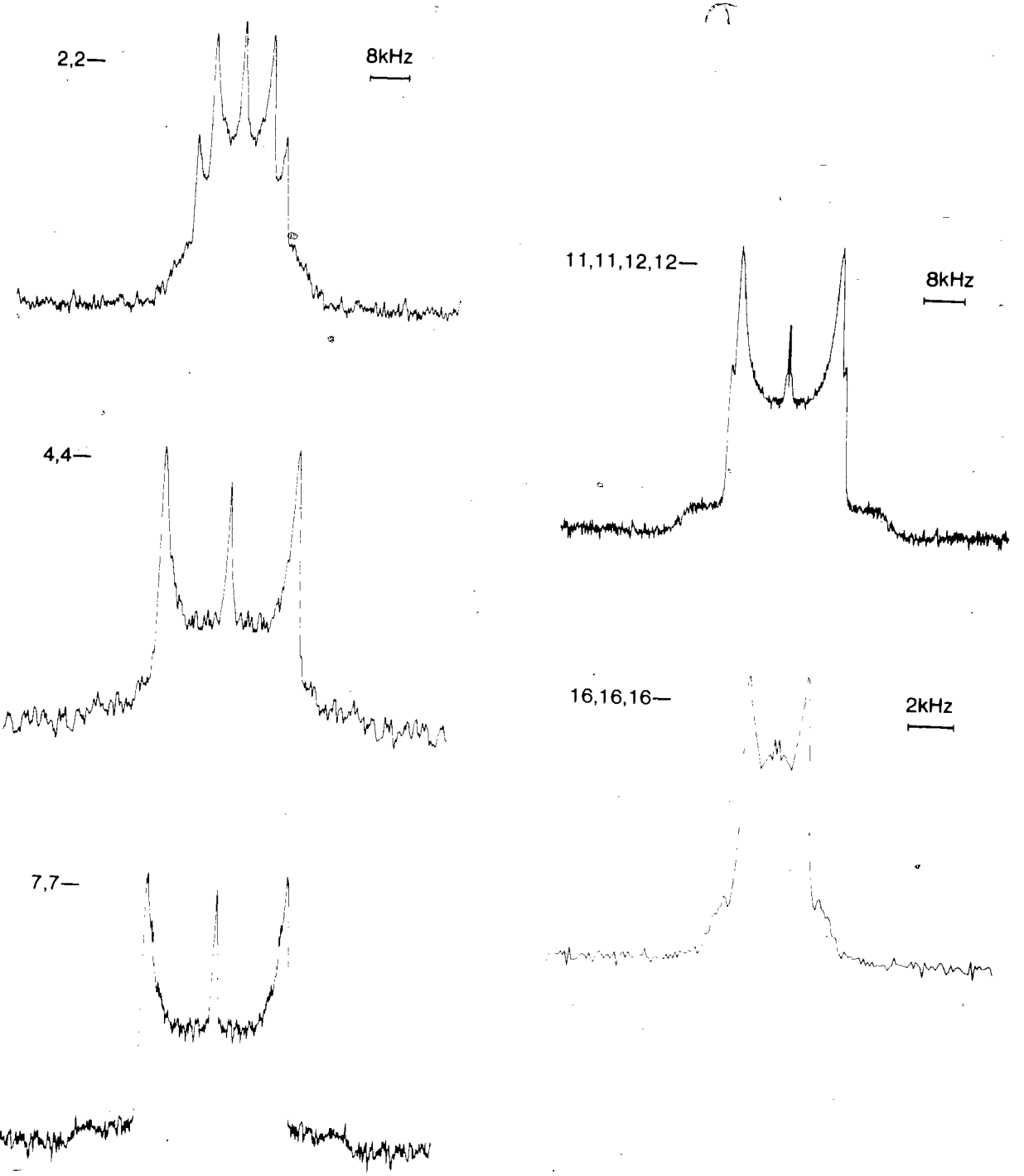
2,2—
8kHz
4,4—
7,7—
11,11,12,12—
8kHz
16,16,16—
2kHz

Since the purpose of the present study was to compare the organizational order in unilamellar vesicles obtained from selectively deuterated palmitic acid and selectively deuterated phospholipids, the liposomes containing ~5 mol % deuterated phosphatidylcholine were diluted to 3 mLs with deuterium depleted water and subsequently sonicated (see Material and Methods). The deuterium NMR spectra of ~7% w/v egg phosphatidylcholine unilamellar vesicles at 25°C are shown in Figure 30. The spectra for the 2-, 4- and 7- positions do not provide an excellent fit to a single Lorentzian line. Whereas, the ^2H NMR spectra for the 11,12 and 16- positions do show a good fit to a single Lorentzian line. These results are in agreement with those obtained from selectively deuterated palmitic acids in unilamellar vesicles.

We have obtained a size distribution of vesicles by the negative staining method. Two separate samples of vesicles containing [11,11,12,12-$^2H_4$], [16,16,16-$^2H_3$]- phosphatidylcholine were examined. The results from the two samples were pooled to reflect the size distribution present in all of the samples studied. Sizes wre categorized into six fractions,with each category having the size range of 40 Å. The results of such an analysis are shown in Figure 31.

Figure 30: Deuterium NMR spectra of approximately 5 mol % phosphatidylcholine selectively deuterated along the sn-2 chain position in unilamellar vesicles of ~7% w/v egg phosphatidylcholine in deuterium depleted water. The position of selective deuteration is indicated to the left of each spectrum. Spectral parameters: 2,2-: sweep width = 50 kHz; data set = 4 K; delay between subsequent pulses = 241 ms; delay before data acquisition = 10 μs; number of acquisitions (NA) = 2.5×10^5; line broadening (LB) = 25 Hz. 4,4-: same as 2,2- except NA = 2.0×10^5; 7,7-: same as 2,2- except NA = 1.5×10^5. 11,11,12,12-: same as 2,2- except NA = 5.0×10^4 delay between subsequent pulses = 291 ms; LB = 10 H; 16,16,16-: same as 2,2- except sweep width = 2 kHz; NA = 5.0×10^3; delay between subsequent pulses = 1.22 s; delay before data acquisition = 50 μs; LB = 1.0 Hz.

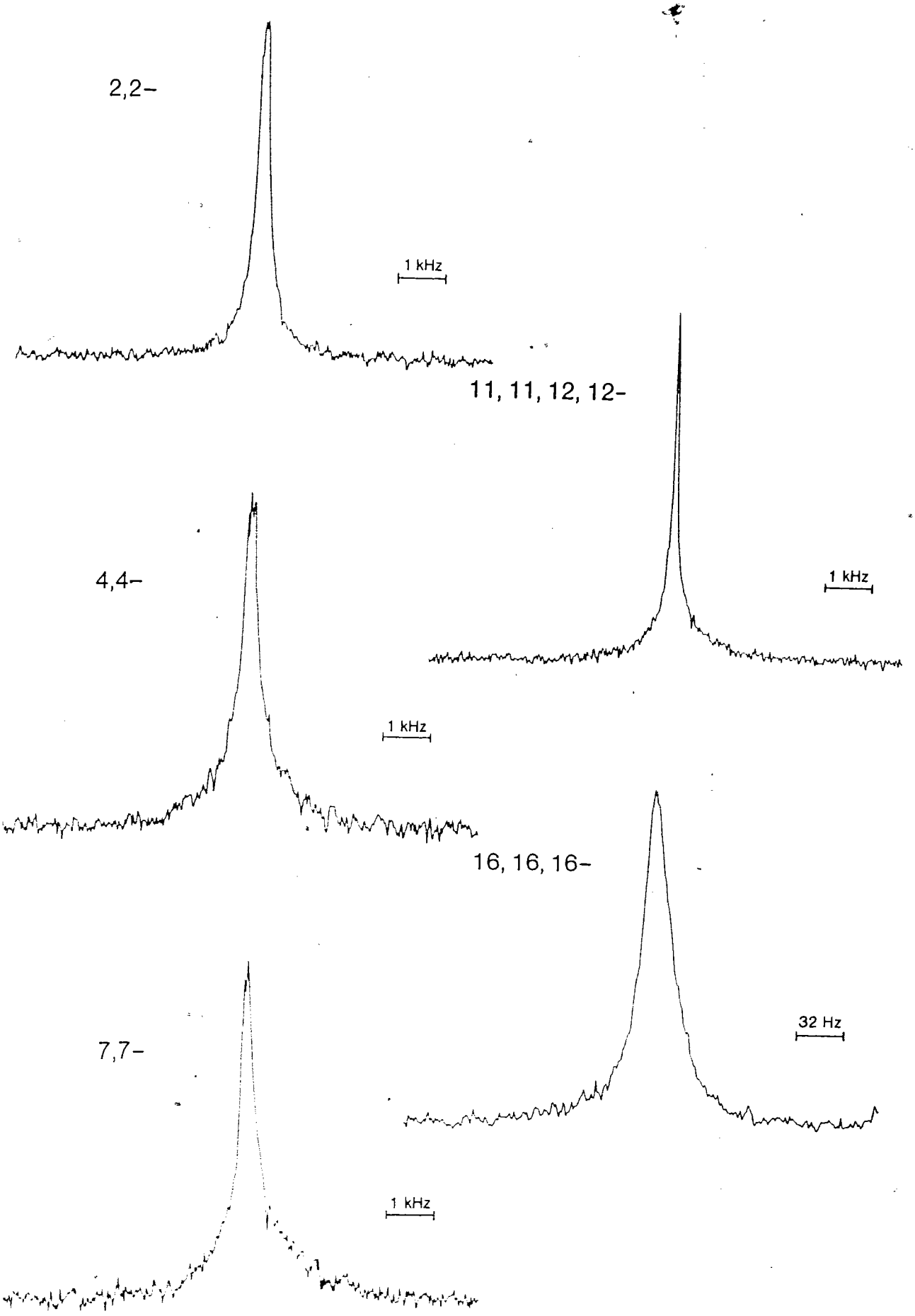
2,2-
1 kHz
11, 11, 12, 12-
1 kHz
4,4-
1 kHz
16, 16, 16-
32 Hz
7,7-
1 kHz

Figure 31: Histogram of Unilamellar Vesicle Sizes Containing Selectively Deuterated Phospholipid.

Figure 31: Histogram of unilamellar vesicle sizes containing selectively deuterated phospholipid

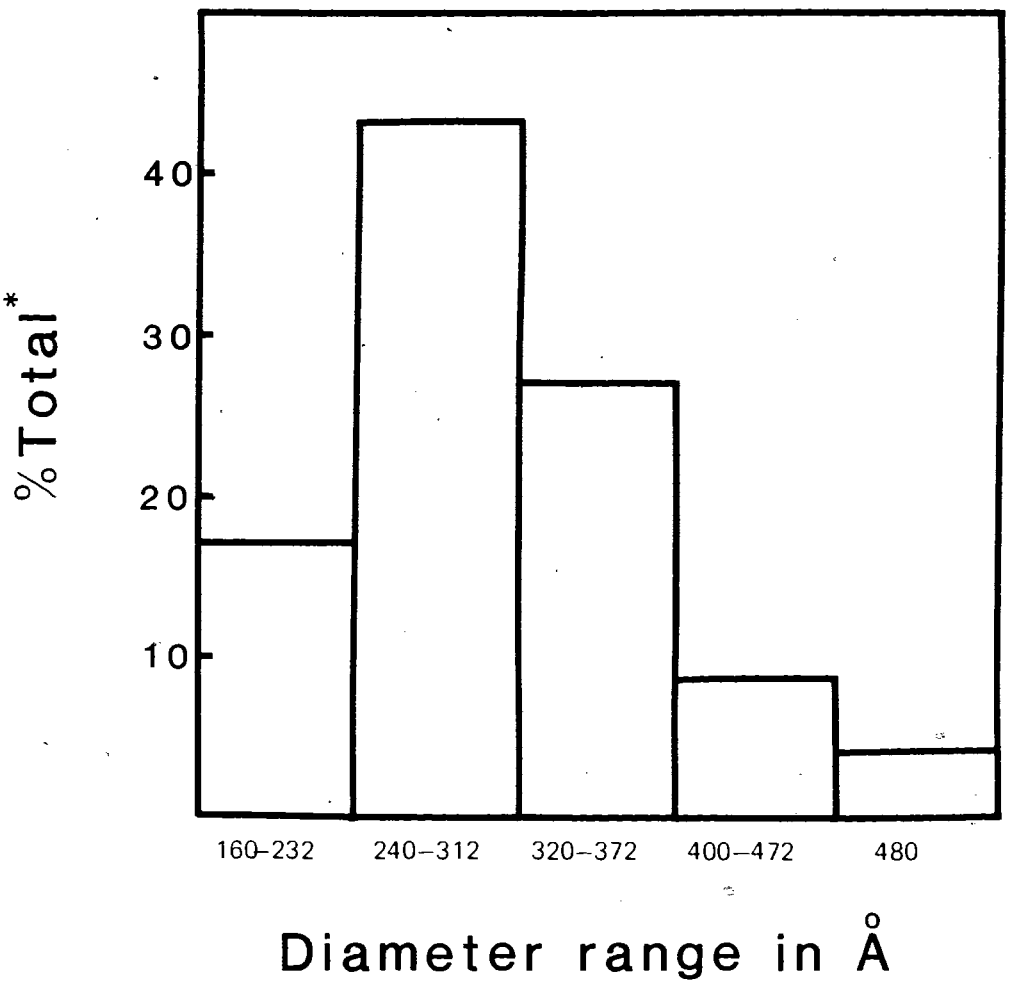

*Total of 975 vesicles were measured.

DISCUSSION

I Molecular Dynamics of Cholesteryl Palmitate in the Reconstituted HDL

Selectively deuterated cholesteryl palmitate has been incorporated into reconstituted HDL particles composed of apoproteins, egg phosphosphatidylcholine and cholesteryl oleate. The molecular motion of cholesteryl palmitate in the core of reconstituted HDL was studied by ^{2}H NMR. The reconstituted HDL was employed as a model of native HDL since its chemical composition can be controlled using artificial lipids. In addition to cholesteryl esters, the core of native HDL also contains triglycerides and cholesterol which may influence the dynamics of cholesteryl esters.

Reconstitution of HDL was performed using the established procedure of Hirz and Scanu (126). This method does not alter the circular dichroic properties of HDL apoproteins (126). The half time of cholesterol efflux from rat hepatoma cells is identical to native HDL indicating the surface properties of reconstituted HDL are similar to native HDL (74). In addition, the high resolution ^{13}C NMR spectrum of reconstituted HDL is essentially identical to that of native HDL (73).

We have also characterized the reconstituted HDL particles using electron microscopy, ^{31}P NMR spectroscopy and chemical analysis. Table III shows the chemical composition of

reconstituted HDL which can be compared with native HDL (Table I). Although a very similar chemical composition to native HDL is found in the reconstituted HDL particle, the protein/phospholipid ratio is slightly lower in reconstituted particles (1.21) than in native HDL_2 (1.39). The diameter of reconstituted HDL is 7.8 nm $\pm$ 1.2 nm is similar to native HDL. But the range of particle size distribution of reconstituted HDL is greater from 6.0 nm to 12 nm. This suggests that the native HDL subclasses HDL_2 and HDL_3 are more homogeneous than the reconstituted particles used in the present study. The reconstituted particles probably represent the entire spectrum of HDL present in human plasma, i.e. both HDL_2 and HDL_3. In addition, ^{31}P NMR line widths of native HDL_3 and of HDL reconstituted using either total lipids or egg phosphatidylcholine (cholesteryl oleate/cholesteryl palmitate are identical within experimental error (Fig. 76) (130). This indicates a similar particle size in the three systems and also suggests that there is no appreciable difference in phospholipid head group conformation (140). Thus, on the basis of electron microscopy ^{31}P NMR and chemical composition, we believe that these particles are good models of native HDL.

^{2}H NMR line widths of selectively deuterated cholesteryl palmitate in reconstituted HDL (Table IV) may be compared with those obtained with the deuterated cholesteryl palmitate in egg phosphatidylcholine unilamellar vesicles. The line widths obtained for deuterated cholesteryl palmitate in the reconstituted HDL particles are very much larger (Table IV) than those for the equivalent position of cholesteryl palmitate deuteration in uni-

lamellar vesicles with the exception of the terminal methyl (59,60) The mean diameter of reconstituted HDL (7.8 nm) is approximately 1/4 that of egg phosphatidycholine vesicles (30 nm); hence, smaller line widths would be expected in reconstituted HDL. Therefore, the larger line widths in reconstituted HDL suggest that ester motion is considerably more restricted in the lipoprotein than in vesicles.

Insight into the dynamic behaviour of deuterated cholesteryl palmitate in reconstituted HDL can be obtained by calculating a theoretical ^2H NMR linewidth for an ester chain undergoing given motions. The simplest case is that of a static all-trans chain embedded in a lipoprotein particle such that particle tumbling is the only motion responsible for line narrowing. A ^2H NMR line width, $\Delta\nu 1/2$, can be calculated using equation 12. Assuming a spherical lipoprotein particle, τe in equation 12 is estimated from the Stokes-Einstein formula (equation 17). For a reconstituted HDL particle, with η = 0.89 cP, $R \sim 40A^o$ and T = 298°K we obtain τe 5.9 x 10^{-8}s; hence, a line width, $\Delta\nu 1/2 = 2350$ Hz is estimated for a rigid C^2H_2 segment. For a deuterium attached to a terminal methyl group, it is also necessary to include the effect of fast rotation about the C-C bond joining it with the adjacent CH_2 group (141), and then we calculate $\Delta\nu 1/2 = 260$ Hz. Clearly, the experimental line widths (Table IV) for deuterated cholesteryl palmitate in reconstituted HDL are much smaller than these predicted values. Therefore, we conclude that cholesteryl ester chain has significant motion inside the lipo-

protein particle.

Our observations are in agreement with those of Hamilton and Cordez (68) who obtained ^{13}C NMR data of native HDL. These authors described the cholesteryl esters in terms of being more "liquid like" than "solid like" - a rather general description. In the case of native HDL, which contains triglycerides, it has been suggested that the dynamic behaviour of cholesteryl esters is similar to that in a triglyceride/cholesteryl ester mixture (67). However, on the basis of our data, it is clear that the presence of triglycerides is not necessary for the ester chains to undergo significant motion. For native HDL the presence of triglycerides and cholesterol certainly could influence the dynamics of cholesteryl ester acyl chains.

The physical state of a cholesteryl oleate/cholesteryl palmitate mixture is solid at approximately 25°C. The fact that there is considerable motion when in reconstituted HDL suggests that the bulk phase packing properties of the ester are altered due to the small size of the HDL core such that chains become more mobile. Cholesteryl ester chain mobility may also be due to the interaction of the ester chains in the core with the phospholipid and/or protein components of the outer monolayer. At present, it is not possible to rule out either or both of these hypotheses. However, it should be noted that native HDL does not show any thermal transitions between 0°C-60°C, whereas its extracted lipids do show a phase transition between 20°C-40°C (40). This suggests that if altered chain packing in HDL was the

sole mechanism leading to chain mobility, then there should be some evidence of a phase transition between 0°C-60°C even though it may be broad and depressed.

The two most popular models for the conformation of cholesteryl esters in HDL particles (Fig. 32) are the "horseshoe" (Structure I) (Edelstein et al., 22) and the extended form (Structure II) (Laggner and Muller, 58). Treating the motions undergone by the ester acyl chain in the lipoprotein as symmetric about the labelled axis (Fig. 32), the quadrupolar splitting, $\Delta\nu_Q$, is modified by a factor $1/2 \langle 3\cos^2\theta - 1\rangle$, where θ is the angle between the symmetry axis for the molecular motion and the C-^{2}H bond, and the angular brackets represent the time average over all conformations of the molecule (95). Hence if cholesteryl palmitate adopted a horseshoe conformation in reconstituted HDL, a dramatic variation f the ^{2}H NMR line width versus chain position in the highly curved region of the acyl chain would be expected as a consequence of the changes in the average value of θ. In phospholipid liposomes containing deuterated cholesteryl ester, a local minimum of quadrupolar splitting is indeed observed at C4-C5 of the ester chain (142). A variation of this form is clearly not the case for the line width of deuterated cholesteryl palmitate in reconstituted HDL. On the other hand, if the ester chain were extended, the variation of the line width versus chain position might be expected to resemble the profile of quadrupolar splittings for the sn-1 chain in phospholipid bilayers, which is known to adopt an extended

Figure 32: Proposed conformation for cholesteryl ester in HDL. I, horseshoe conformation; II, extended conformation. the dashed lines represent the assumed axis of symmetry for the molecular motions.

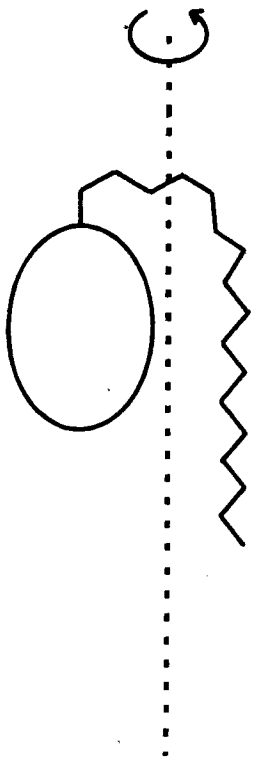

I

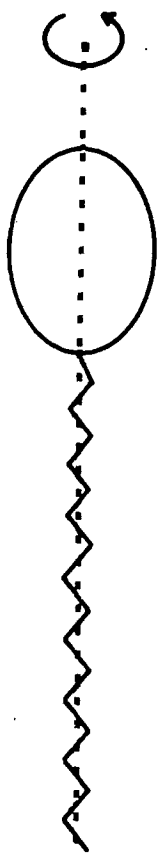

II

conformation (143). This is in fact observed for deuterated cholesteryl palmitate in reconstituted HDL (Table IV). In the present case, we observe a region of relatively constant line widths, which encompasses deuterons on C2-C6, while further down the chain the line widths decrease until reaching a minimum at C/6.

It has been shown that cholesteryl palmitate has finite solubility (up to 5 mol %) in phospholipid model membranes (59-62). Therefore, we expect a small amount of ester to be associated with the phospholipid monolayer of reconstituted HDL. The signal from the monolayer ester will be masked by the core-located ester. Thus the "extended" form probably refers solely to the ester in the core, as the ester in the surface monolayer would probably be in the horseshoe conformation.

For the core located ester our observations are consistent with the extended conformation (Structure II) proposed previously by Laggner and Muller (58). These authors also proposed that the cholesteryl ester molecules were radially distributed within the HDL particles. Assuming such an ordered distribution of cholesteryl palmitate in the lipoprotein, the carbon-deuterium order parameter $|S_{CD}|$ can be calculated using equation 15. Additional assumptions made are the presence of a radial director, and τ_e is due predominantly to the isotropic tumbling of the lipoprotein particle. The absolute values of the order parameter, $|s|$, calculated from the observed ^2H NMR line widths, are

shown in Fig. 33. For comparative purposes, we have also included the values for the sn-1 chain of 1-palmitoyl-2-oleyl phosphatidylcholine multilamellar liposomes. While the shapes of both order parameter profiles are quite similar, the values of $|s|$ for cholesteryl palmitate are higher than those of the equivalent positions of 1-palmitoyl-2-oleoyl phosphatidylcholine. This indicates that the angular excursions undergone by the ester chains in lipoprotein are more restricted than those of the acyl chains in multilamellar phospholipid bilayers. The highest order parameter ($|s| \tilde{} 0.38$) for cholesteryl palmitate is observed at C2 of the acyl chain, which probably reflects the motional restrictions imposed by the rigid cholesteryl moiety. However, the fact that all of the order parameters are less than the value of 0.5 expected for a chain undergoing only rapid rotation about its long axis suggests that significant angular fluctuations do occur. These fluctuations become of larger amplitude approaching the terminal methyl group, as evidenced by the progressive decrease of $|s|$ along the chain.

The longitudinal relaxation times, T_1, for the acyl chain of deuterated cholesteryl palmitate in reconstituted HDL are relatively constant at ~ 15 ms for all the C^2H_2 segments studied, while T_1 for the terminal C^2H_3 group is much larger at approximately 150 ms. This implies that the fast molecular motions responsible for longitudinal relaxation have approximately the same rate for the C^2H_2 segments but are significantly slower than those of the C^2H_3 group. Such a behaviour has been encountered previously for deuterated cholesteryl palmitate in phospholipid

Figure 33: Plot of order parameter versus acyl chain position. Plot of the absolute value for the C-2H order parameter ($|S|$) versus chain position for selectively deuterated cholesteryl palmitate in the reconstituted HDL at approximately 25°C (■___■), and for the sn-1 chain of 1- palmitoyl -2 oleoyl phosphatidylcholine at approximately 27°C C (△___△), Seelig and Seelig (143).

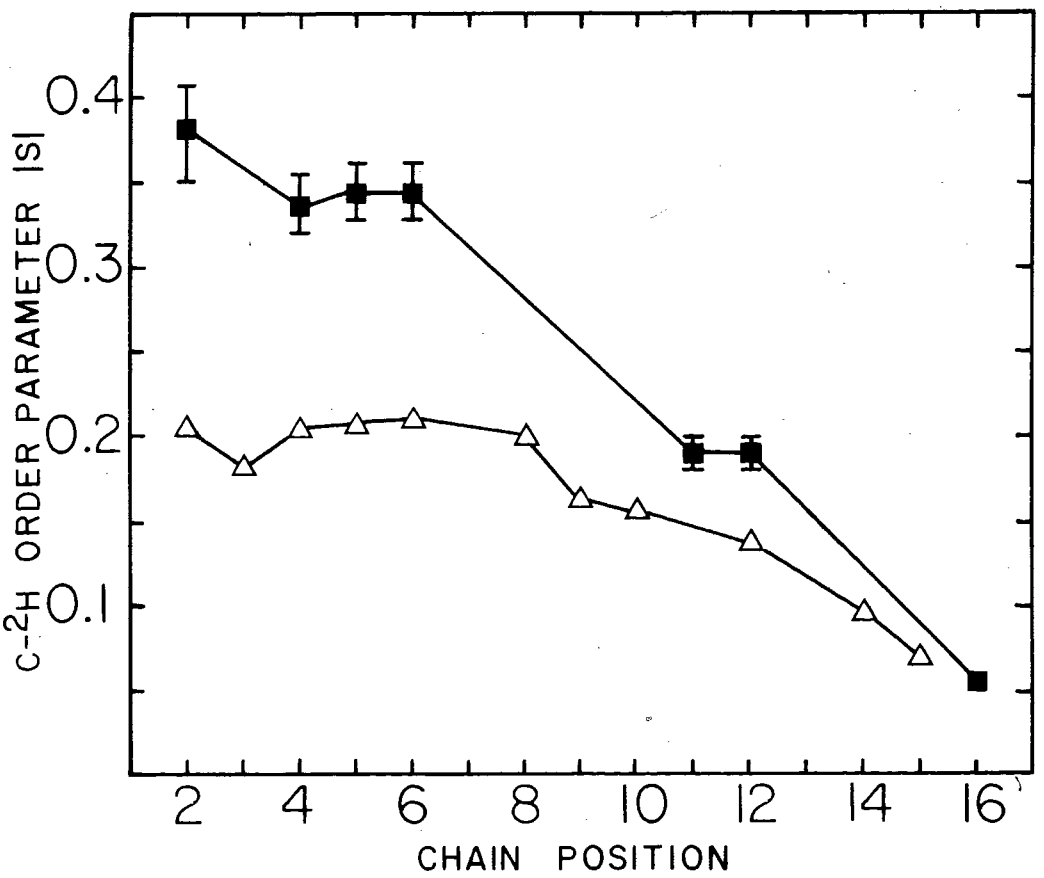
C-^{2}H ORDER PARAMETER |S|
0.4
0.3
0.2
0.1
2
4
6
8
10
12
14
16
CHAIN POSITION

vesicles (59,60). A quantitative interpretation of the longitudinal relaxation times of cholesteryl palmitate in reconstituted HDL is, unfortunately, difficult due to the small size of these particles. For deuterated cholesteryl palmitate in phospholipid vesicles, particle tumbling ($\tau_e \sim 10^{-6}$s) is too slow to appreciably influence T_1, and fast segmental motions appear to dominate longitudinal relaxation (60). This may not be the case for much smaller lipoprotein particles ($\tau_e = 5.9 \times 10^{-8}$s), so that an extreme narrowing condition does not apply.

II Molecular Motions of Phospholipid Surface Monolayer of Native HDL as Inferred from Selectively Deuterated Palmitic Acid.

Small amounts (<5 mol %) of selectively deuterated palmitic acids have been incorporated into native HDL_2 and HDL_3. The intimate association of palmitic acid and HDL was confirmed by Sepharose 4B gel exclusion chromatography (Figures 16 and 11). The electron microscopy studies of HDL_3 and ^{31}P NMR of HDL_3 and HDL_2 indicate that the added fatty acid does not alter the structure of native HDL. The mean diameter of 7.5 ± 1.4 nm for HDL_3 containing ~5 mol % [5,5,6,6-$^2H_4$] palmitic acid is similar to native HDL_3 whose mean diameter was 7.7 ± 1.2 nm in substantial agreement with literature value (Table I) (18). Furthermore, the mean diameter obtained from electron microscopy is in good agreement with the value of 7.8 ± 0.3 nm determined by sedimentation (134). In the case of HDL_2 we have used the value of 10.0 ± 1.0 nm for the hydrodynamic mean diameter as determined from gradient gel electrophoresiss and sedimentation velocity by Anderson et al. (134).

Fatty acids incorporated at low levels (<5 mol %) are known to be reliable probes of the dynamic behavior of phospholipid acyl chains in model membranes (144) and erythrocyte ghost membranes (145). Moreover in a recent comprehensive study, Pauls et al. (144) found that the carbon-deuterium order parameters of as much as 20 mol % of deuterated palmitic acid incorporated into dipalmatoylphosphatidylcholine multilamellar liposomes were within 10% of those of the phospholipid itself.

Tables V and X show that the line widths of selectively deuterated fatty acids in HDL's are dependent upon the position of selective deuteration and the type of lipoprotein. The values for deuterated palmitic acid in HDL_2 are somewhat larger than the equivalent positions of deuteration of palmitic acid in HDL_3. This might be expected as HDL_2 is a larger particle than HDL_3. The variation of line width with the position of deuteration of palmitic acid in both lipoproteins suggests the acyl chains of the surface monolayer possess anisotropic motions. The degree of anisotropy for a carbon-deuterium bond on the palmitic acid can be calculated by using equations (15 and 16). We will assume the anisotropic motions of palmitic acid intercalated into the surface monolayer of HDLs are axially symmetric about a radial director.

In order to calculate the segmental order S_{CD} for deuterated palmitic acid, a knowledge of the effective correlation time, τ_e in equation 16, for the isotropic motions is required (103). By use of our experimentally determined HDL_3 radius (3.75 $\pm$ 0.7 nm), the viscosity η = 0.89 cP of pure water and T = 298°K, we obtain the correlation time for particle tumbling $\tau_t = 4.8 \times 10^{-8}$s. The value of τ_t for HDL_2 using a radius of 5.0 $\pm$ 0.5 nm, η = 0.89 cP, T = 298°K is 1.13×10^{-7}s. The second contribution to τ_e is due to lateral diffusion of a phospholipid molecule around the highly curved lipoprotein surface. We have determined the diffusion coefficient of a number of lipids in both HDL_2 and

vesicles using the method of Cullis (117). Using ^2H- and ^{31}P NMR spectroscopy we find the value of $D = (2.0 \pm 1.0) \times 10^{-8}$ cm^2 S^{-1} for phospholipid in HDL_2 (see below). This approximates the value of $D = (2.5 \pm 0.4) \times 10^{-8}$ cm^2 S^{-1} measured for phospholipid diffusion in egg phosphatidylcholine vesicles at 25°C, but is lower than the value of $D = (7 \pm 1) \times 10^{-8}$ cm^2 S^{-1} for [$^2H_{31}$] palmitic acid in egg phosphatidylcholine vesicles (Wassall, S.R., Gorrissen, H., and Cushley, R.J., unpublished results). Using $D = (2 \pm 1) \times 10^{-8}$ cm^2 5^{-1}, we obtain $\tau_e = 4.8 \times 10^{-8}$s for HDL_3 and $\tau_e = 1.06 \times 10^{-7}$ for HDL_2. From the ^2H NMR line widths in Tables V and X the absolute values of the order parameters $|S_{CD}|$ for the selectively deuterated palmitic acids in HDLs were determined by means of equation 15. The values are listed in Table XV.

For comparison we have also shown the S_{CD} values of selectively deuterated stearic acids in egg phosphosphatidycholine multilamellar liposomes (106).

In HDL_2, the values of S_{CD} are 0.29-30 for deuterons on the C_2-C_6 positions and 0.23 for the 11, 12 positions. These values are somewhat lower than for the corresponding positions in HDL_3. The difference in the order parameters between HDL_2 and HDL_3 has also been observed from the ESR measurement using 5- doxylstearate incorporated into HDLs. More importantly, the acyl chains in the surface monolayer of both HDLs are considerably more ordered than those of the multilamellar liposomes.

TABLE XV: The order parameter $|S_{CD}|$ for selectively deuterated fatty acids in HDL_2 and HDL_3 (palmitic acids at ~25-27°C) and egg phosphatidylcholine multilamellar liposomes (stearic acids at 30°C).

[1]HDL_2	[2]HDL_3	Chain Position		Multilamellar[3] Liposomes
		Palmitic Acid	Stearic Acid	
0.27	0.38	2	2	0.24
0.30	0.38	4	4	0.24
0.30	0.37	5 (6)	7	0.23
0.23	0.23	11 (12)	12	0.17
0.04	0.05	16	18	0.02

[1]Based upon $\tau_e = 1.06 \times 10^{-7}$ s

[2]Based upon $\tau_e = 4.8 \times 10^{-8}$ s

[3]From Stockton *et al.* (106)

Since both HDL_2 and HDL_3 have small diameters (<100Å), this leads to a high degree of curvature for the phospholipids in the surface monolayer. It is conceivable that the high curvature in the surface monolayer may affect the acyl chain packing which may contribute to the observed line width. Therefore, we have studied phospholipid dispersions, i.e. unilamellar vesicles whose surface is also curved as models of the surface monolayer of HDLs.

As stated in the results section, the ^2H NMR lineshapes (Figure 17) for selectively deuterated palmitic acids in the unilamellar vesicles composed of egg phosphatidylcholine/sphingomyelin are a superposition of Lorentzian lines of varying widths produced by vesicles having a distribution of sizes. Therefore, simple line width measurement cannot be used to obtain an order parameter as in the case of HDL. Instead the heterogeneity of vesicle sizes must be categorized by binning the distribution since each fraction (bin) in the sample will result in a Lorentzian line of different width. Small sizes will contribute to the centre of the ^2H spectrum and the larger sizes will be reflected in the wings of the resonance. We have fractionated the vesicle size distribution into six size categories (Figure 19). Using equation 19, a theoretical ^2H NMR line shape was calculated by taking a superposition of spectral lines, statistically weighted in intensity according to the proportion of vesicles in each size category. Spectral simulations were computed for S_{CD} from 0.01 to 0.20 in 0.01 steps. The critical

test for a simulation based upon summing a series of Lorentzian lineshapes of different widths at half height is to be found in the faithfulness of the fit in the wings, i.e. far from the central frequency. Figure 34 shows the best fit simulation of [2,2-$^2H_2$] palmitic acid in unilamellar vesicle spectra. The order parameter $|S_{CD}| = 0.08$ yields a faithful reproduction of the observed spectra, whereas the value of $|S_{CD}| = 0.20$ is clearly much too broad. The best simulations of the other positions of deuteration are shown by dotted lines in Figure 35. For [16,16,16-$^2H_3$] palmitic acid simulations were computed for S_{CD} from 0.01 to 0.02 in 0.001 steps. The order parameters obtained from the simulations are plotted in Figure 36. As the purpose of the unilamellar vesicle study was to compare and contrast the acyl chain ordering with those of the surface monolayer of HDL, we have also plotted the HDL_3 values in Figure 36.

As can be seen in Figure 36, the shape of the order parameter profiles of palmitic acid in HDLs and egg phosphatidylcholine/sphingomyelin unilamellar vesicles are very similar. There is an "order plateau" of almost constant S_{CD} for the first few carbons in the chain followed by a progressive decrease towards the terminal methyl group. The $|S_{CD}|$ values for deuterated palmitic acid in the lipoprotein outer monolayer are considerably higher (~3-5 times) in the plateau region than the equivalent chain position in the vesicle bilayer.

Figure 34: Deuterium NMR spectrum (solid lines) of approximately 5 mol % [2,2-$^{2}H_{2}$] palmitic acid in unilamellar vesicles of 15% W/V egg phosphatidylcholine/beef brain sphingomyelin (85:15 W/W) in deuterium depleted water. The dotted line is a simulation obtained from equation 19 using $|S_{CD}|$ = 0.08 and 0.20.

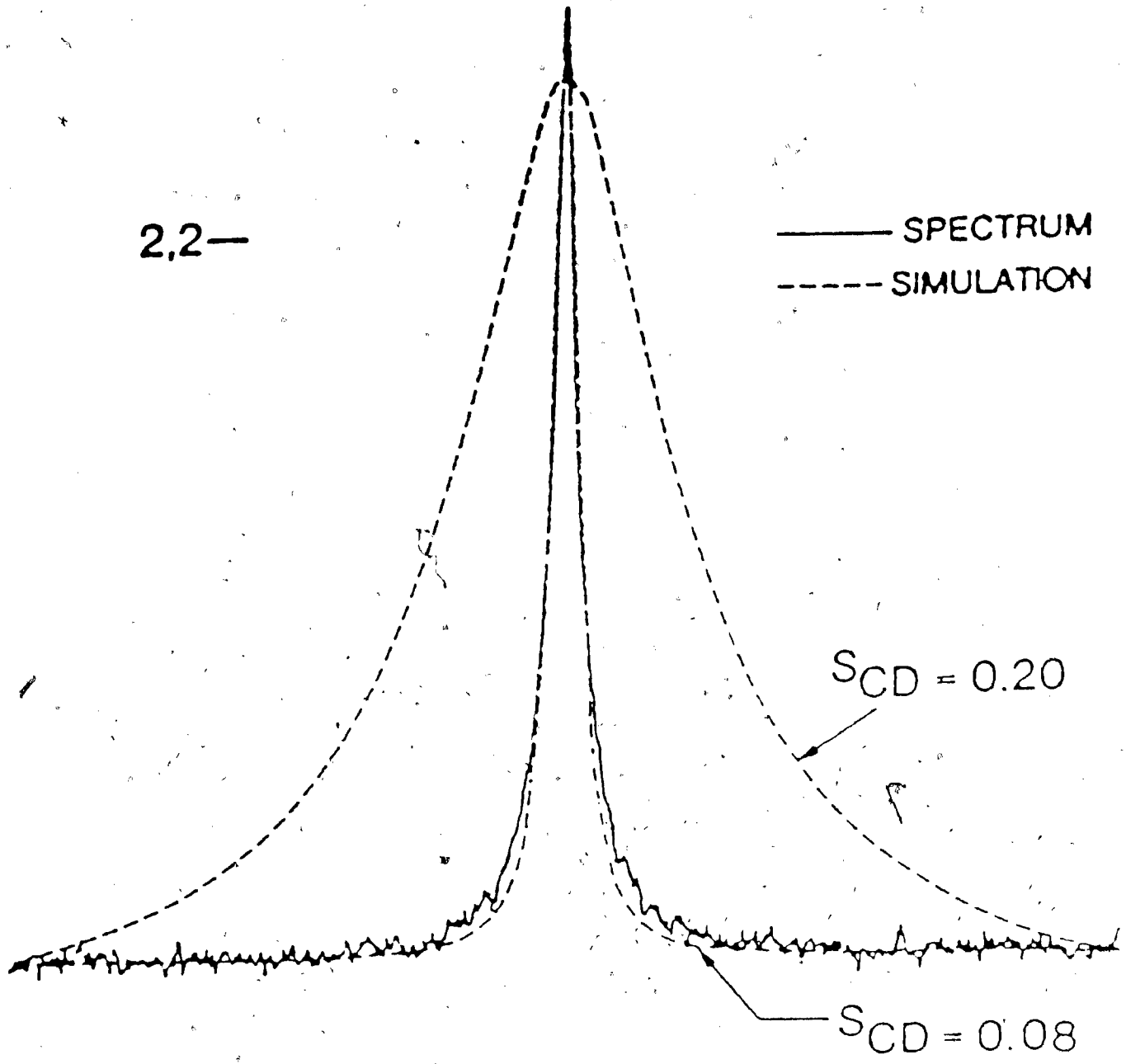
2,2—
SPECTRUM
SIMULATION
$S_{CD} = 0.20$
$S_{CD} = 0.08$

Figure 35: Deuterium NMR spectra (solid lines) of ~5 mol % selectively deuterated palmitic acids in unilamellar vesicles of 15% W/V egg phosphatidylcholine/beef brain sphingomyelin (85:15 W/W) in deuterium-depleted water. Position of selective deuteration is indicated to the left of each spectrum. The dotted lines are the best fit superposition of Lorentzian lines simulating the spectrum by using the order parameter $|S_{CD}|$ indicated.

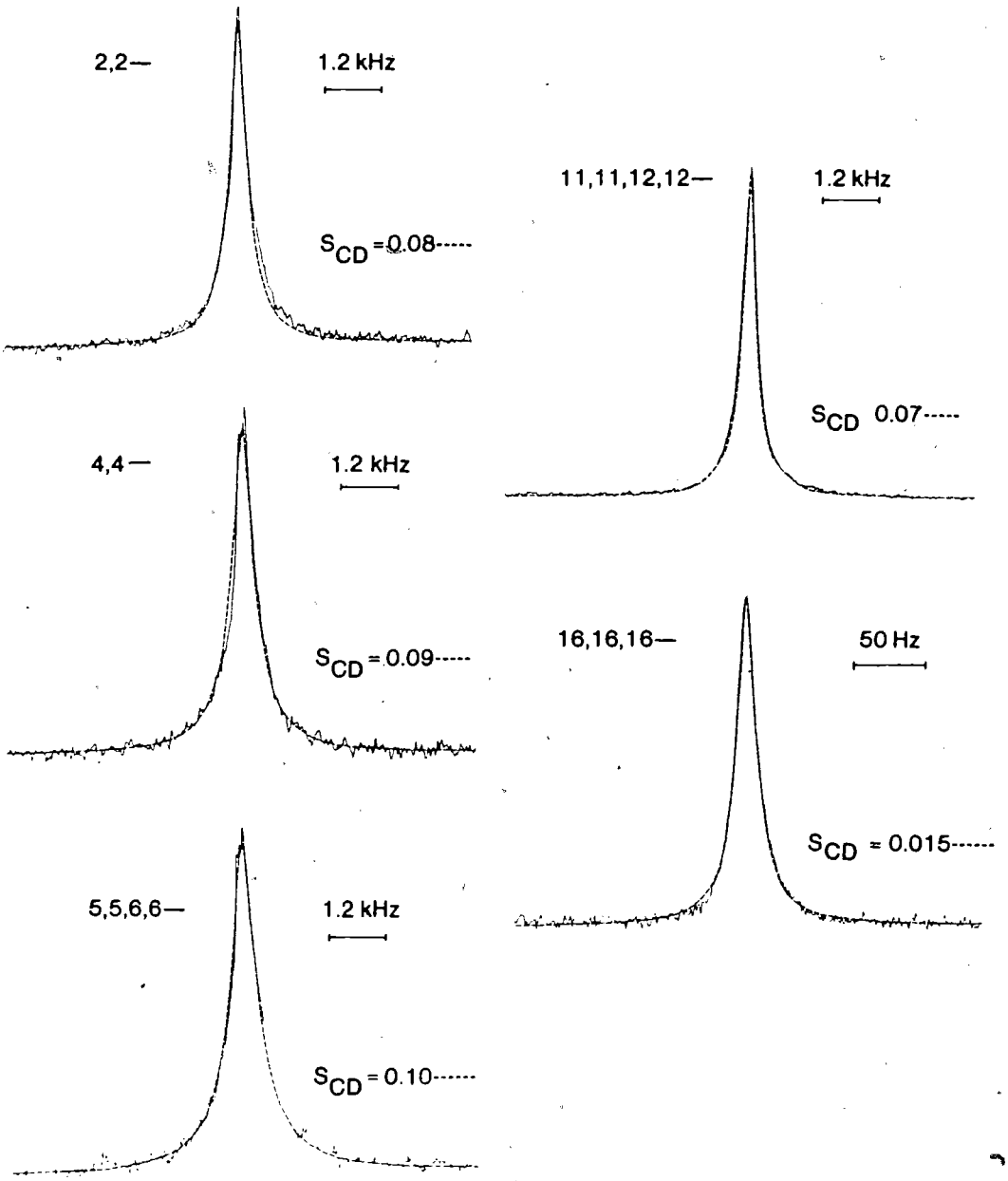
2,2—
1.2 kHz
S_{CD} = 0.08-----
4,4—
1.2 kHz
S_{CD} = 0.09-----
5,5,6,6—
1.2 kHz
S_{CD} = 0.10------
11,11,12,12—
1.2 kHz
S_{CD} 0.07-----
16,16,16—
50 Hz
S_{CD} = 0.015------

Figure 36: Plot of the absolute value of the order parameter $|S_{CD}|$ vs. acyl chain position for selectively deuterated palmitic acid incorporated into HDL_3 (●—●) and into egg phosphatidylcholine/sphingomyelin unilamellar vesicles (■____■) at ~25-27°C. The S_{CD} values for selectively deuterated stearic acids in egg phosphatidylcholine multilamellar liposomes at 30°C (▵____▵), Stockton *et al.* (106), are also included.

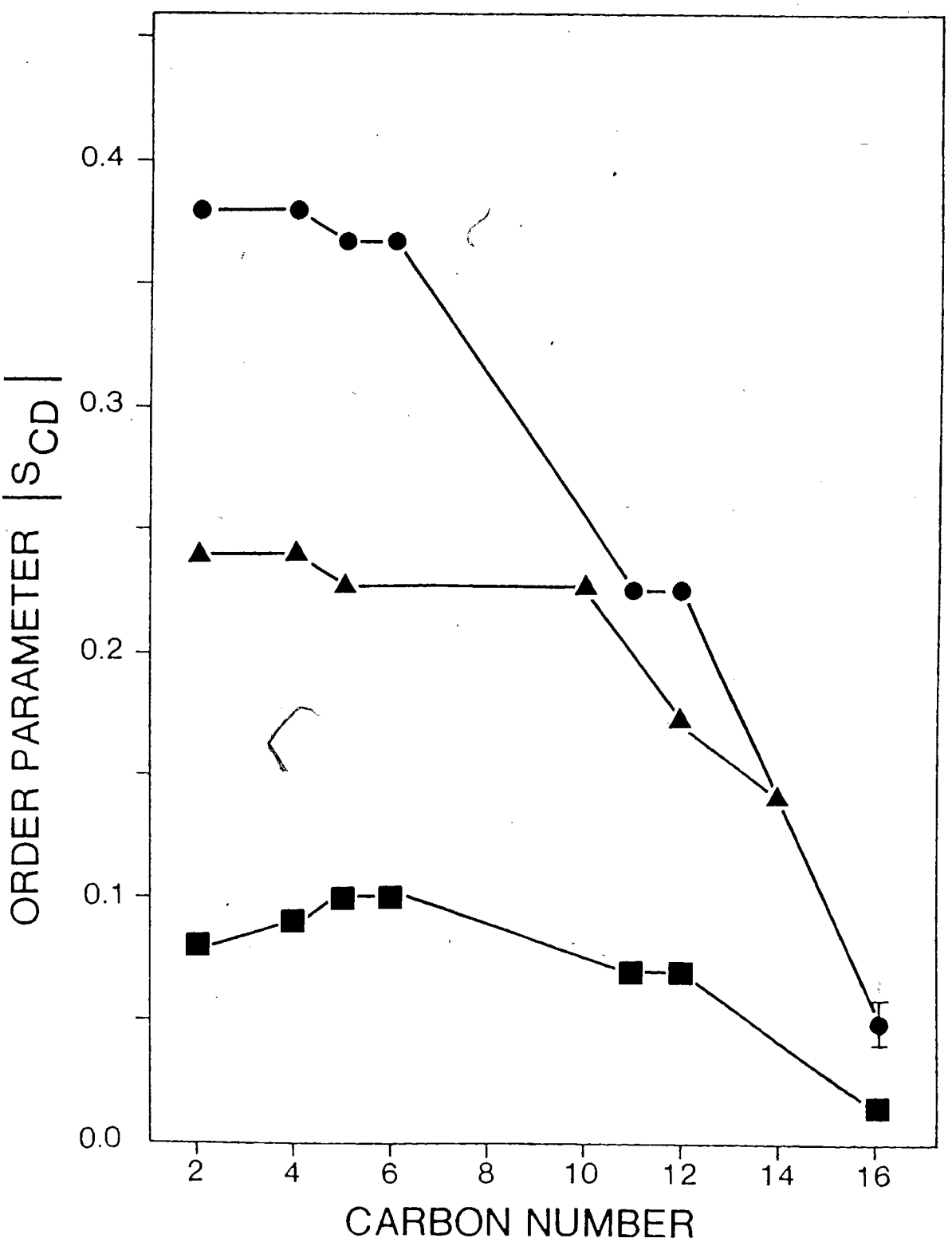
ORDER PARAMETER $|S_{CD}|$
0.4
0.3
0.2
0.1
0.0
2
4
6
8
10
12
14
16
CARBON NUMBER

A possible reason for the higher order of the surface monolayer in HDL's may be due to the presence of cholesterol. In a comprehensive study, Stockton and Smith (146) found that the molecular order of egg phosphatidylcholine multilamellar liposomes in liquid crystalline phase increased linearly with the addition of cholesterol. At approximately 33 mol % cholesterol, the acyl chain molecular order for the positions 2-11 increased approximately 1.7 times. Using the composition of native HDLs, we have found that if all of the cholesterol is associated with the surface monolayers, then mol % cholesterol with respect to the phospholipid in the monolayer are 23.1 and 26.4 for HDL_2 and HDL_3, respectively. Using Figure 11 in Smith et al. (92), we expect an increase in $|S_{CD}|$ of 1.33 times for HDL_2 and 1.47 times for HDL_3. This should be considered an upper limit since there is some evidence that ~40% of the HDL cholesterol may be in the core (74). Therefore we conclude that higher acyl chain order in the monolayer of HDL is not due solely to the presence of cholesterol in the monolayer.

It may be argued that fatty acid in HDL_2 and HDL_3 exhibits a higher orientational order due to the presence of protein in the outer layer. Using the number of protein and phospholipid molecules per particle reported by Verdery and Nicholls (147) we obtain a molar ratio of phospholipid/protein of 14/1 for HDL_3 and 26/1 for HDL_2. At such a low phospholipid/protein ratio a substantial effect of the protein on the behaviour of the phospholipid chains might be expected. However, ^2H NMR studies

of protein/phospholipid model membranes (148,149) indicate that, at least on the ^2H NMR timescale, there is no appreciable acyl chain ordering effect due to the proteins.

Laggner and Muller (58) have proposed a model for the structure of HDL in which cholesteryl esters, triglycerides and perhaps some cholesterol occupy the core of HDL particle and are arranged in a radially symmetric pattern. Such an arrangement would result in the interdigitation of the phospholipid acyl chains, located in the surface monolayer, with the ester and triglyceride acyl chains as well as with the rigid cholesteryl molity of the cholesteryl esters. This interdigitation and the resulting spatial restrictions within the outer monolayer could conceivably result in higher order parameters of the phospholipid chains, hence also fatty acid probes, in HDL.

It is also important to note that the acyl chain order observed for the phosphatidycholine/sphingomyelin vesicles is at least two times lower than egg phosphatidycholine multilamellar liposomes. It may be argued that the presence of 15% sphingomyelin results in the lowering of the acyl chain order in the unilamellar vesicles. However, the ^2H NMR spectrum of ~5 mol % [5, 5, 6, 6- $^2H_4$] palmitic acid in egg phosphatidylcholine vesicles yielded $\Delta\upsilon 1/2$ = 520 Hz which approximates the line width obtained in the presence of sphingomyelin (Table VIII). These results are in contrast to the ^2H NMR and ^1H NMR studies of unilamellar vesicles, where it was concluded that the acyl chains of both vesicles and multilamellar liposomes have the same order

(150,103,106).

The present results with selectively deuterated palmitic acids can be compared directly with the pioneering work of Stockton et al. (106) who studied selectively deuterated stearic acids in egg phosphatidylcholine unilamellar vesicles. The line widths obtained by those authors were 1.2 - 1.3 kHz for positions C_2-C_{10} and 800 Hz for the C_{12} position. These values are considerably larger than obtained in this study. We do not know the basis for this discrepancy. However, as can be seen from equations 16 and 17, the value of the line width obtained depends upon the size of the vesicles; hence, Stockton et al. (106) may have larger vesicles in their preparation than the present study. In calculating the order parameter, S_{CD}, those authors assumed homogeneous (with respect to size) vesicles with a diameter = 20.0 nm. In contrast, we have measured the size of unilamellar vesicles by negative staining electron microscopy. We found vesicles to be very heterogeneous having diameters <25.0 nm to 60.0 nm, with a mean diameter of about 30.0 nm, Figures 18 and 19. The heterogeneity of vesicle sizes has also been observed by Bloom et al. (103). We have considered this heterogeneity in our linewidth analysis (see above).

An objection to our method of size measurement (i.e. negative staining) is that during the staining procedure (drying) vesicles tend to collapse on the grid to produce flattened structures. Therefore, the measured size is artificially higher.

If this were the case, we should expect to see a random distribution of on edge and on face views of the flattened structures in the micrographs. We do not observe this (see Figure 18) and, in fact, most of the structures exhibit circular dimensions. Assuming all of the structures are flattened discs we have calculated the decrease in diameter on transforming a disc to a spherical vesicle. A disc of 8.0 nm thickness and diameter ranging from 20.0 nm to 50.0 nm corresponds to a decrease in diameter from 5-13%. Using these values for the diameter, the value of S_{CD} is only 0.02 higher.

III Selectively Deuterated Phosphatidylcholine in Native HDL_2

As stated earlier, deuterated fatty acids yield a reliable measurement of $|S_{CD}|$ for the HDL phospholipids. Nevertheless, the presence of fatty acid introduces a net negative charge to the HDL particle. Hence the value of $|S_{CD}|$ obtained for the upper position of the acyl chain may be inaccurate. We have, therefore, incorporated (<5 mol %) a phosphatidylcholine selectively deuterated along the sn-2 acyl chain into native HDL_2 particle by mild sonication. This technique yielded an unperturbed lipoprotein particle as shown by ^{31}P NMR (see Results, Section R.V.).

The ^2H NMR line widths obtained for the various positions of deuteration as a function of temperature are shown in Table IX. As in the case of selectively deuterated fatty acid (Section D.II), we have calculated the carbon-deuterium order parameter $|S_{CD}|$ using equations 15 and 16. We have used the literature value of HDL_2 radius = 50Å (138). The $|S_{CD}|$ calculated for the various positions are shown in Table XVI.

At 15°C there is a plateau region of the positions C_2-C_7 of nearly constant $|S_{CD}|$. The order parameter decreases at C_{11}, C_{12} before reaching a minimum at the C^2H_3 segment. These results are in good agreement with the results obtained from selectively deuterated palmitic acid in HDL_2. At 25°C the $|S_{CD}|$ profile of selectively deuterated phospholipid remains the same at 15°C except that the value for the [2, 2- $^2H_2$] position is increased

TABLE XVI: The temperature dependence of the order parameter |SCD| of phosphatidylcholine selectively deuterated along the sn-2 chain incorporated (~5 mol %) into native HDL_2.

Chain Position	|SCD|		
	15°C	25°C	40°C
2-	0.28	0.30	0.32
4-	0.27	0.27	0.28
7-	0.27	0.27	0.28
11,12-	0.22	0.21	0.15
16-	0.05	0.05	0.05

and the [11, 11, 12, 12 - $^2H_4$] position is decreased. As the temperature is raised to 40°C there is a further increase in order at [2, 2 - $^2H_2$] position and a dramatic decrease in S_{CD} for the [11, 11, 12, 12, - $^2H_4$] position.

By analogy to multilamellar liposomes where the 2 position of the sn-2 chain has smaller quadrupolar splittings than the rest of the plateau region, we expect a smaller line width for the 2 position of the sn-2 chain labelled phospholipid in HDL_2 (96). In fact a higher value of the line width and consequently the $|S_{CD}|$ is observed, compared to the remaining position of the plateau region, at all temperatures studied. Furthermore, the increase in $|S_{CD}|$ for the upper positions of the selectively deuterated phospholipid acyl chains in HDL_2 with temperature is in contrast to a uniform decrease in $|S_{CD}|$ observed for the deuterated phospholipid in multilamellar liposomes (96). On the basis of the above observation, we believe that either the conformation or the ordering of the phospholipids is different in HDL_2 as compared with the phospholipids in multilamellar liposomes. We favour the conformation hypothesis because such a hypothesis is also put forth to account for the large ^{31}P chemical shift anisotropy measured for HDL_2 (see Section D.V, pp.187-204). We suggest that the phospholipid headgroup is extended in HDL_2 i.e. the O-P-O plane is parallel to the monolayer surface.

The increase in order parameter for the upper region of the hydrocarbon chain obtained as the temperature is increased is

also observed in potassium palmitate bilayers (151). This is explained by the fact that the polar group of the soap molecular is anchored at the lipid/water interface. At lower temperature in the L_α phase, the molecular axis is not strictly parallel to the bilayer normal. But higher temperatures, the area per polar head group is larger, and the molecular axis becomes essentially parallel to the bilayer normal. Thus an increase in the apparent order parameter, $|S_{CD}|$, is observed. Such a hypothesis may also explain the order parameter increase with temperature observed for the selectively deuterated phospholipid in HDL_2 monolayer.

Another possibility for an increase in $|S_{CD}|$ observed with increase in temperature for the upper region of the acyl chains is "liquid-protein" interaction. It should be noted that such an interaction has not been observed on the ^2H NMR timescale for fluid lipids (148-149). We consider this possibility because the HDL apoproteins are significantly different than those proteins studied previously. The HDL apoproteins are surface proteins, i.e. they do not traverse the HDL particle (41). These apoproteins are arranged in an amphipathic helix which orients parallel to the curvature of the HDL surface (42). It has been proposed that the ionic (polar amino acid residues) may interact with the zwitterionic phosphate headgroup of HDL phospholipids. It is conceivable that, as the temperature is raised the protein occupies a greater surface area on the HDL_2 particle and through electrostatic interaction restricts the motions of the headgroup; hence an increase in $|S_{CD}|$ for the upper portion of the phospholipids is observed.

The disordering effect in the C11, C12 region of the phospholipid acyl chains may be interpreted as follows. At higher temperatures the area per polar headgroup is larger causing an increase in the lateral pressure within the HDL_2 monolayer. The anchoring of the polar headgroup maintains the higher order in the upper region at higher temperatures. The increase in area for the acyl chains reduces the order for the lower region of the acyl chains.

It is also possible to argue that increase in disorder at higher temperature observed for the C11, C12 region is due to the intercalation of the core constituents into the monolayer. Upon heating, the core constituents (cholesteryl esters) become disordered; hence their ordering effect on the phospholipid acyl chains would be reduced. This effect being greatest at the C11, C12 position may reflect the extent of interdigitation of the core components.

It is clear from the above comments that the temperature dependence of $|S_{CD}|$ is not fully understood at present. Further research is required to clarify this important point.

IV Longitudinal Relaxation Times

The ^2H NMR longitudinal relaxation times measured for selectively deuterated palmitic acids in HDL_2 and HDL_3 (Tables VII and VI) and for selectively deuterated phospholipid (Table X) exhibit a profile in which the relaxation rate $1/T_1$ is approximately constant at $\sim 70 \pm 20 S^{-1}$ for positions 2-11,12 and falls off to $\sim 5\ S^{-1}$ at the 16 position. The shape of this profile, with its plateau region of approximately constant values for the upper portion of the acyl chain, is qualitatively similar to that observed for liquid crystalline dipalmitoylphosphatidylcholine membranes (152). In contrast, the actual rates in HDL's are, apart from the terminal methyl, a factor of >2 X greater than in the phospholipid bilayers. Although the difference in resonant frequency ν_o of the two sets of measurements (38.8 vs. 54.4 MHz) may be a significant contributing factor, the higher longitudinal relaxation rates suggest that the molecular motion(s) responsible are slower in the lipoprotein monolayer than in the model membrane and/or the presence of additional motion(s) in the case of HDL_3. ^{13}C NMR relaxation times for HDL that are shorter than for liposomes prepared from HDL lipids have been reported previously (48,49).

No definitive interpretation of spin lattice relaxation in lipid bilayers has been presented. Analysis solely in terms of a fast correlation time representing segmental motions is inadequate, since, in particular, a dependence of resonance frequency is observed of the form

$$\frac{1}{T_1} = A\tau_f + B/Wo^{1/2}$$

where A and B are constants. Slow collective order fluctuations described by a distribution of correlation times (111) and diffusion of defects (e.g. kinks) up and down the acyl chains (112) are the relaxation mechanisms that have been proposed.

Table VI illustrates that the T_1's measured at 25°C for [5,5,6,6-$^2H_4$] palmitic and [16,16,16-$^2H_3$] palmitic acids in HDL_3 increase by ~45 and 17% respectively between 38.8 and 61.4 MHz. ^{13}C NMR relaxation times which increase with resonant frequency have similarly been reported for HDL (53). The trend is thus qualitatively in agreement with the behaviour seen in liquid crystalline phospholipid bilayers. On the basis of the current ^2H NMR data, obtained at only two resonant frequencies, it is not possible to decide upon the exact nature of the molecular motions determining the relaxation in the lipoprotein monolayer. The situation in HDL's is further complicated by the possibility that particle tumbling (τ_t ~10^{-7}s) is itself fast enough to influence the longitudinal relaxation time (153).

Table X shows the T_1 behaviour of deuterated phospholipid in HDL_2 as a function of temperature. As the temperature is increased from 15°C to 40°C the T_1's remain essentially unchanged for the C_2 - C11,12 positions; however, the terminal methyl T_1 is increased from ~150 ms to 240 ms. The invariance of T_1 with

temperature for the upper positions is in contrast to the behaviour of phospholipid bilayers in the liquid-crystalline phase (152). The exact nature of the motions in HDL is not known. However, it could be that the acyl chains of the HDL surface monolayer are less flexible than the corresponding positions of the phospholipid bilayers.

V Diffusion of Phospholipids in HDL_2

Both the sphingomyelin and phosphatidylcholine resonances of HDL_2 had similar ^{31}P NMR linewidths (6 ± 1 Hz at 40 MHz and 29 ± 3 Hz at 102.2 MHz) suggesting these lipids are homogeneously mixed in HDL. We have measured the lateral diffusion coefficient of surface phospholipids in HDL_2 by the method of Cullis (117). In this technique the rotational correlation time of HDL, τ_T, hence the linewidth of HDL_2 phospholipid resonances is varied as a function of the medium viscosity (see Section D.II, pp.45-46). The solvent viscosity can be altered significantly by adding aliquots of glycerol to the sample.

The linewidth, $\Delta\upsilon 1/2$, is given by equation 30 which can be expressed as follows:

$$\frac{1}{\Delta\upsilon_{1/2}-C} = \frac{1}{\eta}\left(\frac{3\ kT}{M_2\ 4\pi R^3}\right) + \frac{6D}{M_2 R^2} \qquad (32)$$

A plot of $(\Delta\upsilon 1/2\text{-}C)^{-1}$ vs η^{-1} gives a straight line for which the ratio of intercept/slope is given by

$$\frac{\text{Intercept}}{\text{Slope}} = \frac{8\pi\ DR}{kT} \qquad (33)$$

Thus, making no assumptions for the value of second moment, M_2, D can be obtained provided R is known.

From the ^{2}H NMR and ^{31}P NMR linewidth variation as a function of the solvent viscosity (Tables XI and XIII) we have obtained plots of $(\Delta\nu_{1/2}\text{-C})^{-1}$ vs η^{-1}. Both ^{31}P NMR (Figure 37) and ^{2}H NMR (Figure 38) data give a good fit to a straight line. The solid line is the least squares fit to the data, with correlation coefficient = 0.9956 and 0.9907 ^{31}P NMR data (Figure 37) and ^{2}H NMR data (Figure 38), respectively. The dotted lines in Figures 37 and 38 are drawn through extremes of the error limits. Using a radius of 5.0 nm for HDL_2, we obtain D = (2±1) x 10^{-8} cm^2 s^{-1} for ^{31}P NMR data (~25°C) D = (1.6±1) x 10^{-8} cm^2 s^{-1} for ^{2}H NMR data (~25°C). These values proximate those obtained for pure phospholipid bilayers (117).

Employing the equations 15, 16 and 30 and D = 2.0 x 10^{-8} cm^2 s^{-1}, a theoretical variation of linewidths can be generated for the solvent viscosities employed. Such predicted linewidths are plotted (solid lines) on Figures 25, 28. Close agreement is found between the experimental data and those predicted by equation 30.

In calculating the theoretical curve we have used the value of the second moment obtained from the graph for both the ^{2}H and ^{31}P data (Figures 28 and 25). Using S_{CD} = 0.02 we calculate the residual second moment M_{2R} to be 2.04±0.5 x 10^{7} s^{-2} which is in substantial agreement with the value of 2.14 x 10^{7} s^{-2} obtained from a $(\Delta\nu_{1/2}\text{-C})^{-1}$ vs η^{-1} plot (Figure 38).

Figure 37: Plot of $(\Delta\nu 1/2\text{-}C)^{-1}$ vs. η^{-1} obtained from ^{31}P NMR (undecoupled at 102.2 M Hz) line widths of native HDL_2 containing 16-[$^2H_3$] phosphatidylcholine as a function of glycerol concentration.

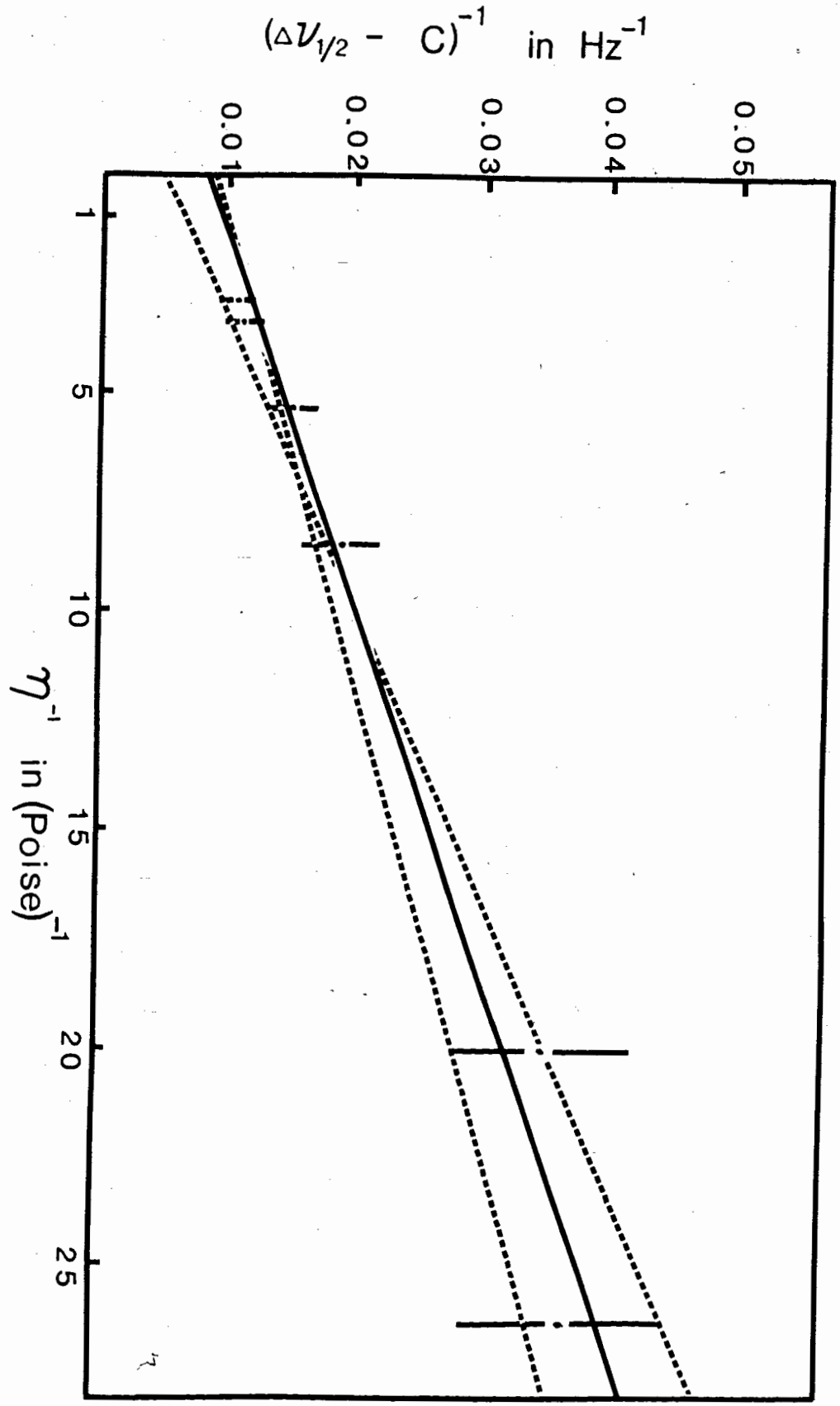
$(\Delta\nu_{1/2} - C)^{-1}$ in Hz^{-1}
0.01
0.02
0.03
0.04
0.05
1
5
10
15
20
25
η^{-1} in $(Poise)^{-1}$

Figure 38: Plot of $(\Delta\upsilon 1/2\text{-}C)^{-1}$ vs. η^{-1} obtained from ^2H NMR line widths methyl deuterated phosphatidylcholine in HDL_2 as a function of glycerol concentration.

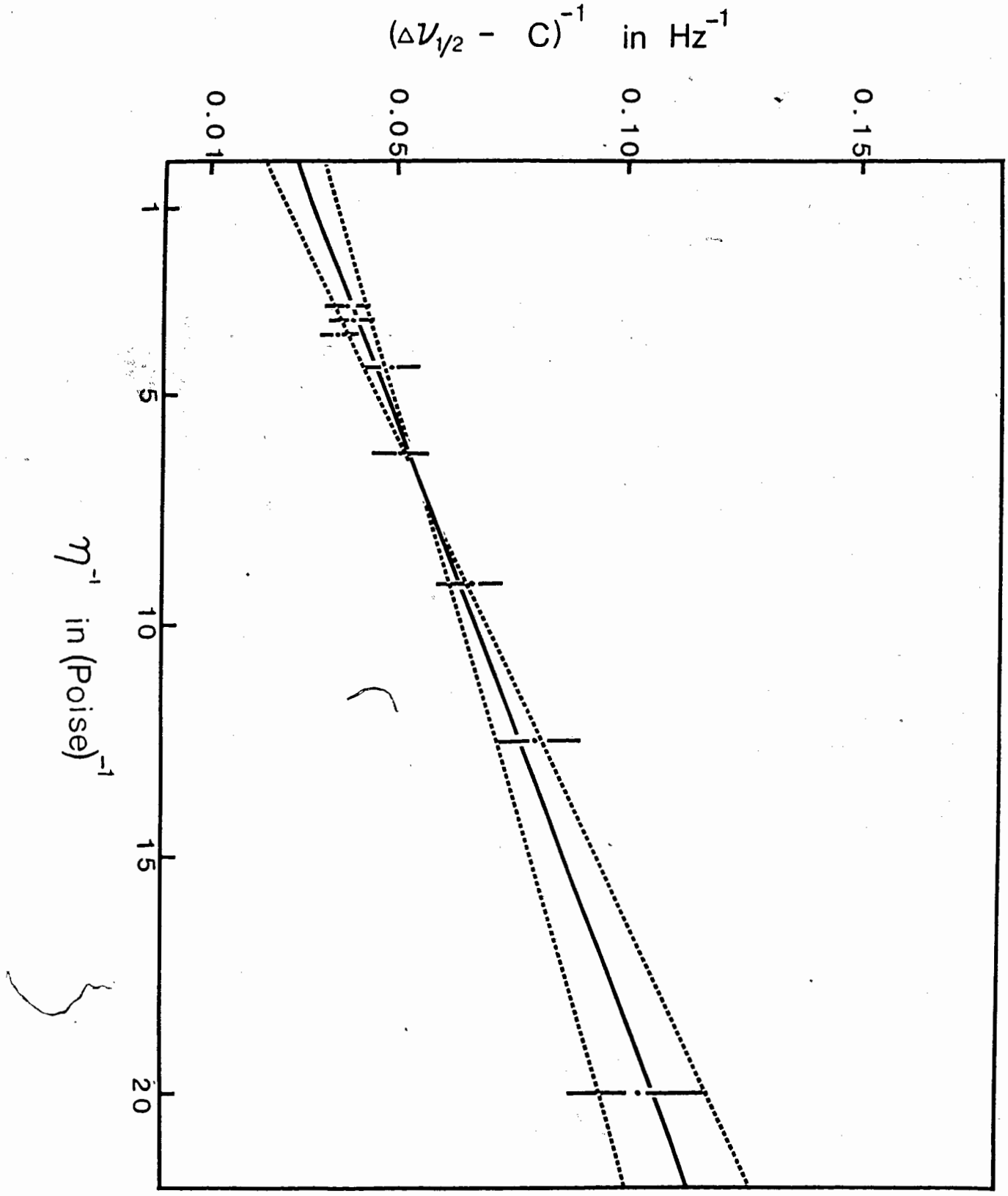
$(\Delta\nu_{1/2} - C)^{-1}$ in Hz^{-1}
0.01
0.05
0.10
0.15
1
5
10
15
20
η^{-1} in $(Poise)^{-1}$

The value of the residual chemical shift anisotropy obtained from the ^{31}P NMR data (Figure 37) of HDL = 75±10 ppm is considerably larger than $\Delta\sigma$ = 40 ppm for phospholipid bilayers. In order to account for the discrepancy we have varied the lateral diffusion coefficient and the radius of the particle. Assuming $\Delta\sigma$ = 40 ppm and R = 5.0 nm, we have obtained theoretical curves for D = 0, D = 5 x 10^{-9}, and D = 2.5 x 10^{-8}, which are plotted on Figure 39. It is apparent that none of the values of lateral diffusion coefficient fit the experimental data. In Figure 40 the value of R was varied from 6.0 to 8.0 nm, with $\Delta\sigma$ = 40 ppm and D = 2 x 10^{-8} cm^2 s^{-1}. A satisfactory fit to the experimental data is observed when R = 7.0 nm. This value of R for HDL_2 is considerably larger than reported in the literature (134). Anderson et al. (134) have measured the radius of particles from the density range = 1.063 - 1.125 g mL^{-1}, which is similar to the preparation in the present study. Using negative staining electron miscroscopy, sedimentation velocity and gradient gel electrophorosis the values of diameter obtained were 11.0 ±0.5 nm, 10.0 ± 0.5 nm, respectively. Therefore it is unlikely that we have underestimated the size of HDL_2 to such a large extent. The large value of $\Delta\sigma$ obtained for HDL_2 may indicate differences in the headgroup conformation and/or motion betwen HDL_2 and phospholipid bilayers. The value of the ^{31}P residual chemical shift anisotropy is known to depend upon the motions of the headgroups in phospholipid bilayers (115). For dipalmitoyl phosphatidyl choline bilayers $\Delta\sigma$ decreases from ~69 ppm in the gel phase at -10°C to ~45 ppm in the liquid

Figure 39: Plot of ^{31} NMR Line Width of HDL_2 as a Function of Solvent Viscosity. The Dotted Lines are Calculated Fits with the Different Lateral Diffusion Coefficient, D, and using $\Delta\sigma$ = 40 ppm and Radius = 50.0Å.

The variation of ^{31}P linewidth of HDL_2 as a function of solvent viscosity

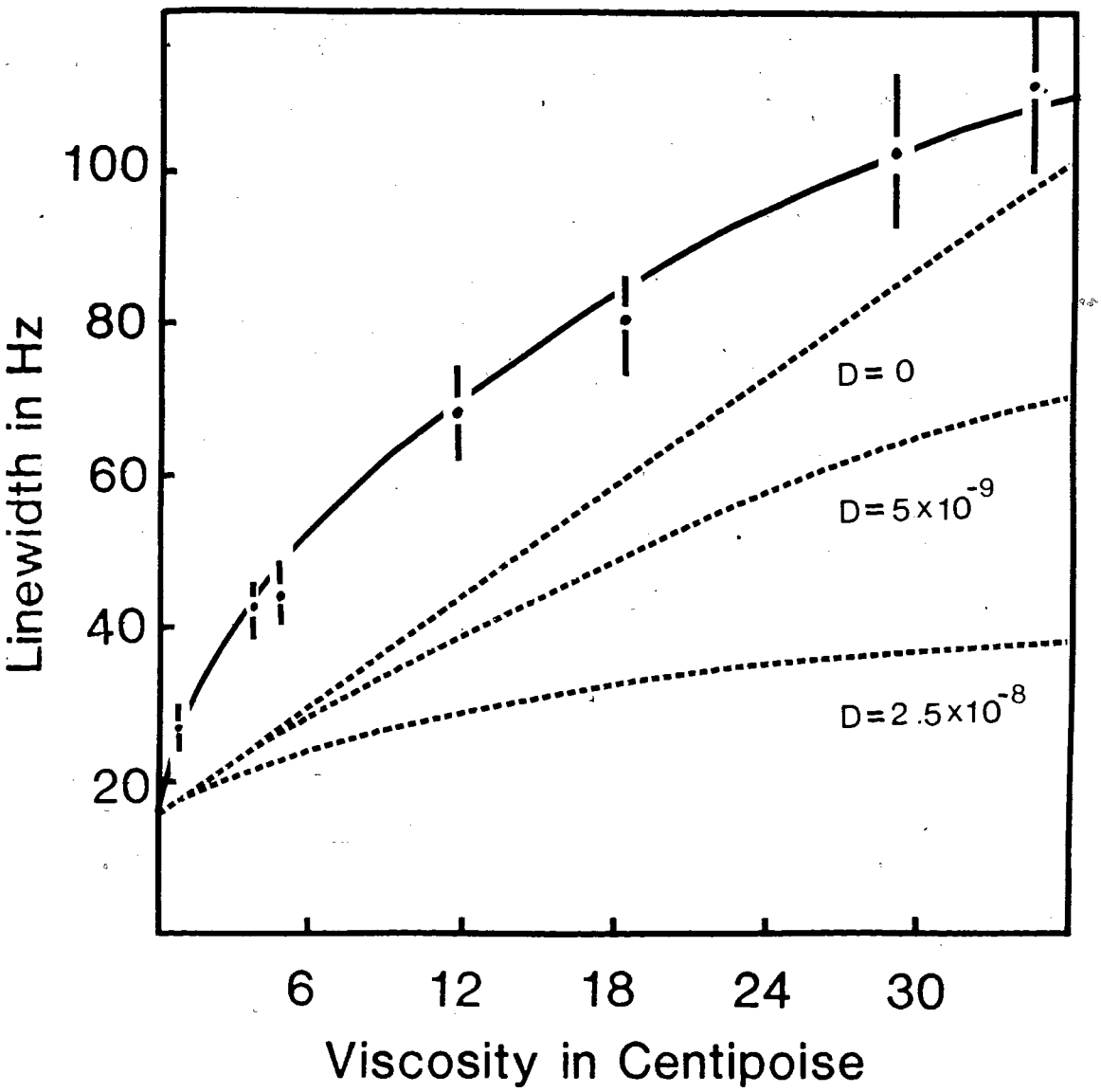

Figure 40: Plot of ^{31}P NMR Line Width of HDL_2 as a Function of Solvent Viscosity. The Dotted Lines are Calculated Fits with Different Radii and using $\Delta\sigma$ = 40 ppm and D = 2.0×10^{-8} cm^2 s^{-1}.

The variation of ^{31}P linewidth of HDL_2 as a function of solvent viscosity

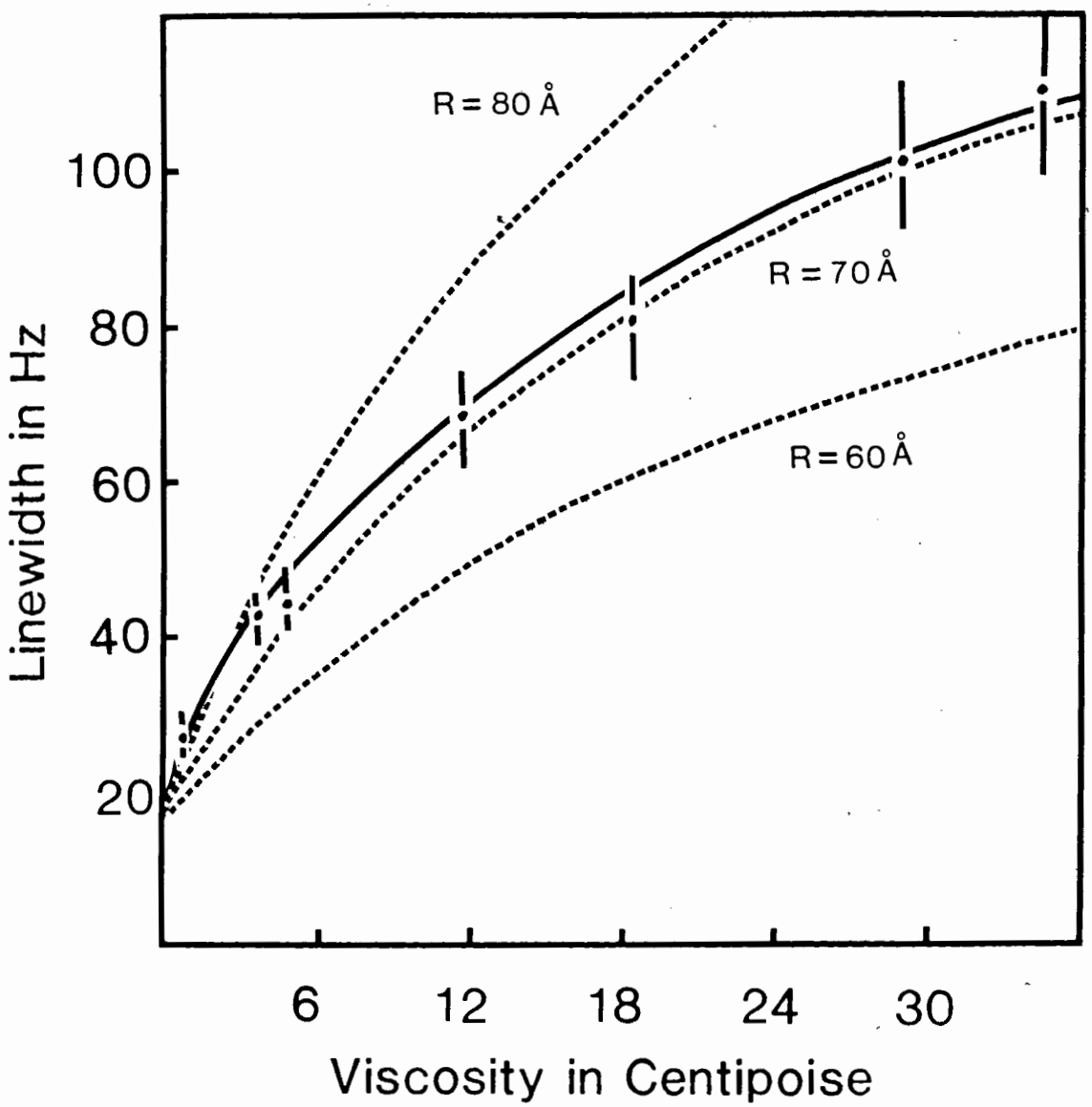

crystalline phase at 48°C (115). This decrease in $\Delta\sigma$ is attributed to the onset of rapid rotation about the C(2)-C(3) axis of the glycerol backbone and wobbling of the headgroup coupled with the conformational transitions. The large value of $\Delta\sigma$ observed for HDL_2 cannot solely be due to the absence of the above mentioned motions as the HDL_2 phospholipids are well above the gel-liquid crystalline phase transition at 25°C. This is borne out by the fact that the lateral difusion coefficient, D = 2×10^{-8} cm^2 s^{-1} at $\sim$25°C which is similar in value (117, 89) to the pure phospholipid bilayers in the liquid crystralline state.

The headgroup conformation of egg phosphatidylcholine bilayers have been examined by neutron diffraction and of dipalmitoylphosphatidyl-choline bilayer by ^{31}P NMR (114,154). The H_2O/D_2O differential neutron diffraction results are consistent with the choline group being in the plane of the bilayer. The ^{31}P result of the dipalmitoylphosphatidyl-choline in the liquid-crystalline phase, with $\Delta\sigma$ ~45 ppm is consistent with the O-P-O plane of the headgroup being oriented 50° with respect to the bilayer plane (154). Griffin et al. (154) have also calculated $\Delta\sigma$ for dipalmitoylphosphatidylcholine bilayer in both the gel and liquid crystalline phase with the O-P-O plane parallel to the bilayer plane. The extended conformation of the headgroup yields spectra whose breadth is ~80 ppm in the liquid crystalline phase. This value is coincident with the value of $\Delta\sigma = 75 \pm 10$ ppm obtained for HDL_2.

Since the residual chemical shift anisotropy of HDL_2 is considerably larger than that of phospholipid bilayers, the possibility that glycerol altered the HDL_2 structure was considered. The effect of glycerol on the ^{31}P NMR of phospholipid multilamellar liposomes has been studied by Cullis (117), who observed no change in the residual chemical shift anisotropy even at 85% glycerol concentration. Glycerol also has no effect on the dipalmitoylphosphatidycholine multilamellar liposomes in the liquid crystalline phase as shown by X-ray diffraction (155). However, glycerol causes extensive interdigitation of the acyl chain below the liquid-crystalline phase. Following these observations we believe that glycerol probably has very little direct affect on the phospholipid headgroup in HDL_2, but could affect the HDL_2 apoprotein structure and thereby cause changes in the phosphate group conformation.

Control experiments were performed to check the indirect effect of glycerol on the HDL_2 structure. Firstly, an η = 26 cp sample was diluted to η = 19 cp. The ^{31}P NMR linewidth of the diluted sample was 84 Hz, which is in close agreement to that obtained from Figure 25. Secondly, exhaustive dialysis of the η = 19 cp solution yielded a linewidth in close agreement with native HDL_2. To alleviate the problems associated with glycerol, we have attempted to measure the ^{31}P residual chemical shift anisotropy by examining HDL_2 in the absence of any perturbants.

By substituting equation (31) into equation (30) we obtain

$$\Delta \upsilon_{1/2} = \frac{16\pi}{45} \Delta\sigma^2 \upsilon_o^2 \tau_e + C$$

where υ_o is the resonance frequency. Thus, a plot of $(\Delta\upsilon 1/2 - C)$ vs. υ_o^2 yields a straight line from which the value of $\Delta\sigma$ can be obtained provided τ_e is known. We have measured the undecoupled ^{31}P NMR linewidth of HDL_2 at three different frequencies (Table XII). Using $\tau_e = 1.06 \times 10^{-7}$ s and the slope from the graph in Figure 41 we calculate $\Delta\sigma$= 69 ppm. This is in substantial agreement with the $\Delta\sigma = 75 \pm 10$ ppm obtained from the viscosity experiment. However, as the linewidth measurements have large (±10%) uncertainty associated with them and the fact that we have only three points describing a straight line, the $\Delta\sigma$ obtained from the field dependence is probably not very accurate. Thus, further research is required to establish the origin of the apparently large value of $\Delta\sigma$ in HDL_2.

Figure 41: Plot of ($\Delta\nu_{1/2}$-C) vs. ν_o^2 of ^{31}P NMR (undecoupled) line widths of native HDL_2 obtained at different resonance frequencies.

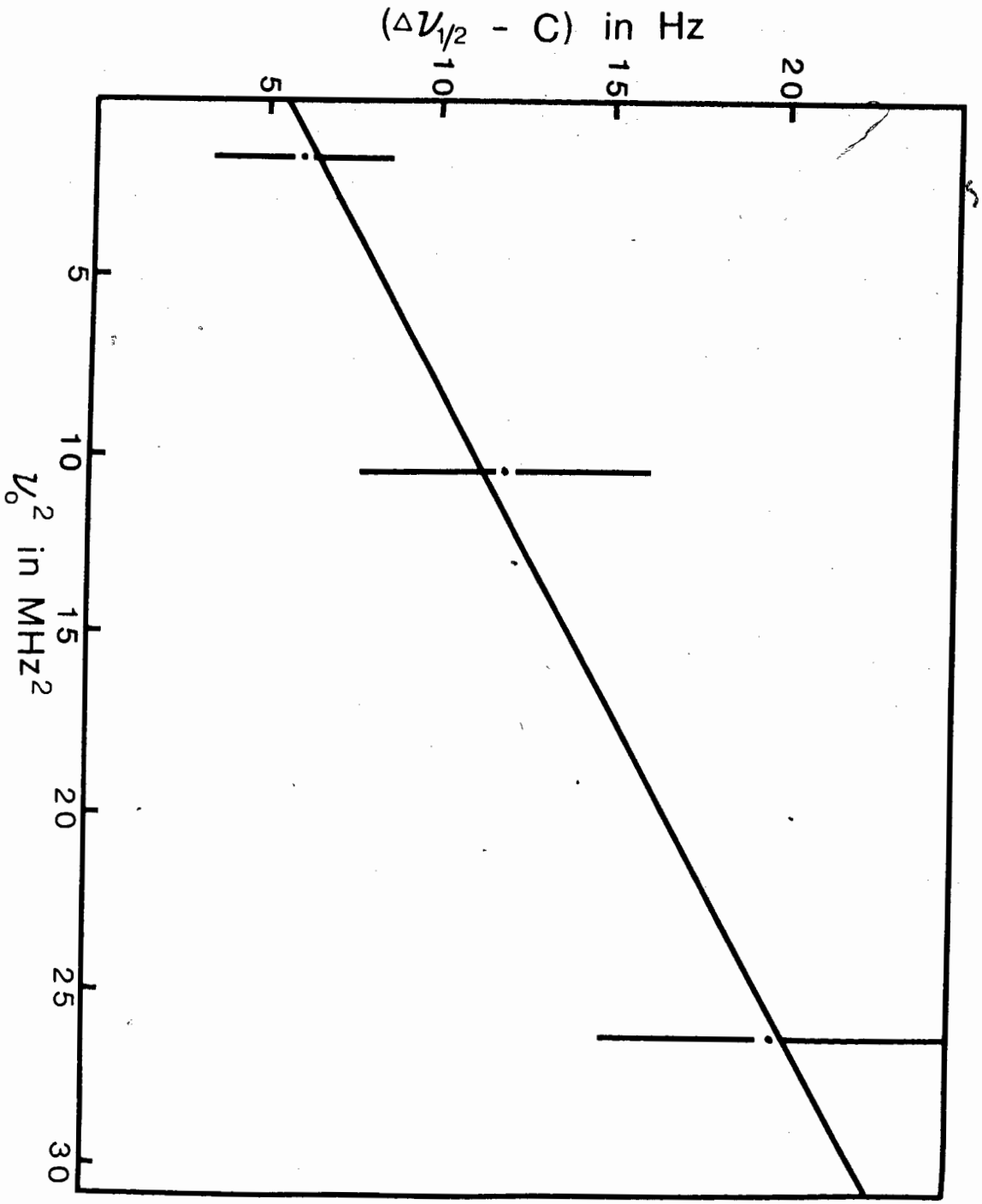
$(\Delta\nu_{1/2} - C)$ in Hz
5
10
15
20
ν_o^2 in MHz^2
5
10
15
20
25
30

VI The Acyl Chain Orientational Order of Deuterated Phospholipids in Membranes

Previously, from the results obtained using selectively deuterated palmitic acid, it was concluded that the orientational order in unilamellar vesicles is at least two times lower than the corresponding liposomes (Section D.II, pp. 163-178). Although fatty acids reflect the orientational order of phospholipids in multilamellar liposomes adequately, the possibility remains that they may alter the unilamellar bilayer structure. For example, fatty acids are known to induce vesicle fusion (135). Therefore, we have examined the acyl chain order using selectively deuterated phospholipids.

Unilamellar vesicles of egg phosphatidylcholine containing (<5 mol %) sn-2 chain labelled phosphatidylcholine derived from egg lysolecithin and selectively deuterated palmitic acid were prepared by sonication. The ^2H NMR spectra of such vesicles are shown in Figure 30.

Fast isotropic tumbling of the vesicle and the lateral diffusion of the phospholipid averages the quadrupolar interaction such that the quadrupolar splitting disappears. Hence, the spectra have to be analysed using equation 19 to obtain S_{CD}. Here, in obtaining $|S_{CD}|$ we have ignored the contribution to the line width resulting from local segmental motion (i.e. the $1/T_1$ term in equations 15 and 19) and any other slow motions. Therefore, we report only an upper limit of S_{CD}.

The correlation time, τ_e, requires the knowledge of the radius of particle and the value of the lateral diffusion coefficient of phospholipid molecules. The radius of the particle was obtained directly from electron micrographs of negatively stained vesicles. We have measured the phospholipid diffusion coefficient at 25°C in egg phosphatidycholine vesicles by the method of Cullis (117) and found $D = (2.5 \pm 0.5) \times 10^{-8}$ $cm^2\ s^{-1}$.

Unilamellar vesicles have an additional problem in that they are heterogeneous with respect to size. Hence a superposition of Lorentzian lines is observed. We have measured their size distribution, shown in Figure 31. Employing equation 19 we have simulated the spectra (Figure 42) in exactly the same manner as described in the vesicles containing selectively deuterated palmitic acids (see pp.167-168). The order parameters which exhibit best visual fits are shown in Figure 42 and Table XVII.

For comparison we have examined the orientational order of multilamellar liposomes made from the same lipid mixture as unilamellar vesicles. The quadrupolar splittings obtained from the various positions of selective deuteration are shown in Table XIV. We have calculated $|S_{CD}|$ using equation 8, which are shown in Table XVII. The two values of $|S_{CD}| = 0.09$ and 0.14 is obtained for the 2 position of the sn-2 chain are due to inequivalence of the two deuterons (137). The value of $|S_{CD}| = 0.22$ for (C4) and 0.23 for (C7) position are representative of

Figure 42: Deuterium NMR spectra (solid lines) of approximately 5 mol % sn-2 chain labelled phosphatidylcholine in unilamellar vesicles of ~7% W/V egg phosphatidylcholine in deuterium depleted water. The position of selective deuteration is indicated to the left of each spectrum. The dotted lines are the best fit superposition of Lorentzian lines using the order parameter indicated.

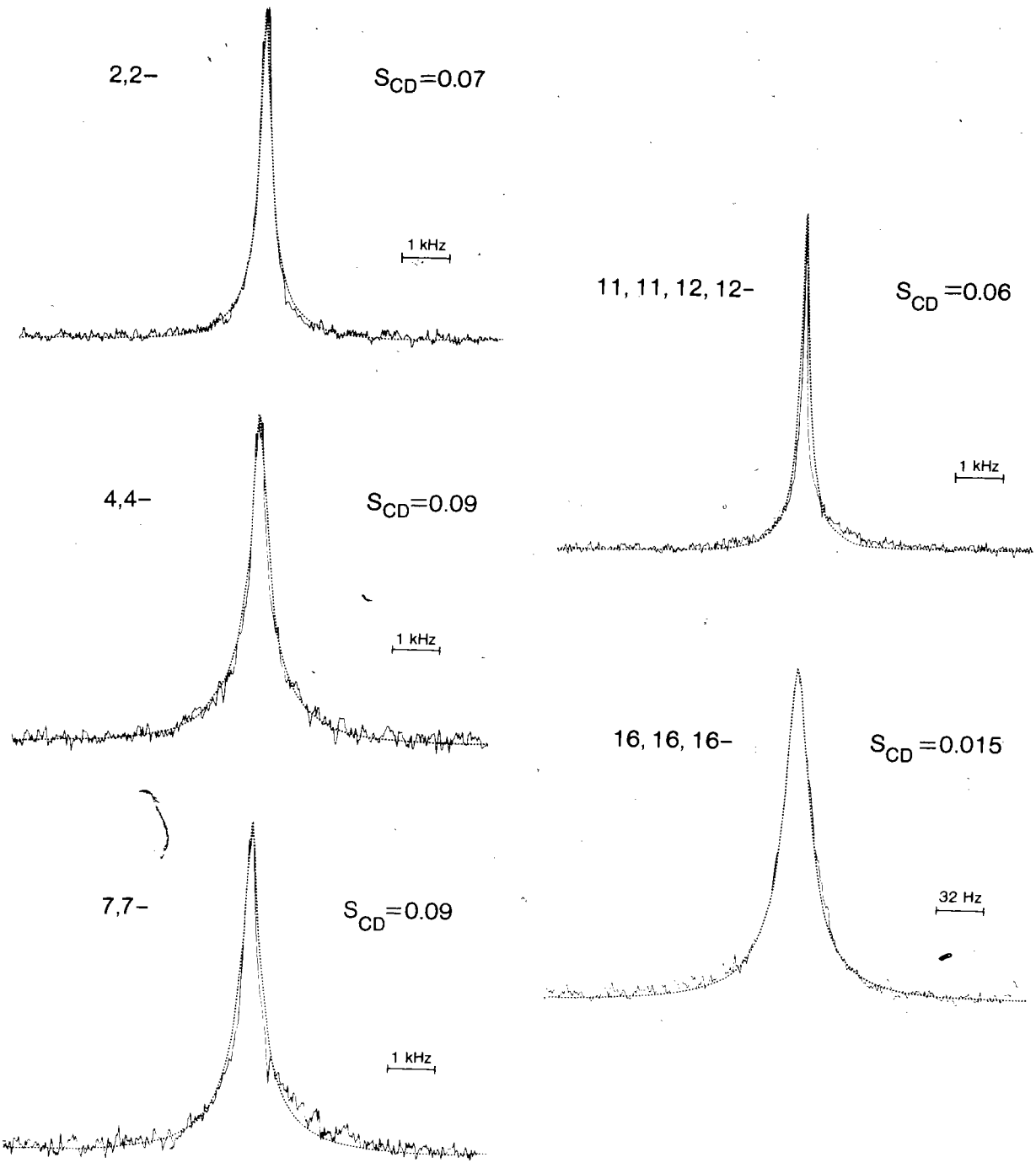
2,2-
S_{CD}=0.07
1 kHz
11, 11, 12, 12-
S_{CD} =0.06
1 kHz
4,4-
S_{CD}=0.09
1 kHz
16, 16, 16-
S_{CD} =0.015
32 Hz
7,7-
S_{CD}=0.09
1 kHz

TABLE XVII: Order parameter $|S_{CD}|$ for sn-2 chain labelled phosphatidylcholine in egg phosphatidylcholine unilamellar vesicles and multilamellar liposomes at 25°C.

Deuterium position on sn-2 acyl chain	$\|S_{CD}\|$	
	Vesicles	Liposomes
2-	0.09	0.09, 0.14
4-	0.09	0.22
7-	0.09	0.23
11,(12)-	0.06	0.18, 0.16
16-	0.015	0.02

the "order parameter plateau" which extends to C10 as shown in other multilamellar dispersion (106,96). The order parameter decreases at 0.18 and 0.16 at C11, C12 before reaching a minimum of 0.02 at C^2H_3. These results are quite similar to those obtained from dipalmitoylphosphatidycholine multilamellar bilayers (143).

Based upon an inspection of the results in Table XVII we are led to conclude that acyl chain order in unilamellar vesicles is approximately one-half of that found in multilamellar liposomes. These results of deuterated phospholipids are in agreement with those obtained from selectively deuterated palmitic acids (107).

The differences in hydrocarbon chains of multilamellar bilayers and unilamellar vesicles are also seen in the gel to liquid-crystalline phase transition (82). Multilamellar dipalmitoyl phosphatidylcholine liposomes undergo a highly cooperative (nearly isothermal) gel to liquid-crystalline phase transition at ~41.2°C. In contrast, small unilamellar vesicles made from the same lipid have broad gel to liquid-crystalline phase transition at about 36.9°C. The enthalpy associated with unilamellar vesicle phase transition is approximately 50% of that of multilamellar liposomes. It is suggested that the phospholipid acyl chain in highly curved unilamellar vesicles have different packing compared to phosphatidylcholine packing in an essentially planar bilayer of multilamellar liposomes. Our ^2H NMR results show these differences quantitatively in acyl chain packing in

two systems.

The lower values of the carbon-deuterium order parameter in vesicles may account for several interesting observations in the literature: insulin binds to small unilamellar vesicles of egg phosphatidylcholine, but not to corresponding multilamellar liposomes (156); protein can transfer from erythrocyte membranes into small unilamellar vesicles but do not transfer into multilamellar liposomes (158); and phospholipid exchange proteins utilize small unilamellar vesicles as effective substrates but are not active with multilamellar liposomes (157).

CONCLUSIONS

Human plasma high density lipoproteins are spherical microemulsions consisting of an apolar (cholesteryl esters and triglycerides) core surrounded by an outer phospholipid monolayer. Surface bound apoproteins stabilize the microemulsions. In the present investigation, we have studied the molecular motions and conformation(s) of lipids in HDL_2 (density = 1.063 - 1.125 g/mL) and HDL_3 (density = 1.125-1.21 g/mL) by ^2H and ^{31}P NMR. The lipoprotein particles were characterized by electron microscopy, gel exclusion chromatography and wet chemistry.

For comparison, the model membranes, unilamellar vesicles, having a phospholipid composition similar to HDL were also studied by ^2H NMR.

High Density Lipoproteins

Reconstituted high density lipoprotein was prepared by sonication and preparative ultracentrigation of mixtures containing the apoproteins of HDL_3, egg phosphatidylcholine, cholesteryl oleate and acyl chain deuterated cholesteryl palmitate in aqueous buffer. The resulting structures have a size and chemical composition very similar to native high density lipoproteins (Table III). The ^2H NMR line widths for the deuterons on the chain positions C2 - C6 varied from 350-430 Hz (Table IV). Such a variation is consistent with an average ester conformation wherein which the ester acyl chain is extended. This conclusion is in

contrast to the HDL models proposed on the basis of compositional analysis (22), but agrees with the model proposed on the basis of low-angle x-ray diffraction (58).

Furthermore, a theoretical line width was calculated for the deuterated cholesteryl palmitate in reconstituted HDL. Using a radius = 4.0 nm, a line width of 2350 Hz is expected for an all-trans C^2H_2 segment of solid cholesteryl palmitate in the core of reconstituted HDL. Thus, the narrow line widths observed (Table IV) indicate that the cholesteryl palmitate acyl chains have considerable anisotropic motions when in the core of reconstituted HDL.

A possible reason for the presence of anisotropic motion is that the small size of the core may prevent the ester from packing as it does in the bulk phase, therefore, leading to chain mobility. Another explanation may be that the ester acyl chains interdigitate into the surface of monolayer and the ester chains are influenced by surface components, i.e. the phospholipids or apoproteins. Whatever may be the explanation, it should be noted that the cholesteryl ester chains have mobility even in the absence of triglycerides. Hamilton and Cordes (68) have proposed that the motions of the cholesteryl moiety are due primarily to the triglycerides in HDL.

The orientational order S_{CD}, of the phospholipid surface monolayer of HDL_2 and HDL_3 was monitored by incorporating

~5 mol % selectively deuterated palmitic acid into native HDL. At ~25°C, the average order parameter, S_{CD}, for the C-D bonds at chain positions C2-C6 = 0.29 and 0.38 for HDL_2 and HDL_3, respectively (Table XV). These values may be compared to the equivalent positions on selectively deuterated stearic acid in egg phosphatidylcholine multilamellar dispersions where S_{CD} = 0.21 (106). The higher orientational order in HDL may be due to the presence of cholesterol in the surface monolayer, lipid-protein interactions, partial interdigitation of the core components into the surface monolayer and/or high curvature of the surface monolayer. These possibilities are discussed in Section D.II, pp. 163-178.

We have also incorporated sn-2 chain deuterated phosphatidylcholine into the surface monolayer of HDL_2. The line widths were 430-360 Hz for the deuterons on chain positions C2-C7 at 15 °C (Table IX). These results are in good agreement with those of deuterated palmitic acid (see above). But the C-D order parameter for the positions were higher than the rest of the positions in the "plateau region" (Table XVI). This is in contrast to the results obtained for the 2 positions of sn-2 of phospholipids in multilamellar dispersions (96). We suggest that the C2 segment of the sn-2 chain of HDL phospholipids has different conformation than in multilamellar liposomes. Possible reasons for the above difference are discussed in Section D.III, pp.179-186.

The lateral diffusion coefficient, D, of phospholipids in

HDL_2 was also determined by the method of Cullis (117) using ^2H and ^{31}P NMR. A value of $D = (2\pm1) \times 10^{-8}$ cm^2 s^{-1} at ~25°C was obtained using both ^2H and ^{31}P NMR. This value indicates that phospholipids in the HDL surface are in the liquid-crystalline phase.

The ^{31}P residual chemical shift anisotropy (CSA) calculated from the viscosity dependence of ^{31}P NMR line width of HDL_2 was ~75 ppm, whereas, CSA of ~45 ppm is observed in phospholipid bilayers (115). In another experiment, HDL_2 ^{31}P NMR line width was obtained as a function of the Larmor frequency. A CSA ~69 ppm was calculated. The apparently higher value of the residual chemical shift anistropy for HDL_2 compared to a bilayer may reflect conformational and/or motional differences of the head group in the two systems. Griffin *et al.* (154) have calculated a CSA ~80 ppm for phospholipid bilayers where the O-P-O plane is parallel to the surface of the bilayer plane. This suggests that the phospholipid head group in HDL has an extended conformation.

^2H NMR longitudinal relaxation times were measured for the selectively deuterated palmitic acids in HDL_2 and HDL_3 (Tables VI and VIII) are approximately 15 ms for C^2H_2 and 170 ms C^2H_3. These values are shorter than those found in phospholipid bilayers (152), suggesting that the molecular motions are more effective in the lipoprotein monolayer than in the model membrane. In HDL, the particle tumbling (τ_t ~10^{-7}s) may itself influence the longitudinal relaxation.

The T_1's for selectively deuterated phosphotidylcholine in HDL_2 were also measured as a function of temperature. The T_1's for C^2H_2 segments from C2-C11,12 was the same within experimental error. This result contrasts with the temperature dependence behaviour of phospholipid bilayers in the liquid crystalline phase.

The T_1's for 5,5,6,6-[$^2H_2$] palmitic and 16,16,16-[$^2H_3$] palmitic acid in HDL_3 increase by ~45 and 17% respectively between 38.8 and 61.4 MHz. The frequency dependence of T_1 may indicate the presence of slow motions of the form shown in bilayers (111,112). Clearly, much research is required to explain the differences in HDL and phospholipid bilayers.

Unilamellar Vesicles

The higher orientational order observed for phospholipids in HDL than for multilamellar dispersions may be due to the high curvature of the HDL surfaced. Therefore, we have studied unilamellar vesicles composed of egg phosphatidylcholine/sphingomyelin/selectively deuterated palmitic acid whose surface is also highly curved. The average order, S_{CD}, for the "plateau region" was 0.09. This value is approximately 3-5 times lower than that found in HDL. Furthermore, the S_{CD} = 0.09 for the highly curved unilamellar vesicles is at least two times lower than that found in much less curved multilamellar lipo-

somes. For comparison with selectively deuterated palmitic acid in bilayers, we have incorporated phosphatidylcholine, selectively deuterated along the sn-2 chain in egg phosphatidylcholine multilamellar liposomes and unilamellar vesicles. In the case of multilamellar liposomes, the value of S_{CD} was 0.09, 0.014 (C2), 0.22 (C4) and 0.23 (C7). These values of S_{CD} are significantly different, C_{CD} = 0.07 (C2), 0.09 (C4) and 0.09 (C7) from those obtained for unilamellar vesicles. We therefore conclude that the acyl chain orientational order of highly curved unilamellar vesicles is at least two times lower than in multilamellar liposomes.

This significant finding may have important consequences. Firstly, care must be exerted in extrapolating the results obtained from unilamellar vesicles to the planar regions of the biological membranes. Secondly, unilamellar vesicles are excellent models for the highly curved regions of biological membranes. The biological activity associated with the curved regions such as cristae in the mitochondria may be in part due to the structure of the phospholipid acyl chains. Recently, Madden et al. (160) have shown that the coupling ratio of the cytochrome c oxidase reconstituted system increases as the size of the vesicles is decreased.

REFERENCES

(1) Small, D.M. (1981) in Membranes, Molecules, Toxins and Cells (Bloch, K., Bolis, L., and Tosteson, D.C., eds), pp.11-34, John Wright, PSG Inc., Boston, USA.

(2) Eisenberg, S., and Olivecrona, T. (1979), J. Lipid Res. 20 614-623.

(3) Goldstein, J.L., and Brown, M.S. (1977), Ann. Rev. Biochem. 46 897-930.

(4) Goldstein, J.L., Ho, Y.K., Brown, M.S., Innerarity, T.L. and Mahley, R.W. (1980), J. Biol. Chem. 255 1839-1848.

(5) Goldstein, J.L., Ho, Y.K., Basu, S.K. and Brown, M.S. (1979), Proc. Natl. Acad. Sci., USA, 76 333-337.

(6) Miller, G.J. and Miller, N.E. (1975), Lancet I 16-19.

(7) Koelz, H.R., Sherrill, B.C., Turley, S.D. and Dietschy, A.M. (982), J. Biol. Chem. 256 7362-7370.

(8) Tall, A.R. and Small, D.M. (1978), New England J. Med. 299 1232-1236.

(9) Redgrave, T.G., and Small. D.M. (1979) J. Clin. Invest. 64 162-171.

(10) Glomset, J.A. and Norurm, K.R. (1973), Adv. Lipid Res. 11 1-65.

(11) Schwartz, C.C., Vlahce vic, Z.R., Berman, M., Meadows, R., Nisman, M, and Swell, L. (1982), J. Clin. Invest. 70 105-116.

(12) Takinen, M.R., Kashyap, M.L., Srivastava, L.S., Ashraf, M., Johonson, J.D., Perisutti, G., Brady, D., Glueck, C.J., and Jackson, R.L. (1982), Atherosclerosis 41 381-394.

(13) Grosser, J., Schrecker, O., and Green, H. (1981), J. Lipid Res. 22 437-442.

(14) Tall, A.R., Blum, C.B., Forester, G.P. and Nelson, C.A. (1982), J. Biol. Chem. 257 198-207.

(15) Morton, R.E., and Zilversmit, D.B. (1983), J. Biol. Chem. 258 11751-11757.

(16) Nestel, P.J. and Billington, T. (1980), Artery 7 395-403.

(17) Forte, G.M., Nichols, A.V., and Glaeser, R.M. (1968), Chem. Phys. Lipids 2 396-408.

(18) Forte, T., and Nichols, A.V. (1972), Adv. Lipid Res. 10 1-41.

(19) Morrisett, J.D., Jackson, R.L., and Gotto, A.M. (1975), Ann. Rev. Biochem. 44 183-207.

(20) Morrisett, J.D., Jackson, R.L. and Gotto, A.M. (1977), Biochem. Biophys. Acta 472 93-133.

(21) Osborne, J.C. and Brewer, H.B. (1977), Adv. Protein Chem. 31 253-337.

(22) Edelstein, C., Kezdy, F.J., Scanu, A.M., and Shen, B.W. (1979), J. Lipid Res. 20 143-153.

(23) Smith, L.C., Pownall, H.J. and Gotto, A.M. (1978) Annu. Rev. Biochem. 47 751-777.

(24) Pownall, H.J. and Gotto, A.M. (1983) Phospholipids and Athesosclerosis, ed. P. Avogaro, M. Mancini, G. Ricci and R. Pavletti, Raven Press, New York.

(25) Baker, H.N., Delahunty, T., Gotto, A.M., Jackson, R.L. (1974), Proc. Natl. Acad. Sci., USA, 71 3631-3632.

(26) Brewer, H.B., Fairwell, T., Larue, A., Ronan, R., Houser, A., and Bronzert, T.J. (1978), Biochem. Biophys. Res. Commun. 80 623-630.

(27) Brewer, H.B., Lux, S.E., Ronan, R., and John, K.M. (1972), Proc. Natl. Acad. Sci., 69 1304-1308.

(28) Nestruck, A.C., Suzue, G., and Marcel, Y.L. (1980), Biochem. Biophys. Acta 617 110-121.

(29) Shipley, G.G., Atkinson, D., and Scanu, A.M. (1972), J. Supramol. Struct. 1 98-104.

(30) Laggner, P., Kratky, O., Kostner, G., Sattler, J., and Holasek, A. (1972) FEBS Lett. 27 53-57.

(31) Scanu,A.M., Reader, W., and Edelstein, C. (1968), Biochim. Biophys. Acta 160 32-45.

(32) Shore, V.G., Siu-way, Sae, A., and Shore, B. (1978) Biochim. Biophys. Acta 529 319-330.

(33) Shonfield, G., Bradshaw, R.A., and Chen, J.S. (1976) J. Biol. Chem. 251 3921-3926.

(34) Karlin, J.B., Juhn, D.J., Starr, T.I., Scanu, A.M. and Rubenstein, A.H. (1976), J. Lipid Res. 17 30-37.

(35) Mao, S.J.T., Sparrow, J.T., Gilliam, E.B., and Gotto, A.M. (1977) Biochemistry 16 4150-4156.

(36) Shepherd, J., Gotto, A.M., Taunton, O.D., Caslake, M.J. and Farish, E. (1977) Biochim. Biophys. Acta 489 486-501.

(37) Stoffel, W. (1983), in Phospholipids and Atherosclerosis (Avogaro, P., Mancini, M., and Ricci, G. eds) pp. 115-130, Raven Press, New York.

(38) Grow, T.E. and Fried, M. (1975) Biochem. Biophys. Res. Commun. 66 352-356.

(39) Grow, T.W., and Fried, M. (1977) Biochem. Biophys. Res. Commun. 75 117-124.

(40) Tall, A.R., Deckelbaum, R.J., Small, D.M., and Shipley, G.G. (1977) 487 145-153.

(41) Segrest, J.P., Jackson, R.L., Morrisett, J.D. and Gotto, A.M. (1974) FEBS Lett. 38 247-253.

(42) Segrest,J.P. and Feldmann, R.J. (1977) Biopolymers 16 2053-2065.

(43) Skipski, V.P. (1972) in Blood Lipids and Lipoproteins (Nelson, G.J., ed.) pp. 371-583, Wilely-Interscience, New York.

(44) Assmann, G., Sokolsky, E.A., and Brewer, H.B. (1974), Proc. Natl. Acad. Sci., USA, 71 549-553.

(45) Henderson, T.O., Kruski, A.W., Davis, L.G., Glonek, T., and Scanu, A.M. (1975), Biochemistry 14 1915-1920.

(46) Pattnaik, N.M., Kezdy, F.J. and Scanu, A.M. (1976), J. Biol. Chem. 251 2782-2786.

(47) Assman, G., and Brewer, H.B. (1974), Proc. Natl. Acad. Sci., USA, 71 989-994.

(48) Stoffel, W., Zierenberg, O., Tungal, B.D., and Schreiber, E. (1974), Hoppe-Seyler's Z. Physiol. Chem. 355 1381-1390.

(49) Stoffel, W., Zierenberg, O., Tungal, B.D., and Schreiber, E. (1974), Proc. Natl. Acad. Sci., USA, 71 3696-3700.

(50) Andrews, A.L., Atkinson, D., Barratt, M.D., Finer, E.G., Hauser, H., Henry, R., Leslie, R.B., Owens, N., Phillips, M.C. and Robertson, R.N. (1976) Eur. J. Biochem. 64 549-557.

(51) Chapman, D., Leslie, R.B., Hirz, R. and Scanu, A.M. (1969), Nature 221 260-261.

(52) Chapman, D., Leslie, R.B., Hirz, R. and Scanu, A.M. (1969), Biochem. Biophys. Acta 176 524-536.

(53) Brainard, J.R., Knapp, R.D., Patsch, J.R., Gotto, A.M., and Morrisett, J.D. (1980), Ann. N.Y. Acad. Sci. 348 299-317.

(54) Scanu, A.M. (1979) in The Biochemistry of Atherosclerosis (Scanu, A.M., Wissler, R.W., and Getz, G.S., eds.) pp. 3-8, Marcel Dekker, New York.

(55) Scanu, A.M. (1972), Biochim. Biophys. Acta 265 471-508.

(56) Shen, B.W., Scanu, A.M. and Kezdy, F.J. (1977), Proc. Natl. Acad. Sci., USA, 74 837-841.

(57) Verdery, R.B., and Nichols, A.V. (1975), Chem. Phys. Lipids 14 123-124.

(58) Laggner, P. and Muller, K.W. (1978), Q. Rev. Biophys. 11 371-425.

(59) Gorrissen, H., Tulloch, A.P., and Cushley, R.J. (1980), Biochemistry 19 3422-3429.

(60) Cushley, R.J., Gorrissen, H., and Wassall, S.R. (1980), Can. J. Chem. 58 2433-2441.

(61) Forrest, B.J. and Cushley, R.J. (1977), Atherosclerosis 309-318.

(62) Grover, A.K. and Cushley, R.J. (1979), Atherosclerosis 32 87-91.

(63) Jonas, A., and Jung, R.W. (1974) Biochem. Biophys. Res. Commun. 66 651-657.

(64) Jonas, A. (1977), Biochim. Biophys. Acta 486 10-22.

(65) Hamilton, J.A., Talkowski, C., Williams, E., Avila, E.M., Allerhand, A., Cordes, E.H., and Camejo, G. (1973), Science 180 193-195.

(66) Hamilton J.A., Talkowski, C., Childers, R.F., Williams, E., Allerhand, A., and Cordes, E.H. (1974), J. Biol. Chem. 249 4872-4878.

(67) Hamilton, J.A., Oppenheimer, N., and Cordes, E.H. (1977), J. Biol. Chem. 252 8071-8080.

(68) Hamilton, J.A. and Cordes, E.H. (1978), J. Biol. Chem. 253 5193-5198.

(69) Ladbrooke, B.D., Williams, R.M. and Chapman, D. (1968), Biochim. Biophys. Acta 150 333-340.

(70) Small, D.M. (1970) in Surface Chemistry of Biological Systems (Blank, M. ed.) pp. 55-83, Plenum Press, New York.

(71) Avila, E.M., Hamilton, J.A., Harmony, J.A.K., Allerhand, A., and Cordes, E.H. (1978), J. Biol. Chem. 253 3983-3987.

(72) Hauser, H. and Kostner, G.M. (1979), Biochim. Biophys. Acta 573 375-381.

(73) Lund-Katz, S. and Phillips, M.C. (1981), Biochem. Biophys. Res. Commun. 100 1735-1742.

(74) Lund-Katz, S. and Phillips, M.C. (1984), Biochemistry 23 1130-1138.

(75) Coffin, S., Limm, M., and Cowburn, D. (1984), J. Magn. Reson. 59 268-274.

(76) Lee, A.G., Birdall, N.J.M. and Metcalfe, J.C. (1974) in "Methods in Membrane Biology, Vol.2" (Korn, E.D., ed.) Plenum Press, New York, pp.2-156.

(77) Luzzati, V., Gulik-Krzywicki, T. and Tardieu, A. (1968), Nature 218, 1031-1034.

(78) Levine, Y.K. and Wilkins (1971), Nature New Biol. 230, 69-72.

(79) Wilkins, M.H.F., Blaurock, A.E. and Engleman, D.M. (1971), Nature New Biology, 230, 72-76.

(80) Tardieu, A., Luzzati, V. and Reman, F.C. (1973), J. Mol. Biol. 75, 711-733.

(81) McConnell, H.M. and McFarland, B.G. (1972), Ann. N.Y. Acad. Sci. 195, 207-217.

(82) Scheetz, M.P. and Chan, S.I. (1972), Biochemistry 11,4573-4581.

(83) Bangham, A.D. an Horne R.W. (1964), J. Mol. Biol. 8, 660-668.

(84) Gent, M.P.N. and Prestegard, J.H. (1974), Biochemistry 13, 4027-4033.

(85) Huang, C. and Mason, J.T. (1978), Proc. Natl. Acad. Sci., USA 75, 308-310.

(86) Huang, C. (1969) Biochemistry 8, 344-351.

(87) Forge, A., Knowles, P.E. and Marsh, D. (1978), J. Membrane Biol. 41, 249-263.

(88) Litchenberg, D. and Zilberman, Y. (1979), J. Magn. Reson. 34, 491-497.

(89) Mackay, A.L., Burnell, E.E., Nichol, C.P., Weeks, G., Bloom, M. and Valic, M.I. (1978), FEBS Lett. 88, 97-100.

(90) Gent, M.P.N. and Prestegard, J.H. (1977), J. Magn. Reson. 25, 243-262.

(91) Taylor, M.G. and Smith, I.C.P. (1980), Biochim. Biophys. Acta 599 140-149.

(92) Smith, I.C.P., Stockton G.W., Tulloch, A.P., Polnaszek, C.F. and Johnson, K.G. (1977), J. Colloid and Interface Sci. 58 439-451.

(93) Seelig, J. (1978), Progr. Colloid and Polymer Sci. 65 172-179.

(94) Jacobs, R.E. and Oldfield, E. (1981), NMR of membranes, Progr. NMR Spectr. 14 113-136.

(95) Seelig, J. (1977), Quart. Rev. Biophys. 10, 353-418.

(96) Davis, J.H. (1983), Bichim. Biophys. Acta 737 117-171.

(97) Mantsch, H.H., Saito, H., and Smith, I.C.P. (1977) in Progress in the Nuclear Magnetic Resonance Spectroscopy (Emsley, J.W., Feeney, J. and Sutcliffe, L.H., eds.) Vol. 11, pp. 212-272, Pergamon Press, London.

(98) Seelig, J., Seelig, A. and Tamm, L. (1982) in Lipid Protein Interactions (edited by P.C. Jost and O.H. Griffith), Vol. 2, pp. 127-149.

(99) Seelig, J. and Seelig A. (1974), Biochem. Biophys. Res. Commun. 57 406-411.

(100) Peterson, N.O. and Chan, S.I. (1977), Biochemistry 16 2657-2667.

(101) Wolber, P.K. and Hudson, B.S. (1981), Biochemistry 20 2800-2810.

(102) Dufourc, E.J., Smith, I.C.P. and Jarrell, H.C. (1984), Biochemistry 23 2300-2309.

(103) Bloom, M., Burnell, E.E., Mackay, A.L., Nichol, C.P., Valic, M.I. and Weeks, G. (1978) Biochemistry 17 5750-5762.

(104) Smith, I.C.P. (1982), Bulletin of Magnetic Resonance 3 120-132.

(105) Abragam, A. (1961), The Principles of Nuclear Magnetism, Clarendon Press, Oxford.

(106) Stockton, G.W., Polnaszek, C.F., Tulloch, A.P., Hasan, F. and Smith, I.C.P. (1976), Biochemiostry 15 954-966.

(107) Parmar, Y.I., Wassall, S.R., and Cushley, R.J. (1984), J. Amer. Chem. Soc. 106 2434-2435.

(108) Jardetzky, O., and Roberts, G.C.K. (1981) in NMR in Molecular Biology, pp. 10-68, Academic Press, New York.

(109) Brown, M.F. and Davis, J.H. (1981), Chem. Phys. Lett. 79 431-435.

(110) Bloom, M. and Smith, I.C.P. (1985) to be published in Progress in Protein-Lipid Interaction (J.J.H.M. du Pont and A. Watts) Elsevier.

(111) Brown, M.F. (1982) J. Chem. Phys. 77 1576-1599.

(112) Kimmich, R., Schmur, G., and Scheurmann, A. (1983) Chem. Phys. Lipids 32 271-322.

(113) Jeffrey, K.R., Wong, T.C., Burnell, E.E., Thompson, M.J., Higgs, T.P. and Chapman,N.R. (1979), J. Magn. Reson. 36 151.

(114) Büldt, G. and Wohlgemuth, R. (1981), J. Memb. Biol. 58 81-100.

(115) Seelig, J. (1978) Biochim. Biophys. Acta 515 105-140.

(116) Cullis, P.R. and DeKruijff, B. (1979) Biochim. Biophys. Acta 559 399-420.

(117) Cullis, P.R. (1976) FEBS Lett. 70 223-228.

(118) McLaughlin, A.C., Cullis, P.R., Berden, J.A. and Richards, R.E. (1975), J. magn. Reson. 20 146-165.

(120) Grover, A.K. and Cushley, R.J. (1979) J. Labelled Compd. Radiopharm. XVI 307-313.

(121) Singleton, W.S., Gray, M.S., Brown, M.L., and White, J.L. (1965) J. Am. Oil Chem. Soc. 42 53-56.

(122) Richter, H., Srey, C., Winter, K., and Furst, W. (1977) Pharmazie 32 164.

(123) Havel, R.J., Elders, H.A. and Bragdon, J.H. (1955) J. Clin. Invest. 34 1345-1353.

(124) Scanu, A.M. (1966) J. Lipid Res. 7 295-306.

(125) Scanu, A.M., Toth, J., Edelstein, C., Koga, S., and Stiller, E. (1969) Biochemistry 8 3309-3316.

(126) Hirz, R. and Scanu, A.M. (1970) Bioochim. Biophys. Acta 207 364-367.

(127) Ames, B.N. (1966) in Methods in Enzymology (Newfeld, E.F. and Gimburg, V., eds.), Vol. 8, p.15, Academic Press, New York.

(128) Rudel, L.L. and Morris, M.D. (1973), J. Lipid Res. 14 164-166.

(129) Lowry, O.H., Rosebrough, N.J., Farr, a.L. and Randall, R.J. (1951), J. Biol. Chem. 193 265-275.

(130) Glonek, T., Henderson, T.O., Kruski, A.W., and Scanu, A.M. (1974), Biochim. Biophys. Acta 348 155-161.

(131) Keith, A.D., Melhorn, R.J., Freeman, N.K. and Nichols, A.V. (1973) Chem. Phys. Lipids 10 223-236.

(132) Schroeder, F., Goho, E.H., and Heimberg, M. (1979) J. Biol. Chem. 254 2456-2463.

(133) Sklar, L.A., Doody, M.C., Gotto, A.M. and Pownall, H.J. (1980), Biochemistry 19 1294-1301.

(134) Anderson, D.W., Nichols, A.V., Forte, T.M. and Lindgren, F.T. (1977) Biochim. Biophys. Acta 493 55-68.

(135) Kantor, H.L., Mabrey, S., Prestegard, J.H. and Sturtevant, J.M. (1977) Biochim. Biophys. Acta 466 402-410.

(136) Kantor, H.L. and Prestegard, J.H. (1975) Biochemistry 14 1790-1795.

(137) Engel, A.K. and Cowburn, D. (1981) FEBS Lett. 126 169-172.

(138) Seelig, a. and Seelig, J. (1975) Biochim. Biophys. Acta 406 1-5.

(139) Davis, J.H. (1979), Biophys. J. 27 339-358.

(140) Burnell, E.E., Cullis, P.R. and de Kruijff, B. (1980), Biochim. Biophys. Acta 603 63-69.

(141) Valic, M.I., Gorrissen, H., Cushley, R.J. and Bloom, M. (1979) Biochemistry 18 854-859.

(142) Gorrissen, H., Mackay, A.L., Wassall, S.R., Valic, M.I., Tulloch, A.P. and Cushley, R.J. (1981) Biochim. Biophys. Acta 644 266-272.

(143) Seelig, A. and Seelig, J. (1977), Biochemistry 16 45-50

(144) Pauls, K.P., Mackay, A.L., Bloom, M. (1983) Biochemistry 22 6101-6109.

(145) Davis, J.H., Maraviglia, B., Weeks, G. and Godin, D.V. (1979), Biochim. Biophys. Acta 550 362-366.

(146) Stockton, G.W. and Smith, I.C.P. (1976), Chem. Phys. Lipids 17 251-264.

(147) Verdery, R.B. and Nichols, A.V. (1974), Biochem. Biophys. Res. Commun. 57 1271-1278.

(148) Paddy, M.R., Dahlquist, F.W., Davis, J.H., and Bloom, M. (1981), Biochemistry 20 3152-3162.

(149) Bienvenue, A., Bloom, M., Davis, J.H. and Devaux, P.F. (1982) J. Biol. Chem. 257 3032-3038.

(150) Finer, E.G. (1974) J. Magn. Reson. 13 76-86.

(151) Davis, J.H. and Jeffrey, K.R. (1977) Chem. Phys. Lipids 20 87-104.

(152) Brown, M.F., Seelig, J. and Haberlen, U. (1979), J. Chem. Phys. 70 5045-5053.

(153) Parmar, Y.I., Gorrissen, H., Wassall, S.R., and Cushley, R.J. (1983), J. Biol. Chem. 258 2000-2004.

(154) Griffin, R.G., Powers, L. and Pershan, P.S. (1978) Biochemistry 17 2718-

(155) McDaniel, R.V., McIntosh, T.J. and Simon, S.A. (1983) Biochim. Biophys. Acta 731 97-108.

(156) Fwang, F.J., Leung, H.H., and Merriam, J. (1980) Fed. Proc. 39 1761.

(157) Machida, K., and Ohnishi, S.I. (1980) Biochim. Biophys. Acta 596 201-209.

(158) Bouma, S.R., Drislane, F.W, and Huestis, W.H. (1977) J. Biol. Chem. 252 6759-6763.

(159) Vold, R.L., Waugh, J.S., Klein, M.P., and Phelps, D.E. (1968) J. Chem. Phys. 48 3831-3832.

(160) Madden, D.T., Hope, M.J., and Cullis, P.R. (1984) Canadian Biochemical Society Symposium, Banff, Alberta.

(161) Davis, J.H., Jeffrey, K.R., Bloom, M., Valic, M.I., Higgs, T.P. (1976) J. Chem. Phys. 42 390-394.

(162) Wassall, S.R., Treleaven, W.D., Parmar, Y.I. and Cushley, R.J. (1982) Biochem. Biophys. Res. Commun. 107 429-434.

(163) Hatch, S.T. and Lees R.S. (1968) Adv. Lipid Res. 6 1-35.